

S T U D I E S O N T H E S Y N T H E S I S
O F L A Y E R S I L I C A T E S

BY

DOUGLAS S. SNELL

DEPARTMENT OF CHEMISTRY

UNIVERSITY OF GLASGOW

THESIS SUBMITTED FOR THE DEGREE OF

DOCTOR OF PHILOSOPHY

SEPTEMBER, 1975

ProQuest Number: 11018049

All rights reserved

INFORMATION TO ALL USERS

The quality of this reproduction is dependent upon the quality of the copy submitted.

In the unlikely event that the author did not send a complete manuscript and there are missing pages, these will be noted. Also, if material had to be removed, a note will indicate the deletion.



ProQuest 11018049

Published by ProQuest LLC (2018). Copyright of the Dissertation is held by the Author.

All rights reserved.

This work is protected against unauthorized copying under Title 17, United States Code
Microform Edition © ProQuest LLC.

ProQuest LLC.
789 East Eisenhower Parkway
P.O. Box 1346
Ann Arbor, MI 48106 – 1346

"But I won't be plagued by this any more,
just now; if you choose to think the crystals alive,
do, and welcome." — RUSKIN

And in any case —

"Everything not made of asbestos is going
to be burned." — CARLYLE

CONTENTS

	Page
Summary -	iv
Chapter:-	
1 Introduction	1
2 Hectorite	11
3 Tobermorite	32
4 Cadmium Hydroxide	53
5 Copper Hydroxide	62
6 Beryllium and Zinc Hydroxides	82
7 Higher Temperature Work with $Mg(OH)_2$	97
8 General Hypothesis and Suggestions for Further Work.	108
Appendices:-	
I The Synthesis and Properties of Tobermorite, of C-S-H(I) and of C-S-H-Gel, A Review.	117
II The Hypothesis of the Crystal Gene	151
III Selected Literature on the Copper Silicates	156
References -	160

SUMMARY

Magnesium hydroxide reacts with silica gel to form a hectorite-like phyllosilicate. The reaction is believed to involve initial interlayer adsorption of silicate ion into the brucite crystals. Subsequent argillification is thought to occur by dissolution of the adsorbate and recrystallization of the complex magnesium silicate ions thus formed. If this reaction scheme is valid, silicates should be most easily formed from hydroxides whose crystal structure can be easily penetrated by silicate ion.

The reactions with silica gel of the divalent hydroxides of magnesium, calcium, cadmium, copper, zinc and beryllium were investigated. In each case, a 10% aqueous slurry of a mixture of the solid hydroxide with silica gel was refluxed at pH 10. The hydroxide-silica ratio was 0.75, to satisfy the formula of an ideal 2:1 trioctahedral layer silicate. The reactions were followed by infrared spectroscopy and electron microscopy, and evidence was sought for the existence of an initial intrastructural adsorbate. In some cases, differential thermal analysis was used for further characterisation of the samples. The reaction products were, where possible, identified by powder x-ray diffraction and electron diffraction. In the case of polymorphous hydroxides, samples of consisting of single polymorphs were used as starting materials.

Amorphous silica gel has a strong Si-O stretch

band at 1070 cm^{-1} in the infrared. Intrastructural adsorption of silicate ion produces a new Si-O stretch band at around 1020 cm^{-1} . This band increases in intensity as the adsorbate is formed. Recrystallization of the adsorbate leads to further changes in the Si-O stretching pattern. Adsorption leads to the breaking up of the hydroxide crystals, yielding a material of very low particle size having a weak microcrystalline electron diffraction pattern. Recrystallization of this material is not always observed under the reaction conditions used.

With all the hydroxides except $\epsilon\text{-Zn(OH)}_2$ and $\beta\text{-Be(OH)}_2$, the above changes were observed. Recrystallization of the Mg(OH)_2 and $\gamma\text{-Zn(OH)}_2$ adsorbates led to hectorite and hemimorphite, respectively. Ca(OH)_2 and Cu(OH)_2 gave adsorbates which recrystallized partially. The Cd(OH)_2 adsorbate did not recrystallize. $\epsilon\text{-Zn(OH)}_2$ and $\beta\text{-Be(OH)}_2$ did not form adsorbates.

The "adsorbate half-time" is defined from the infrared spectra for each hydroxide, and correlated with the hydroxide structural parameters. Hydroxides with layer or chain structures have short adsorbate half-times, while those with framework structures have long or infinite adsorbate half-times.

The reaction of magnesium hydroxide with Pyrex glass at 115°C in saturated potassium carbonate solution was investigated. A new magnesium silicate phase is reported.

ACKNOWLEDGEMENTS

This work was carried out in the Department of Organic Chemistry, under the direction of Professor R. A. Raphael and Professor G. W. Kirby, to both of whom I am indebted for the award of a Demonstratorship during the course of the research, and in the Department of Inorganic Chemistry.

My supervisors, Dr. Graham Cairns-Smith and Dr. Tom Baird, supported me throughout with help and inspiration, and they have my heartfelt thanks. Professor H.F.W. Taylor, of Aberdeen University, Dr. V.C. Farmer, of the MacAulay Institute for Soil Research, and Dr. Helen Fullarton, of the Agricultural Chemistry Department of Glasgow University, helped with discussions, x-ray diffraction, DTA and x-ray fluorescence analysis.

I would like to thank the following technicians of Glasgow University for their uncomplaining assistance:-

Helen Douglas	-	Electron Microscopy
Elizabeth Breslin	-	Henderson Lab.
Donald Skinner	-	Geochemistry
Fiona Cowan	-	Microanalysis
Freda Lawrie	-	Infrared Lab.

Finally, I am very grateful to my wife, Anne Gildawie, who despite struggling with her own thesis, was always ready to lend a hand in the battle with this one.

Douglas S. Snell

Douglas S. Snell

CHAPTER 1. INTRODUCTION.

Layer silicates are of wide natural occurrence in a variety of structural types. The tendency of silicate ions to polymerize in two dimensions, giving rise to a sheet structure, is responsible for the layer structures of a large group of minerals, examples of which, in order of increasing structural complexity, are given in table 1.01. The most important family of this group is that derived from the combination of one or two silicate sheets with a sheet of hydroxyl ions in octahedral co-ordination around a central cation, thus producing an unit layer consisting of a metal-hydroxide - silica sandwich. One tetrahedral sheet may combine with one octahedral hydroxide sheet to produce a 1:1 or diphormic, phyllosilicate, such as crysotile; or two tetrahedral silicate sheets may sandwich one octahedral layer to give a 2:1 or triphormic phyllosilicate like talc. Further, the central cation may be divalent, and its hydroxide layer trioctahedral, as in brucite and talc; or trivalent with a dioctahedral layer, as in kaolinite or pyrophyllite. Substitution of every fourth silicon atom by an aluminium atom in the tetrahedral layers of triphormic structures produces the micas. Less ordered substitution in octahedral and tetrahedral layers of both diphormic

and triphormic structures produces the clay minerals. In the micas, the pattern of negative charges created on the layer surface by the substitution, are satisfied by interlayer cations, usually K^+ ; in the clay minerals, randomly-distributed negative charges on the layer surfaces are satisfied by exchangeable interlayer cations.

In some cases, in particular among the Tobermorite group of minerals, a layer structure can be formed lacking a phyllosilicate sheet, in which the polysilicate anions are present as chains. This structure is discussed in greater detail in Appendix I.

Materials similar to or identical with the natural layer silicates may be synthesised from mixtures of metal oxides, hydroxides or silicates with silica and water under the appropriate conditions. Such work commonly involves the use of high-pressure reaction vessels at elevated temperatures, the "hydrothermal method", and approximate phase diagrams for metal-oxide-mixture - water systems may be constructed upon identification of the products. (See, for example, Bowen, N.L. and Tuttle, O.F.; "The System $MgO - SiO_2 - H_2O$ ", Bull. Geol. Soc. America (1949), 60, 439-460). It is difficult to make studies on reaction mechanisms using this technique, however, and the formation of transient metastable phases cannot be continuously observed.

The importance of these points in connection with investigations on the hypothesis of the crystal gene, is outlined in Appendix II.

Accordingly, in this work attention has been limited to the study of those phases which can or might be readily synthesised at atmospheric pressure, thus permitting the continuous observation of the silicification process.

The formation of layer silicates at reflux temperature from aqueous slurries of amorphous silica and metal hydroxides appears to require initially the presence of a layer structure hydroxide on which silicate anions can be adsorbed. Thus, phyllosilicates can be formed at reflux temperatures from the hydroxides of magnesium (1), nickel and cobalt (2), and a layer silicate is formed under similar conditions from calcium hydroxide (Appendix I). These hydroxides, together with those of iron(II), cadmium, and manganese(II), crystallize with the CdI_2 (C_6) structure type (3-7), in which octahedrally co-ordinated layers in the a, a' plane are stacked along the c -axis (figure 1.01). No hydrogen bonds are formed between the layers, which are held together only by electrostatic interactions: the principal cleavage is thus (001).

Certain other divalent metal hydroxides are known to crystallize with layer structures.

One of the metastable polymorphs of zinc(II)

hydroxide (8) has a chain structure (Chap. 6), while copper(II) hydroxide is thought to have the hydrogen-bonded layer structure of lepidocrocite (9, figure 1.02). Boehmite (γ -AlOOH) also has this structure (10,11), and the formation of kaolinite at 200°C from silica gel and poorly crystalline boehmite has been claimed (12). A summary of the crystal structure data of these metal hydroxides is presented in table 1.02.

In contrast with the above hydroxides, the structure of β -Be(OH)₂ (13), with a small unit cell, has no layer properties and adsorption of silicate ion would be expected to be limited to the external surfaces of the crystallites.

It is generally recognized that the adsorption of silicate units onto pre-existing hydroxide crystals is only the first step in phyllosilicate formation. In the case of hectorite, the most probable adsorbate is geometrically quite similar to the final product. This leads to a dichotomy between the rates of formation of hectorite estimated from X-ray diffraction data and from DTA. A structure for the initial adsorbate, termed "pseudo-smectite", has been proposed (15). It is suggested that this pseudo-smectite may then provide a source of the type B solution species required for final phyllosilicate formation as suggested by Henin and Caillere (16).

It is possible to follow the silicification of brucite in some detail by infra-red spectrophotometry. The adsorption of silicate ions with disappearance of the surface hydroxyl groups, and the appearance of new hydroxyl groups in the phyllosilicate sheet, are all reflected in changes in the infra-red spectrum of the reacting mixture. It has been attempted to apply this technique to similar reflux reactions between silica gel and the hydroxides of table 1.02, with the exception of $\text{Ni}(\text{OH})_2$, $\text{Fe}(\text{OH})_2$, $\text{Co}(\text{OH})_2$ and $\text{Mn}(\text{OH})_2$, all of which are oxidised by molecular oxygen and must therefore be handled in an inert atmosphere, the maintenance of which during prolonged refluxing is a matter of some experimental difficulty. It has, however, been shown that, in the case of $\text{Fe}(\text{OH})_2$, the stability of the C_6 -hydroxide is enhanced in the presence of colloidal silica (17): this may occur via an adsorptive process.

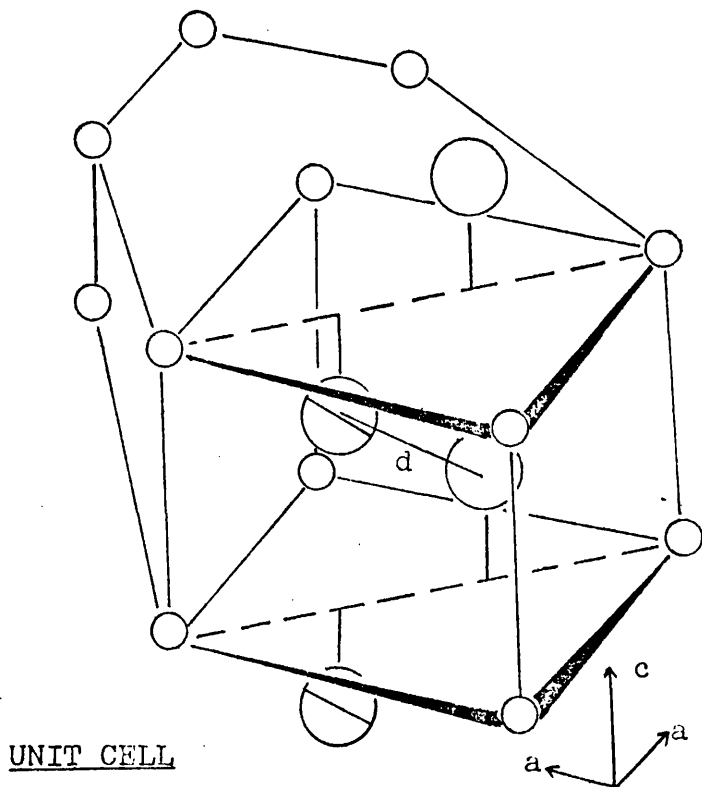
In this study the emphasis is on recognizing the occurrence of the initial adsorptive process and the characterisation, if possible, of the initial adsorbate: subsequent recrystallization of this adsorbate to form a true layer silicate has not been shown to occur in all cases.

Higher reaction temperatures may be achieved at atmospheric pressure by using saturated salt solutions as the reaction medium.

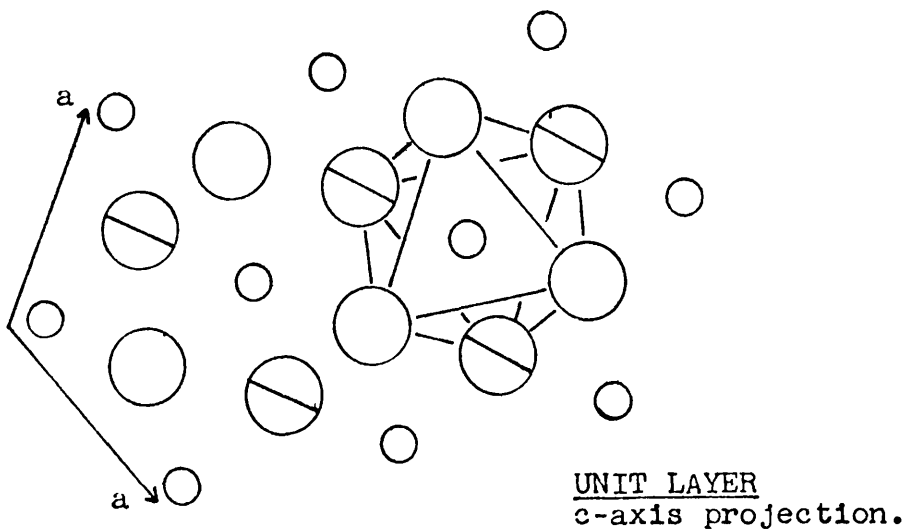
In this way, it was reported (18) that a phlogopite-like material could be prepared by reaction of $\text{Mg}(\text{OH})_2$ with Pyrex in saturated K_2CO_3 solution. Similar reactions have been here attempted, and the product, which was not a mica, is believed to be an entirely new phase, a preliminary report on which is included.

FIGURE 1.1

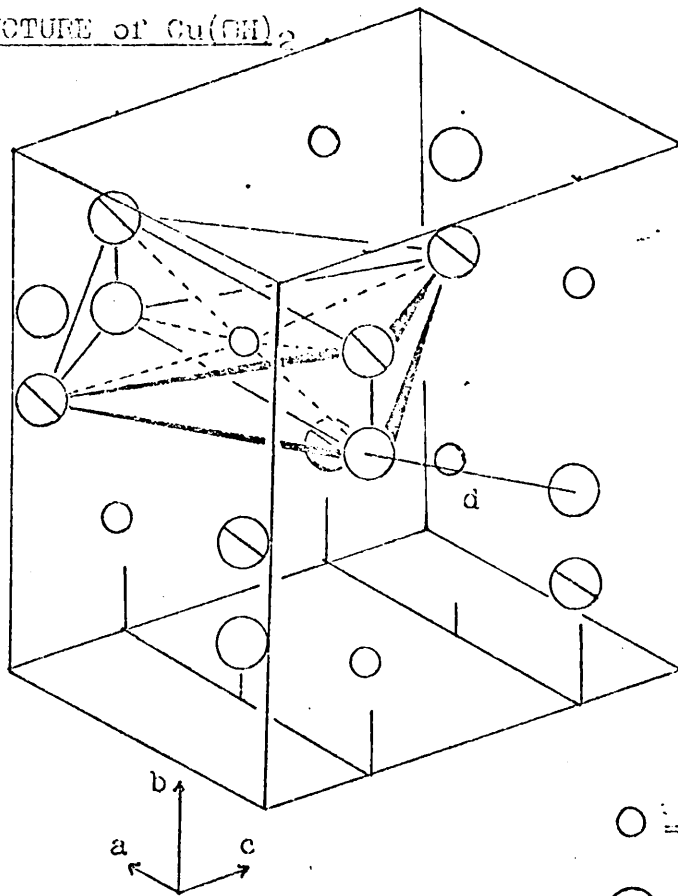
C₆ - STRUCTURE OF METAL HYDROXIDES M(OH)₂



- = metal ion in $(0,0,0)$.
- = hydroxyl ion in $(\frac{2}{3}, \frac{1}{3}, +z)$.
- = hydroxyl ion in $(\frac{1}{3}, \frac{2}{3}, -z)$.
- d = interlayer OH—OH distance.



STRUCTURE of $\text{Cu}(\text{OH})_2$



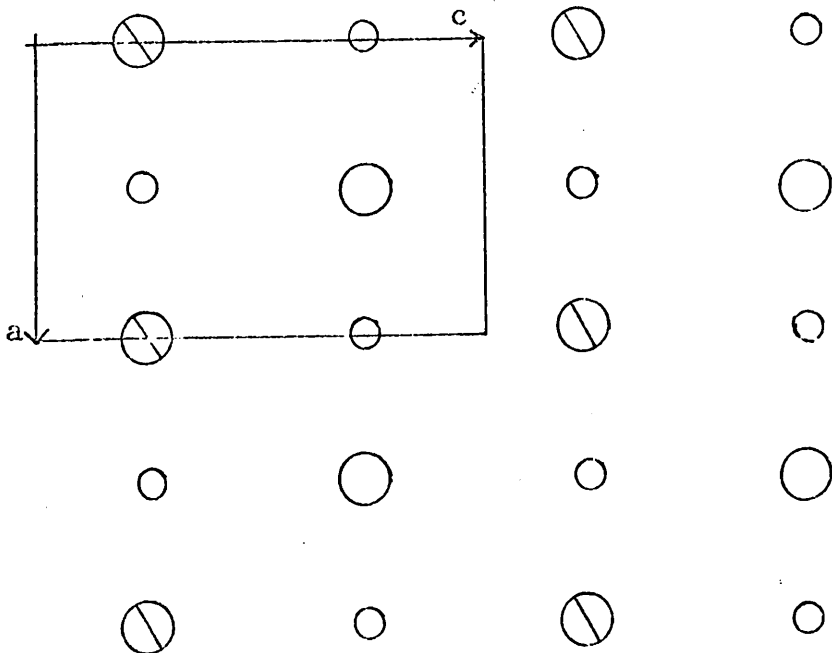
UNIT CELL
Showing
distorted
co-ordination
octahedron.

○ = Copper ion

○ = OH ion, layer
surface

○ = OH ion, intra-
layer

d = interlayer
OH OH distance.



TOP of UNIT LAYER, b-axis projection.

TABLE 1.01.

Examples of Natural Layer Silicates.

Kaolinite	Diocahedral, 1:1
Crysotile	Triocahedral, 1:1
Pyrophyllite	Diocahedral, 2:1
Talc	Triocahedral, 2:1
Hectorite	Triocahedral, 2:1 with Li-for-Mg substitution, octahedral layer.
Montmorillonite	Diocahedral, 2:1 with Al-for-Si substitution, tetrahedral layers.
Micas	Di- and Tri-octahedral: 2:1 with 1 in 4 tetrahedral layer ions being Al ³⁺ , Fe ³⁺ substitution also common.
Chlorites	Wide range of above units with interstratified octahedral layers.
Tobermorites	Distorted triocahedral layer with silicate dreierketten on either side.

TABLE 1.02

Metal Hydroxide Crystal Structure Data.

Ref.	Species	Space Gp.	a	b	c	d
3,7	Ca(OH) ₂	P $\bar{3}$ m1 (H)	3.59		4.90	3.33*
4	Mn(OH) ₂	P $\bar{3}$ m1 (H)	3.34		4.68	3.24*
3	Mg(OH) ₂	P $\bar{3}$ m1 (H)	3.15		4.77	3.22*
4	Co(OH) ₂	P $\bar{3}$ m1 (H)	3.18		4.65	3.18*
5	Ni(OH) ₂	P $\bar{3}$ m1 (H)	3.13		4.61	3.10*
6	Fe(OH) ₂	P $\bar{3}$ m1 (H)	3.26		4.61	3.05*
5	Cd(OH) ₂	P $\bar{3}$ m1 (H)	3.50		4.70	2.98*
9	Cu(OH) ₂	CmCm (O)	2.95	10.59	5.26	2.97*
48	γ -Zn(OH) ₂	Imm2 (O)	23.07	8.04	3.30	2.84**
47	ϵ -Zn(OH) ₂	P2 ₁ 2 ₁ 2 ₁ (O)	5.17	8.54	4.93	2.83***
10,11	γ -AlOOH	AmAm (O)	12.24	3.69	2.86	2.70*
14	γ -FeOOH	AmAm (O)	12.51	3.87	3.06	2.70*
5	β -Be(OH) ₂	P2 ₁ 2 ₁ 2 ₁ (O)	4.61	7.02	4.52	2.67***

a, b, c - lattice parameters (\AA)

d - OH - OH distance, \AA (* = interlayer, ** = inter-chain, *** = between tetrahedra)

H - Hexagonal

O - Orthorhombic

CHAPTER 2. HECTORITE.

2.1 Introduction.

The synthesis of Hectorite under reflux conditions has been the subject of much study (1, 15, 19). The purpose of the present work is to explore the reaction by infra-red spectrophotometry and to relate the spectra to observations made by other techniques, in the hope of finding a means of examining the characteristics of reactions, described in later chapters, with less crystalline products.

2.2 Experimental.

A slurry containing approximately 10% solids by weight was made up with $Mg(OH)_2$, silicic acid and LiF in the proportions $SiO_2:MgO:LiF = 1.5:1.0:0.01$ to satisfy the formula of a natural hectorite, $Si_8(Mg_{5.34}Li_{0.66})O_{20}(OH)_4$. and refluxed in a polypropylene flask for some days at pH 10. Adjustment of the pH was effected by adding small quantities of solid LiOH. Samples of the reaction were taken at regular intervals (Table 2.01) and freeze-dried. Infra-red spectra in the region $4000 - 300\text{ cm}^{-1}$ were recorded, using KBr pressed discs, on a Perkin-Elmer 457 double-beam grating spectrophotometer. Where the use of a heating stage was desired, spectra were run on the more advanced Perkin-Elmer 225. Samples were prepared for

TABLE 2.01.

Run 7 Sample Times.

Sample	Time (mins)	(hours)	(days)
7.01	6		
7.02	60	1	
7.03	119	2	
7.04	180	3	
7.05	240	4	
7.06	303	5	
7.07	359	6	
7.08	420	7	
7.09	480	8	
7.10	575	9.5	
7.11	630	10.5	
7.12	690	11.5	
7.13	756	12.5	
7.14	1443	24	1
7.15	2175	36	
7.16	2901	48	2
7.17	4840	81	3.4
7.18	6509	108	4.5
7.19	8659	144	6

electron microscopy by washing on the centrifuge, and mounting on carbon-film covered copper grids using the droplet technique. Electron micrographs were taken on a Siemens Elmiskop 1A Electron Microscope with double condenser lenses, thin-film apertures and a liquid-nitrogen-cooled anti-contamination stage.

$\text{Mg}(\text{OH})_2$ was freshly precipitated from AnalaR $\text{MgCl}_2 \cdot 6\text{H}_2\text{O}$ solution by addition of AnalaR ammonia solution, washed several times with distilled water, and freeze-dried. The residual water content of the dry powder was estimated by weight loss, complexometry and ion exchange and was taken into account in the preparation of the reaction slurry.

AnalaR LiF, LiOH and Mallinkrodt 100 mesh Silicic acid were used.

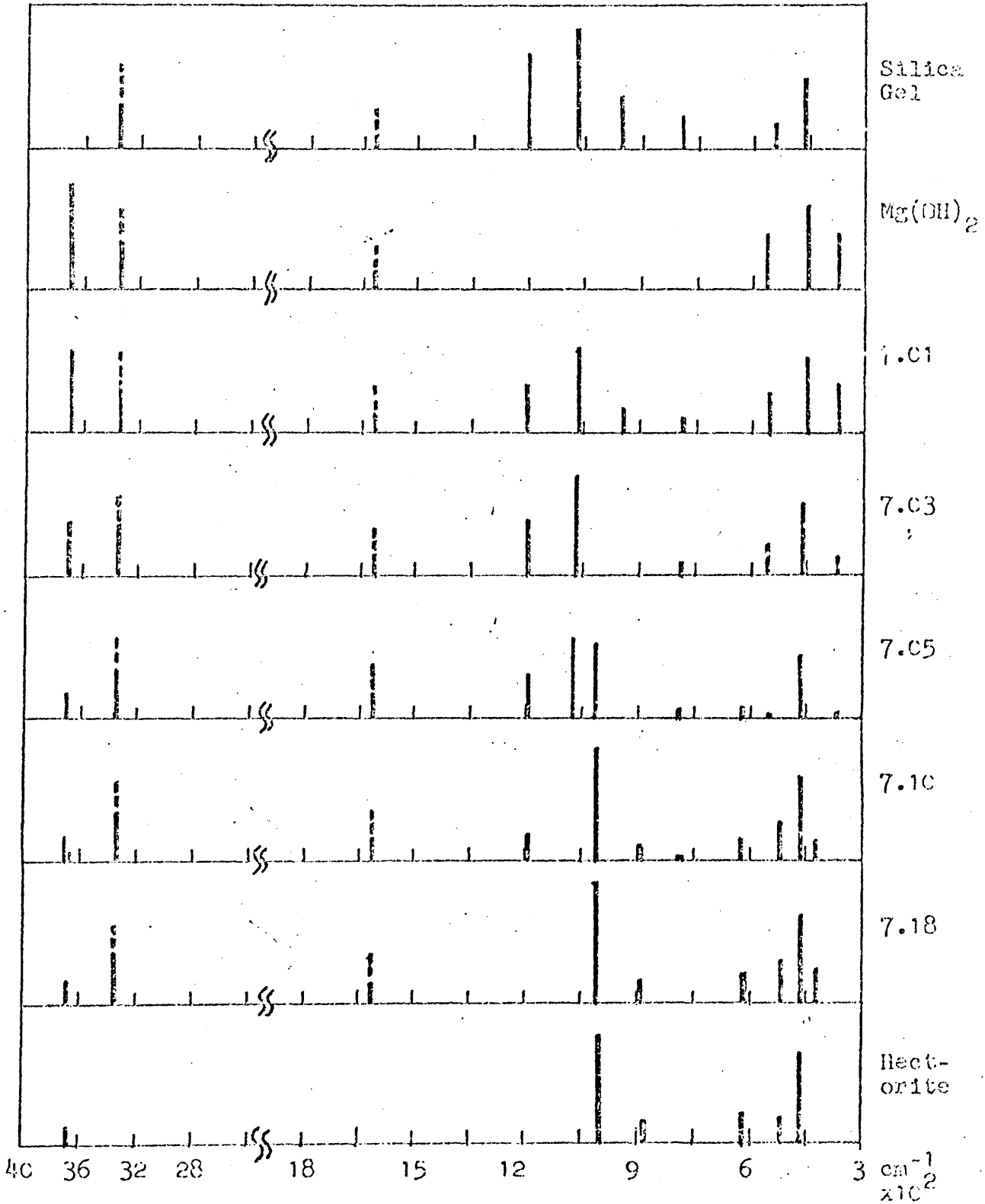
2.3 Results and Discussion.

The infra-red spectra of samples from the reaction are displayed in figure 2.1 in the form of line drawings, in which the length of each line is a measure of the maximum absorbance of each band. Bands of variable intensity due to the absorption of free water molecules occur at 3400 and 1620 cm^{-1} . The spectra of the starting materials and of a natural hectorite (after Farmer, (20)), are also presented.

Before discussing the changes apparent in the spectra, it is important to note that the bands displayed are broad and almost invariably overlap, leading to uncertainties in the positions

FIGURE 2.1

Infra-red Spectra of Samples from Run 7.



of the absorption maxima and in most cases to serious errors in the estimation of absorption intensities. The only sharp bands are those occurring around 3700 cm^{-1} , due to stretching of free hydroxyl groups.

The shapes of the broad overlapping bands, especially in the Si-O stretching region ($1300 - 700\text{ cm}^{-1}$), are useful as an indication of the state of bonding of the silicate anions, and the recorded spectra of the main starting materials, an intermediate stage, (sample 7.05), and a typical product (sample 7.18) are displayed in figures 2.2 to 2.5 respectively. Amorphous silica gel has its main Si - O stretching frequency at 1080 cm^{-1} , and the band is very broad. Ordering of the silicate anions, as sheets or as single ions adsorbed onto a substrate, leads to narrowing of the band and shifting to lower frequencies.

$\text{Mg}(\text{OH})_2$ possesses a single, sharp, very intense O-H stretching band at 3700 cm^{-1} . This band is suitable for semiquantitative treatment, and its decay in intensity during the reaction may be estimated. It is replaced by a much weaker, slightly broader band some 20 cm^{-1} lower in frequency, which may be identified with the higher of the two O-H stretch bands ascribed to Hectorite by Farmer (20). This band is distinguishable in the spectra after

FIGURE 2.2
Intra-red Spectrum of Amorphous Silica Gel

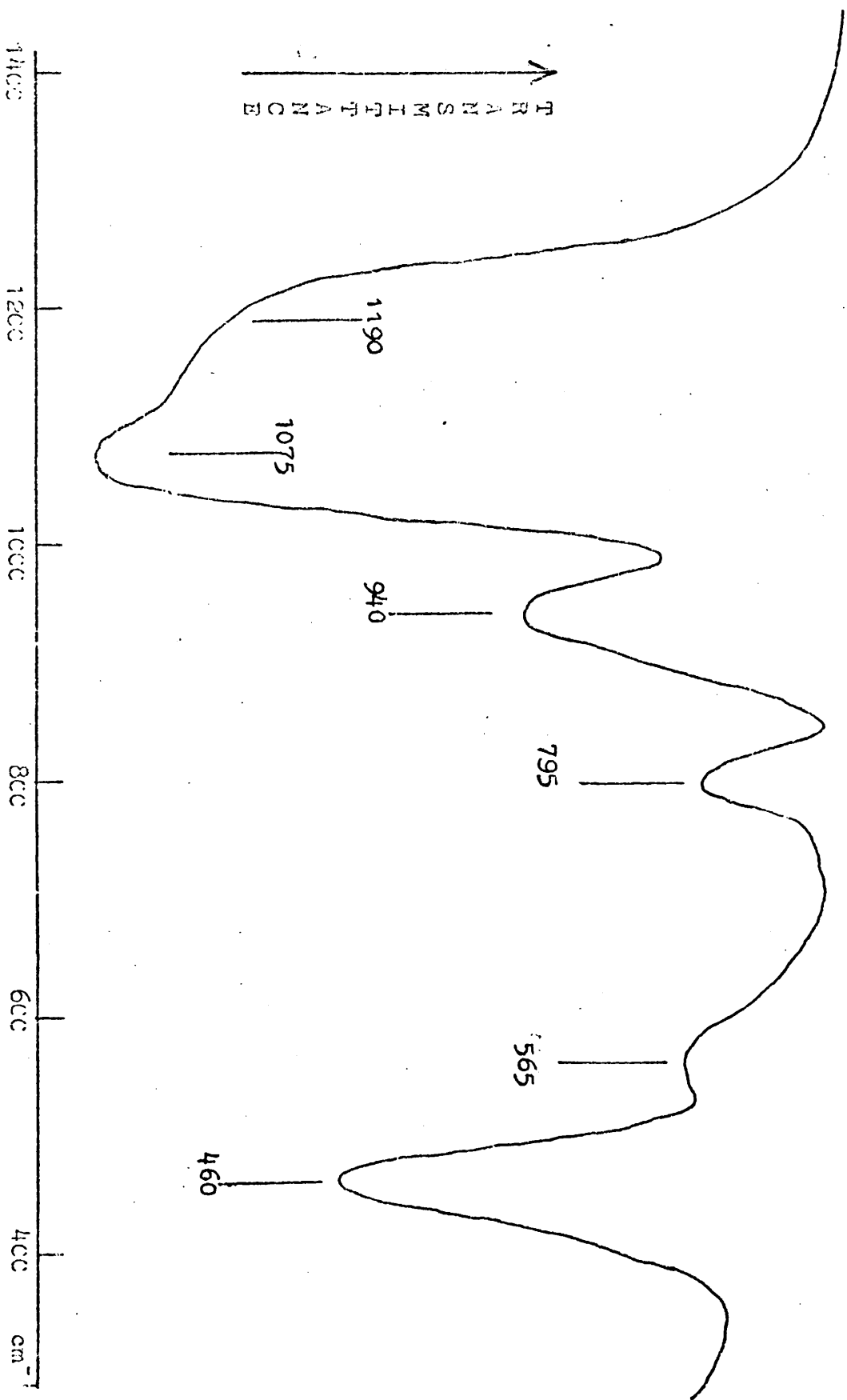


FIGURE 2.3

Infrared Spectrum of $\text{Mg}(\text{OH})_2$

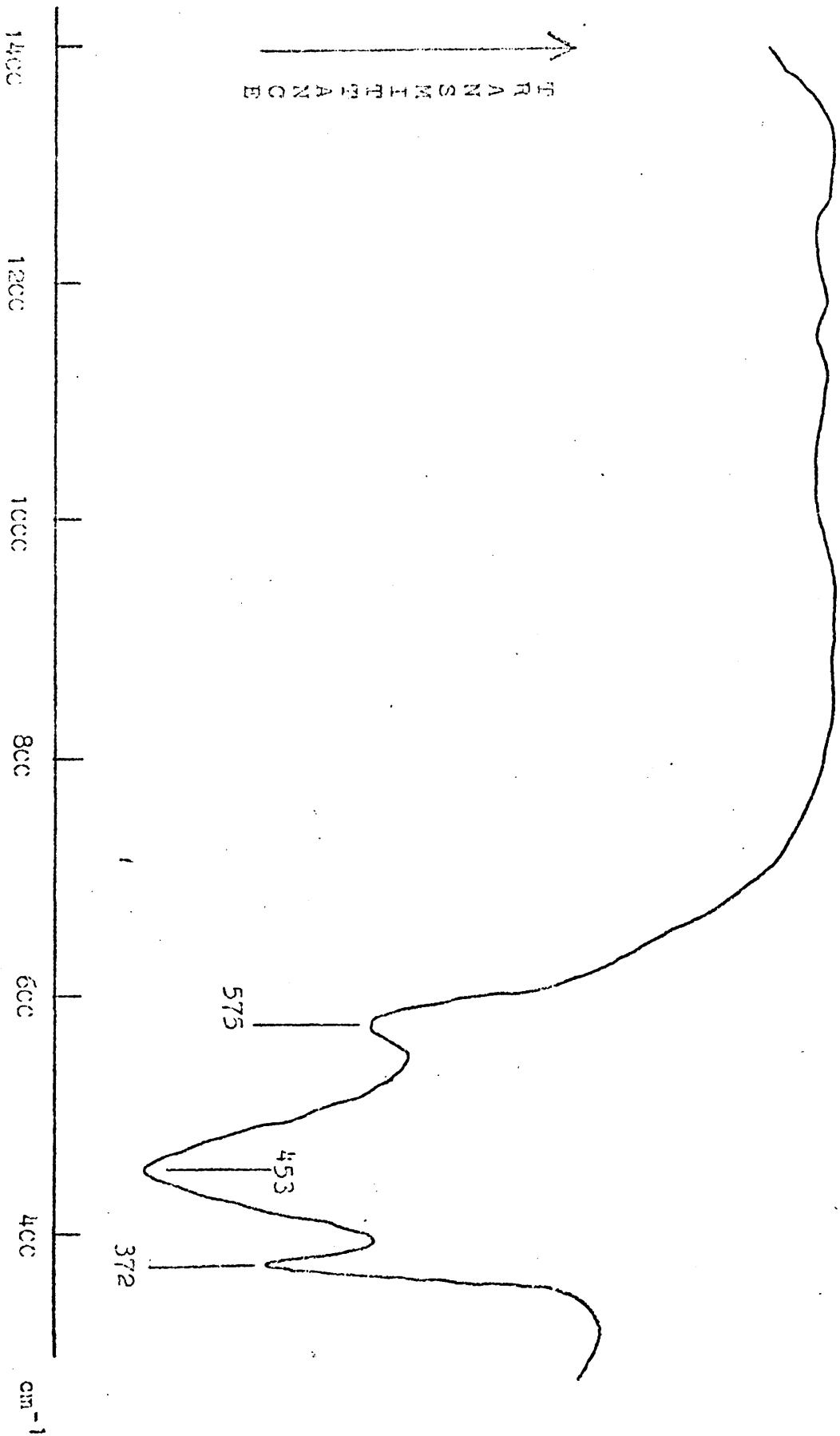


FIGURE 2.4

Infrared Spectrum of Sample 7.05

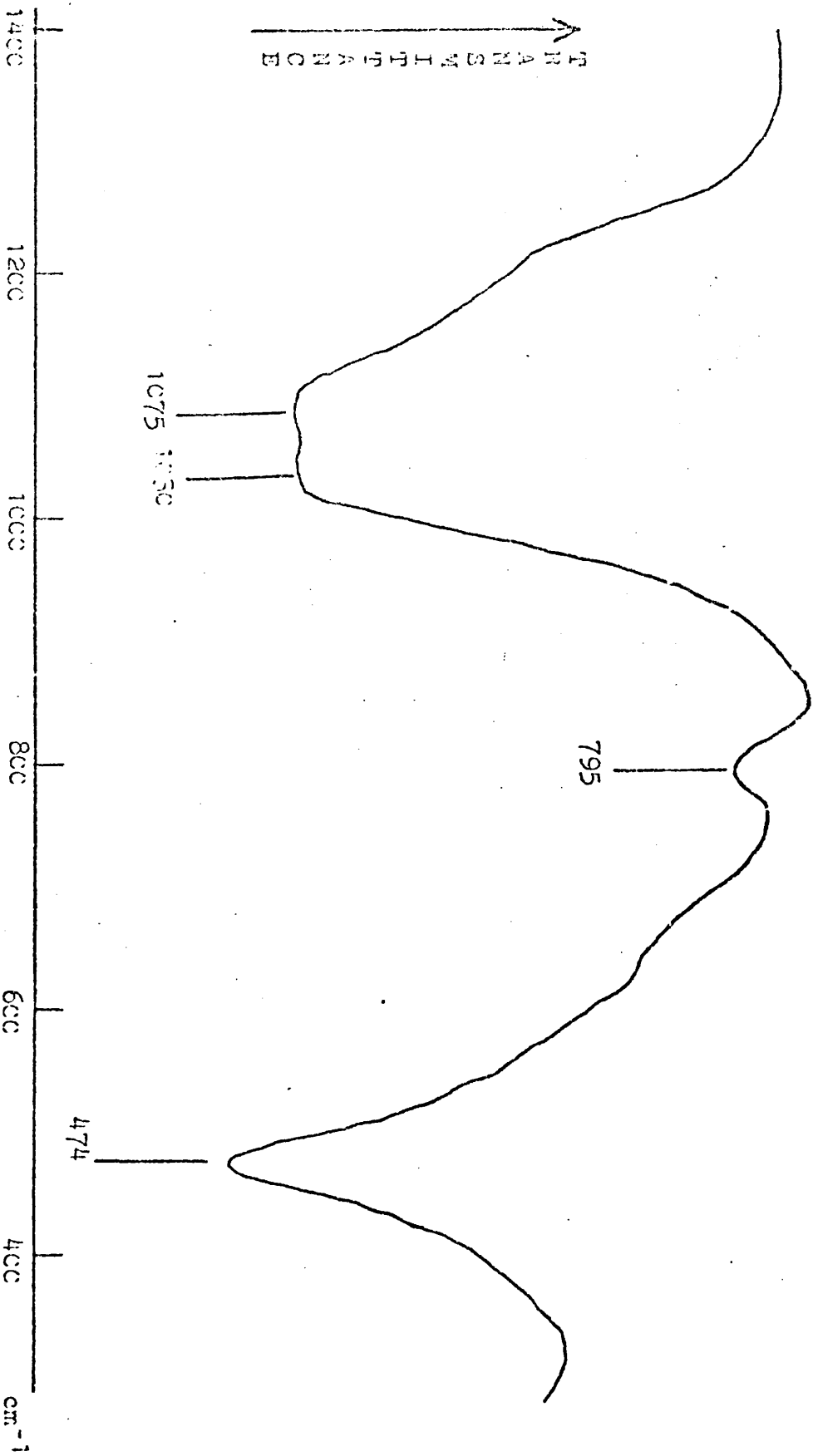
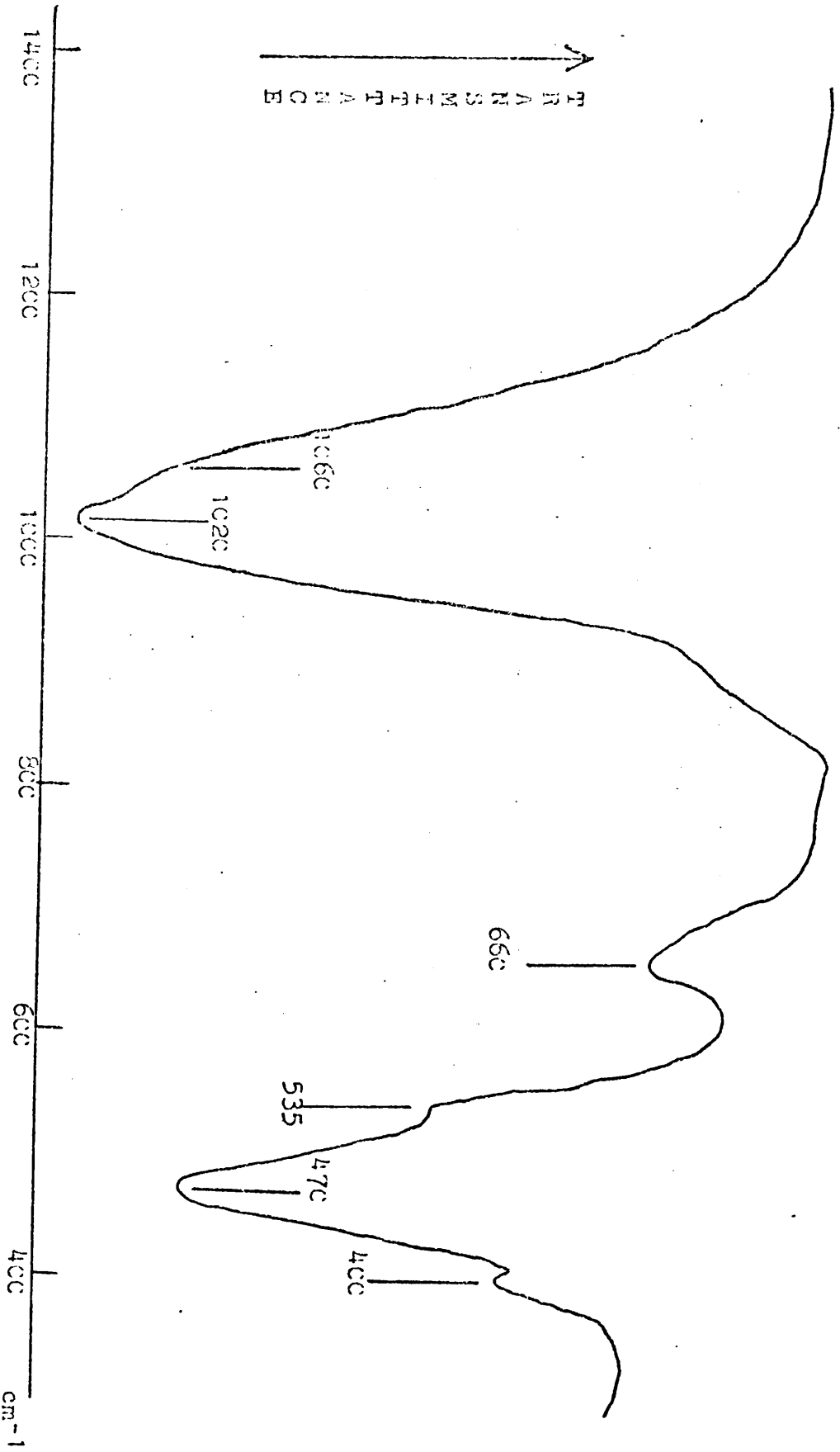


FIGURE 2.5

Infrared spectrum of Sample 7.18



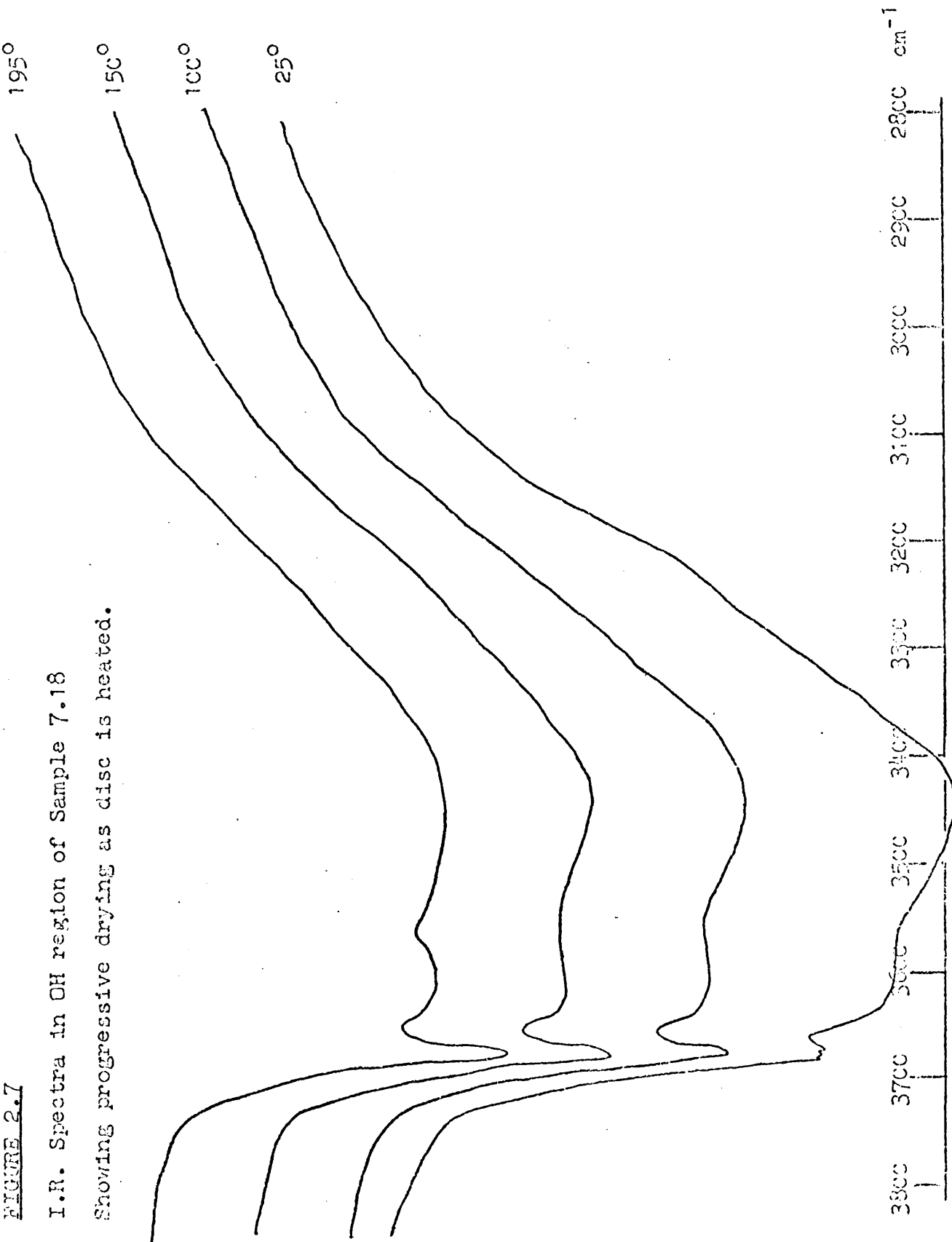
ten hours at reflux and increases in intensity thereafter. The other O-H band, at 3100 cm^{-1} , becomes apparent in later samples and is better resolved on heating the disc to 200°C to effect a partial drying (figure 2.7). It was found that grinding the samples with triethylamine before making up the disc brought about a similar drying, and by this means the 3680 cm^{-1} band could be resolved in samples after six hours at reflux. The use of triethylamine in this way had no other effect on the spectra of the samples, and intensity and absorbance measurements on the 3700 cm^{-1} band were unaffected within the accuracy limits of the measurements. The decay in intensity of the 3700 cm^{-1} band, and the increase in intensity of the 3680 cm^{-1} band, were estimated by the following technique:

Discs containing a known weight of the sample and of KBr were prepared and their spectra recorded. The absorbances of the two bands were measured and converted to the theoretical value expected from a 300 mg. disc containing 1 mg. of sample, denoted $A_{300}/\text{mg.}$, assuming that the absorbances were linearly dependent on the concentration of the sample in the disc and on the disc weight. Repeated measurements showed a standard deviation of $\sim 9\%$, and this was not improved by using the band intensity rather than the absorbance. Grinding was carried out in a vibrating mill to reduce inconsistencies arising from particle

FIGURE 2.7

I.R. Spectra in OH region of Sample 7.18

Showing progressive drying as disc is heated.



size variation.

The results are displayed in figure 2.06 , from which it can be seen that an initial very rapid drop in the intensity of the $\text{Mg}(\text{OH})_2$ band gives way to a more gradual fall, during which the intensity of the Hectorite O -H band rises very slowly. The initial sharp fall is taken to represent an initial rapid coverage of available hydroxide surfaces with silicate ions. Subsequent dissolution of this material, which might be termed "silicated brucite," leads to the formation both of Hectorite and of fresh hydroxide surfaces for adsorption, which therefore proceeds more slowly.

The O-H bending mode of $\text{Mg}(\text{OH})_2$ is apparent as a medium band at 370 cm^{-1} , (figure 2.3). This behaves exactly as the stretch band, vanishing during the reaction and being replaced by a weaker band at 390 cm^{-1} , presumably the O-H bending mode of Hectorite.

Band evolution in the Si-O region is less straightforward. The spectrum of Mallinkrodt 100 mesh silicic acid, figure 2.2, displays a medium band at 950 cm^{-1} due to the Si-O stretching of silanol groups (21). This band is sensitive to the pH of the slurry containing the silica, decreasing in intensity with increasing pH as the silanol groups are progressively deprotonated. Aging of a silica slurry at pH 10 under reflux leads to almost complete removal of this band.

Figure 2.06

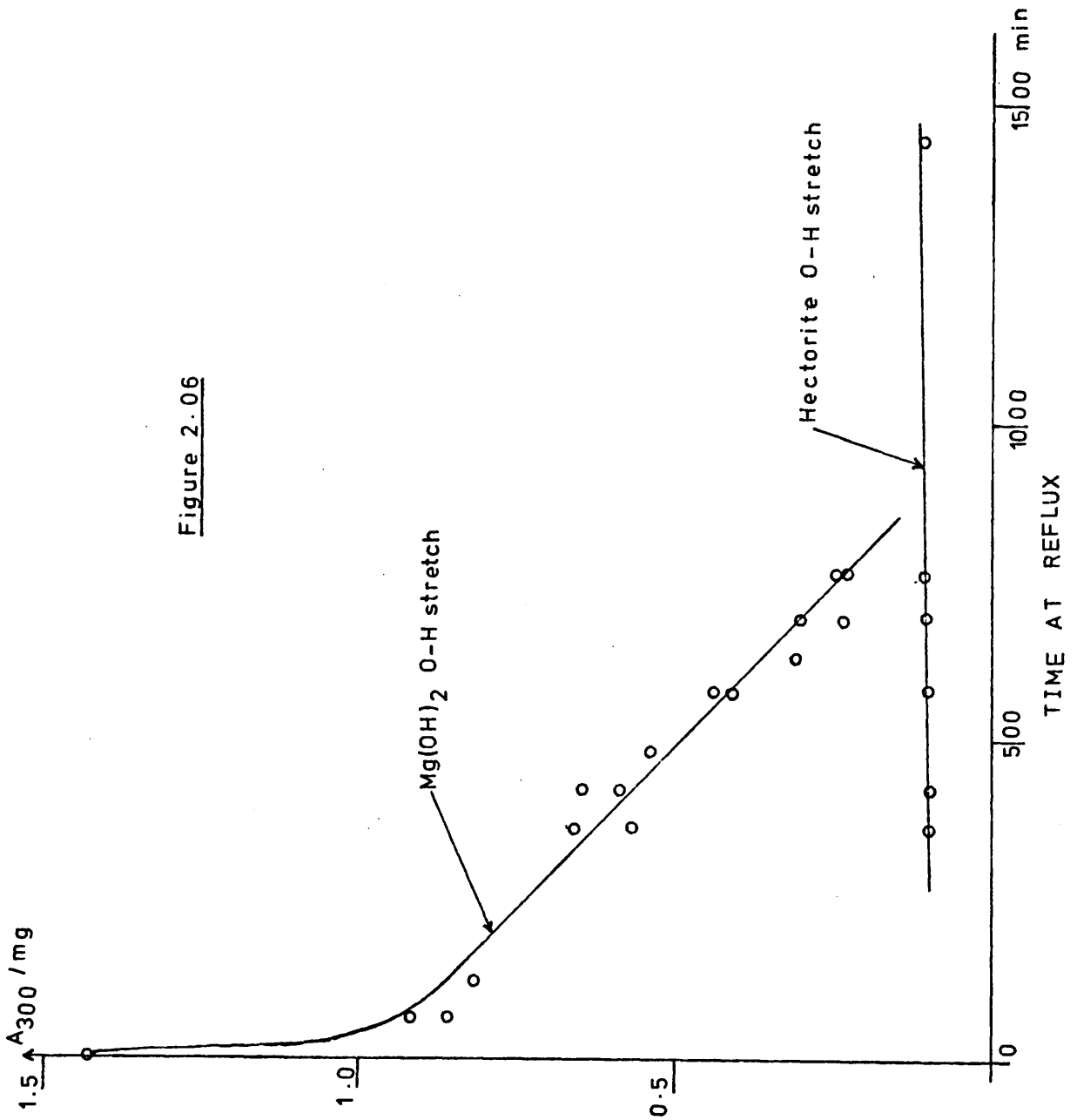
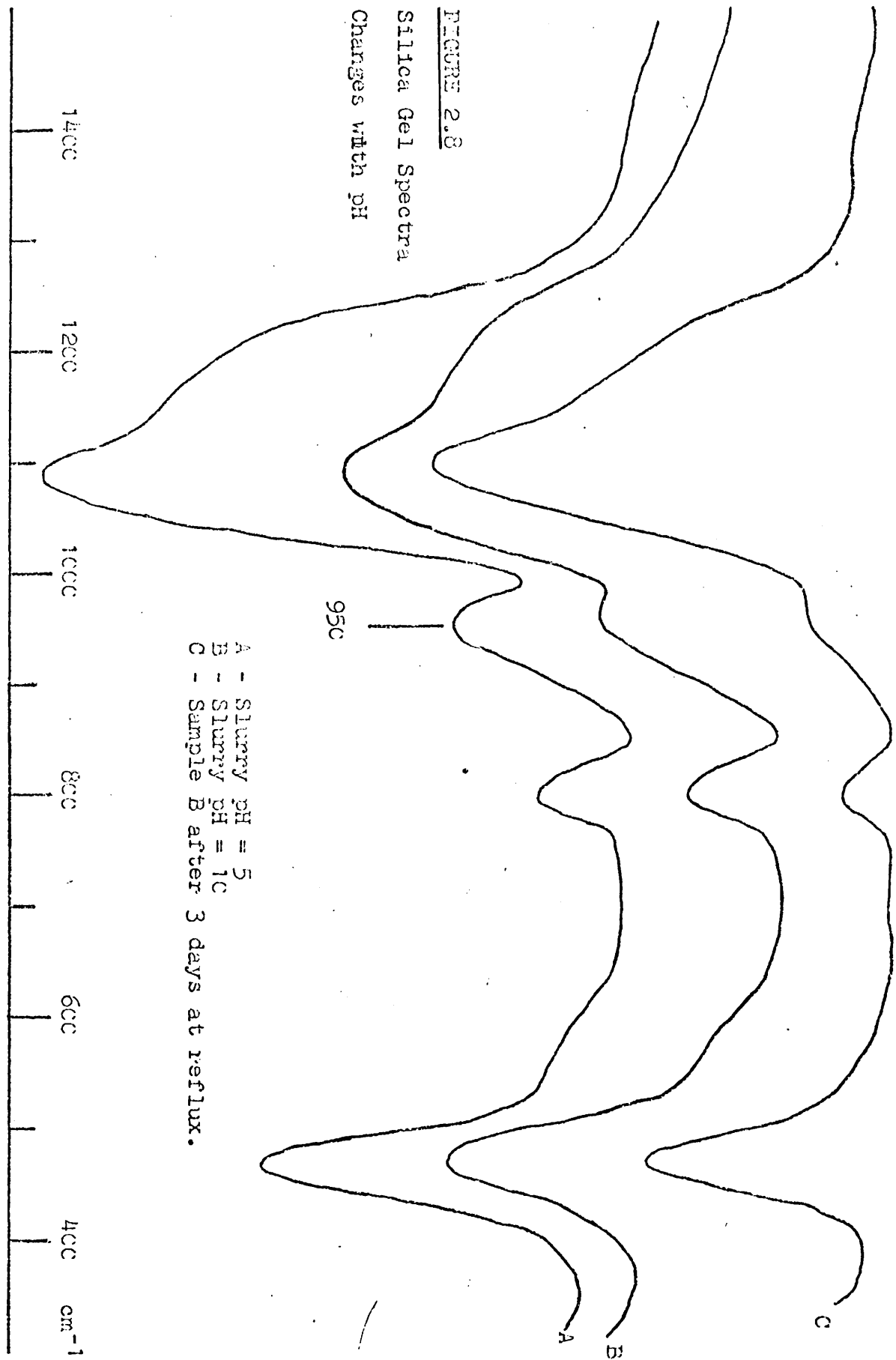


Figure 2.8 shows the spectra of samples taken from silica/water slurries of varying pH values and of a sample taken from a pH 10 slurry after three days at reflux. It will be noted that the weak band at 560 cm^{-1} , hitherto unassigned, shows similar behaviour.

A rough measure of the variation in intensity of the silanol stretch band with pH may be obtained by plotting the ratio of the absorbance of this band to that of the skeletal Si-O band at 470 cm^{-1} , denoted A_{950}/A_{470} , with the pH of the slurry from which the sample was obtained. This is shown in figure 2.9A in the pH range 5 - 10, and appears to have an S-shaped form with the inflexion around pH 8.5. Refluxing of the pH 10 slurry yields figure 2.9B, showing the deprotonation of silanol groups inaccessible, over short periods at room temperature, to the base. The only changes in the spectrum of silica gel on refluxing alone at pH 10, are thus those involving the silanol groups of the gel, skeletal vibrations being unaffected.

During the formation of Hectorite, the rapid deprotonation of the silanol groups of the silica gel is shown by the very early disappearance of the 950 cm^{-1} band (figure 2.1). The principal Si-O stretch band at 1080 cm^{-1} begins to decay and a new Si-O stretch at 1020 cm^{-1} appears. These bands are approximately equally intense by sample 7.05, after four

FIGURE 2.8
Silica Gel Spectra
Changes with pH



- A - Slurry pH = 5
- B - Slurry pH = 10
- C - Sample B after 3 days at reflux.

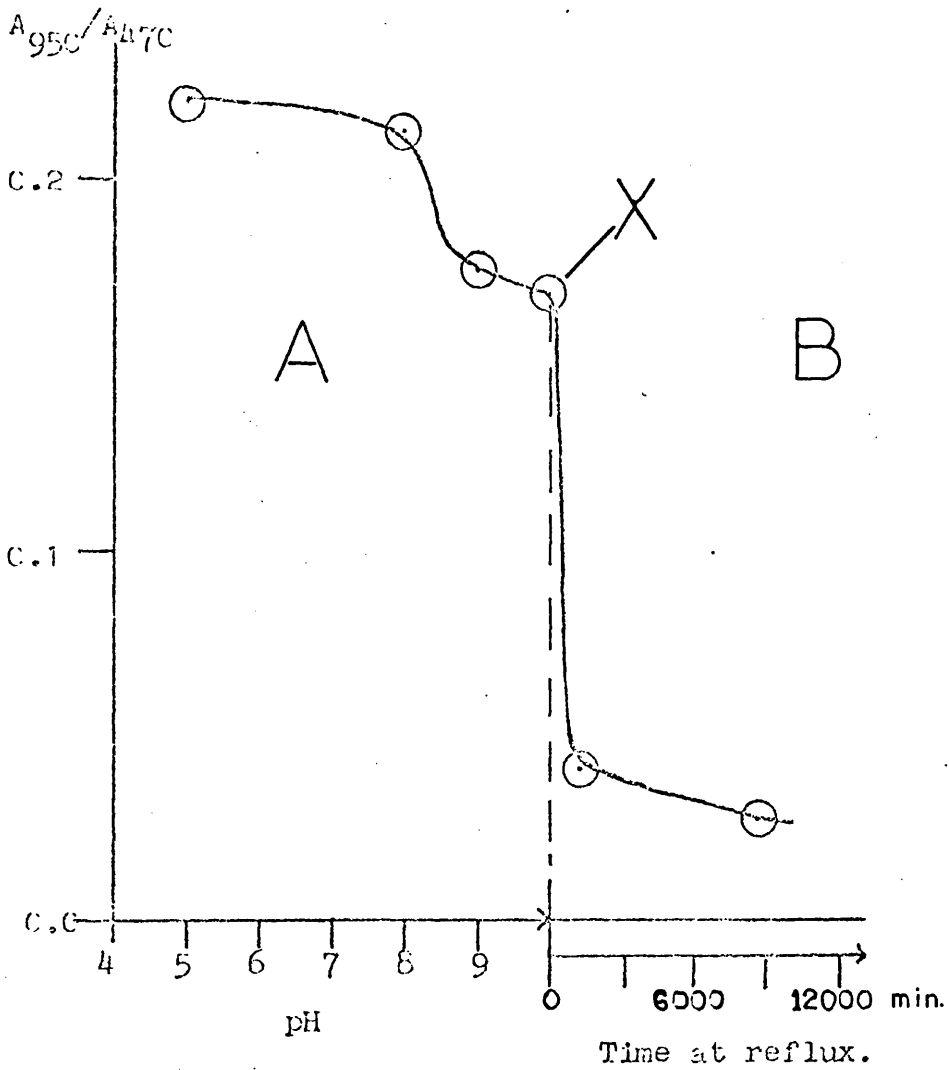


FIGURE 2.9

A - Decrease in Intensity of Si-OH Stretch band (950 cm^{-1}) with pH.

B - Decrease in Intensity of Si-OH Stretch band from pH 10 slurry, with time at reflux.

Point X is common to both graphs.

hours at reflux (figure 2.4). By sample 7.16 the spectrum coincides closely with that of natural Hectorite and the reaction is complete. The development of the O-H librational band at 650 cm^{-1} proceeds in step with that of the O-H stretch band at 3680 cm^{-1} , and it is recognisable as a shoulder by sample 7.05.

Sample 7.18, when shaken with water, formed a sol which could be dried onto polythene sheet and peeled off as a self-supporting film. This film, when exposed to n-butylamine vapour at a pressure of 10 mm. Hg, adsorbed n-butylamine molecules. Examples of the spectra of the films are shown in figures 2.10 to 2.12. Attempts to adsorb pyridine vapour onto the films in order to perform an orientation study such as that of Serratos (22), were unsuccessful.

Electron micrographs of the samples are presented in plates 2.01 to 2.04. The product shows the crumpled-sheet appearance typical of synthetic Hectorites (plate 2.01) and lattice fringe images with a spacing of 1.2 nm. can be obtained in the neighbourhood of the folds (plate 2.02). The selected area diffraction patterns (plate 2.03) of regions of the product show rings corresponding to the known d-spacings of Hectorite. Intermediate samples show regions of broken $\text{Mg}(\text{OH})_2$ crystals interspersed with regions of product, (plate 2.04, sample 7.05) and the SAD pattern shows the presence of both phases. (plate 2.05)

No evidence was found for any regular

Figure 2.10

Sample 7.18 self-supporting film.

A - alone

B - +n-butylamine vapour.

C - n-BuNH₂, liquid film.

OH, NH & CH stretch region.

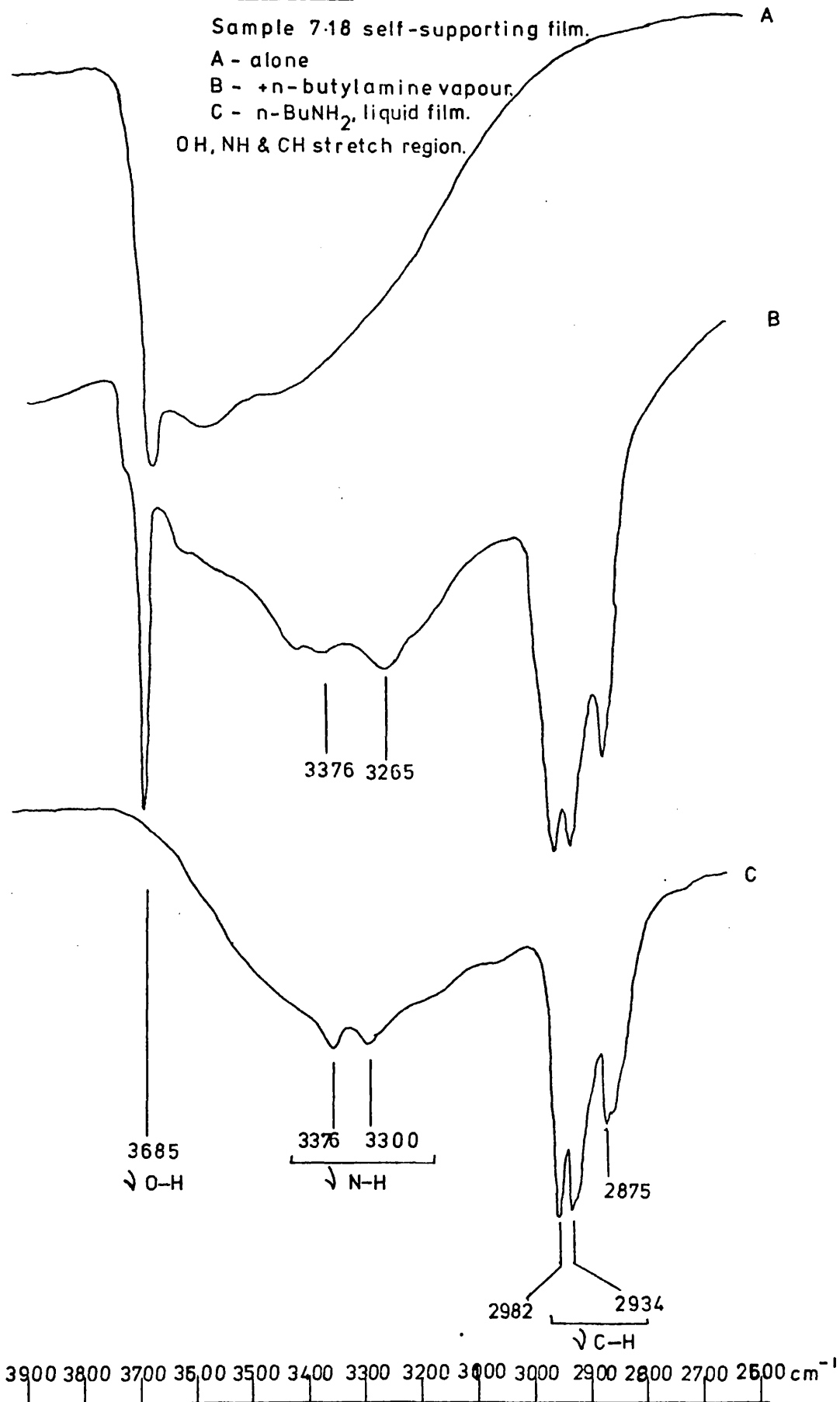


Figure 2.11

As fig. 2.10, deformation region.

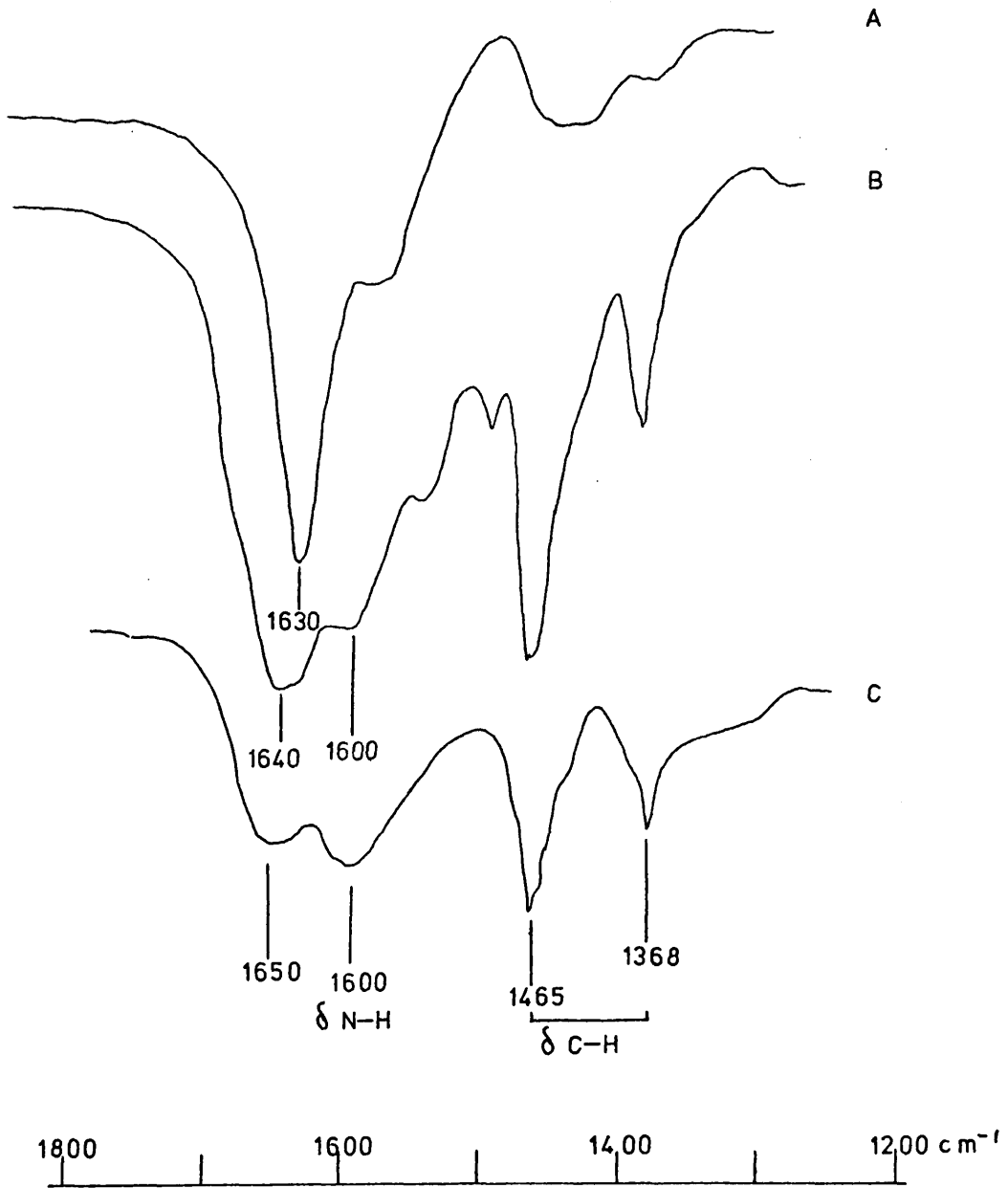
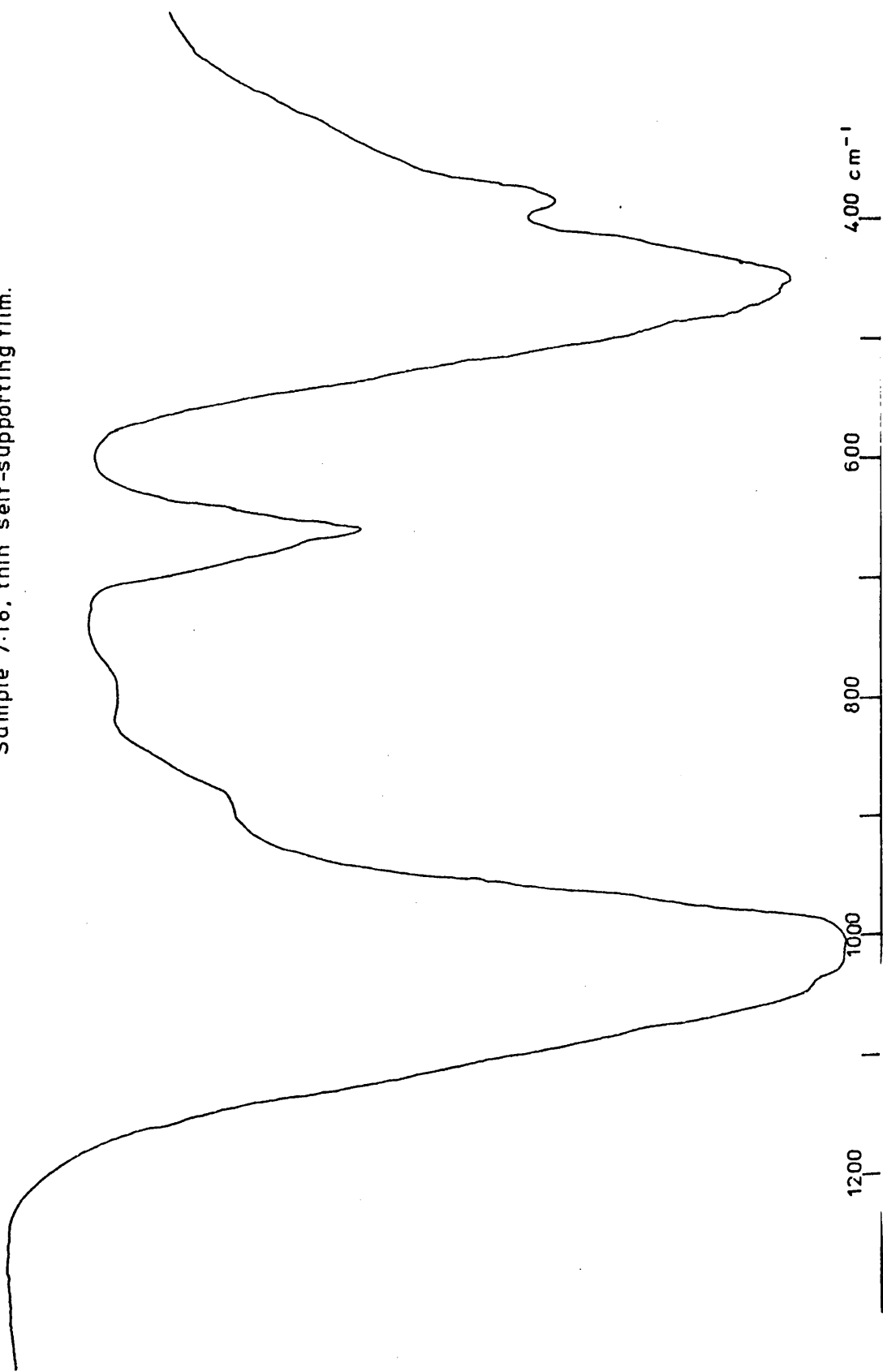


Figure 2.12
Sample 7-18, thin self-supporting film.



intermediate phase such as the "pseudo-smectite" described by Baird et. al. (15). A much lower LiF concentration was used, however, in this work and it may be that the formation of an ordered "pseudo-smectite" requires the presence of substantial amounts of LiF to cause the occurrence of the defect structure described (15).

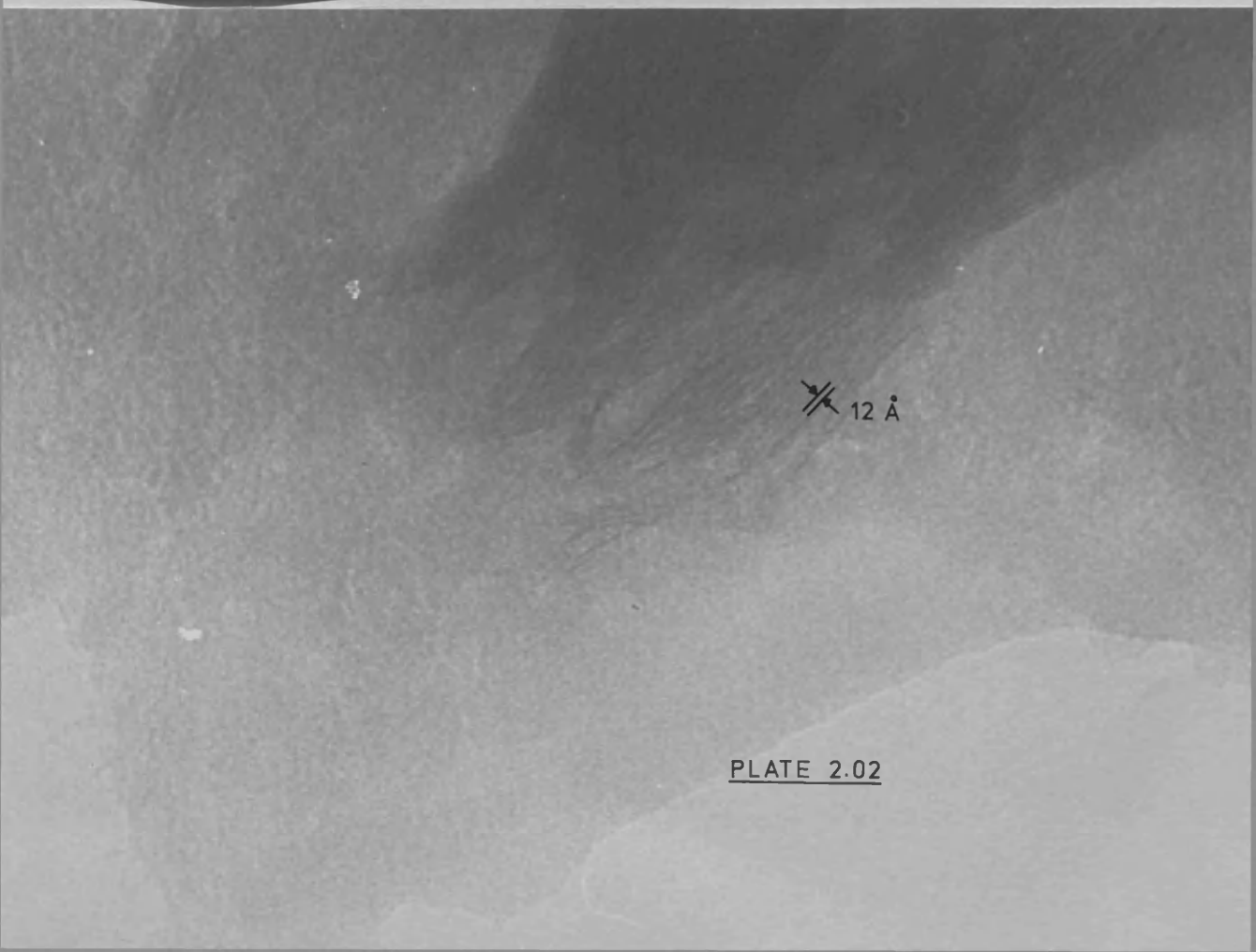
PLATE 2.01

0.25 μ



 12 Å

PLATE 2.02



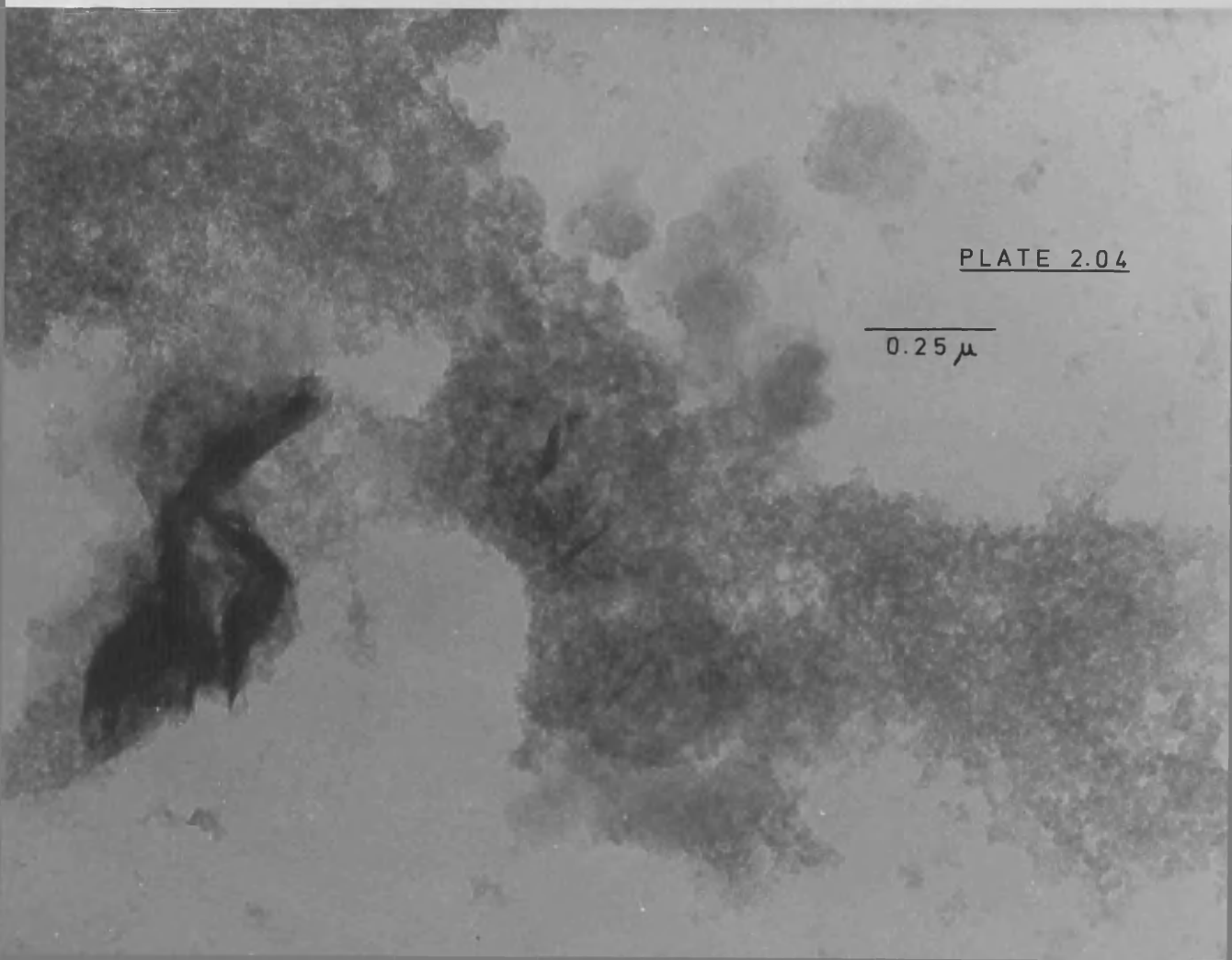
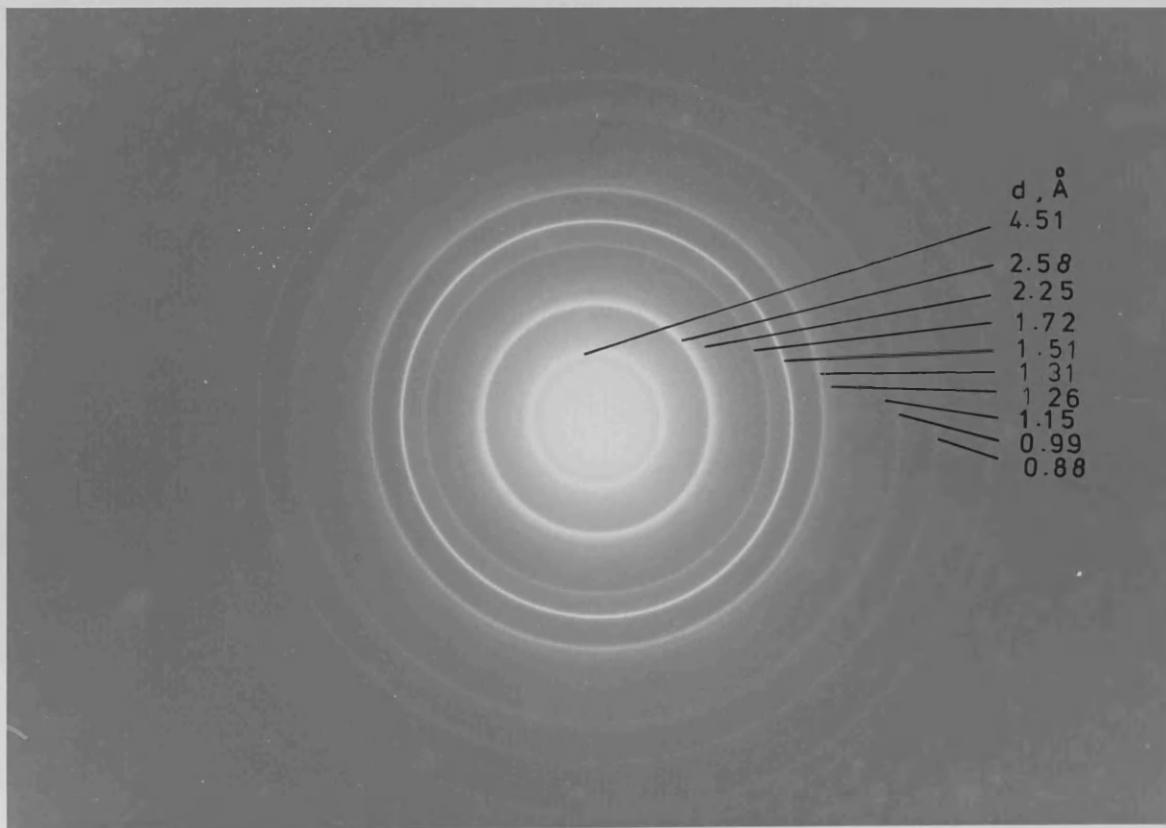


PLATE 2.05

HECTORITE

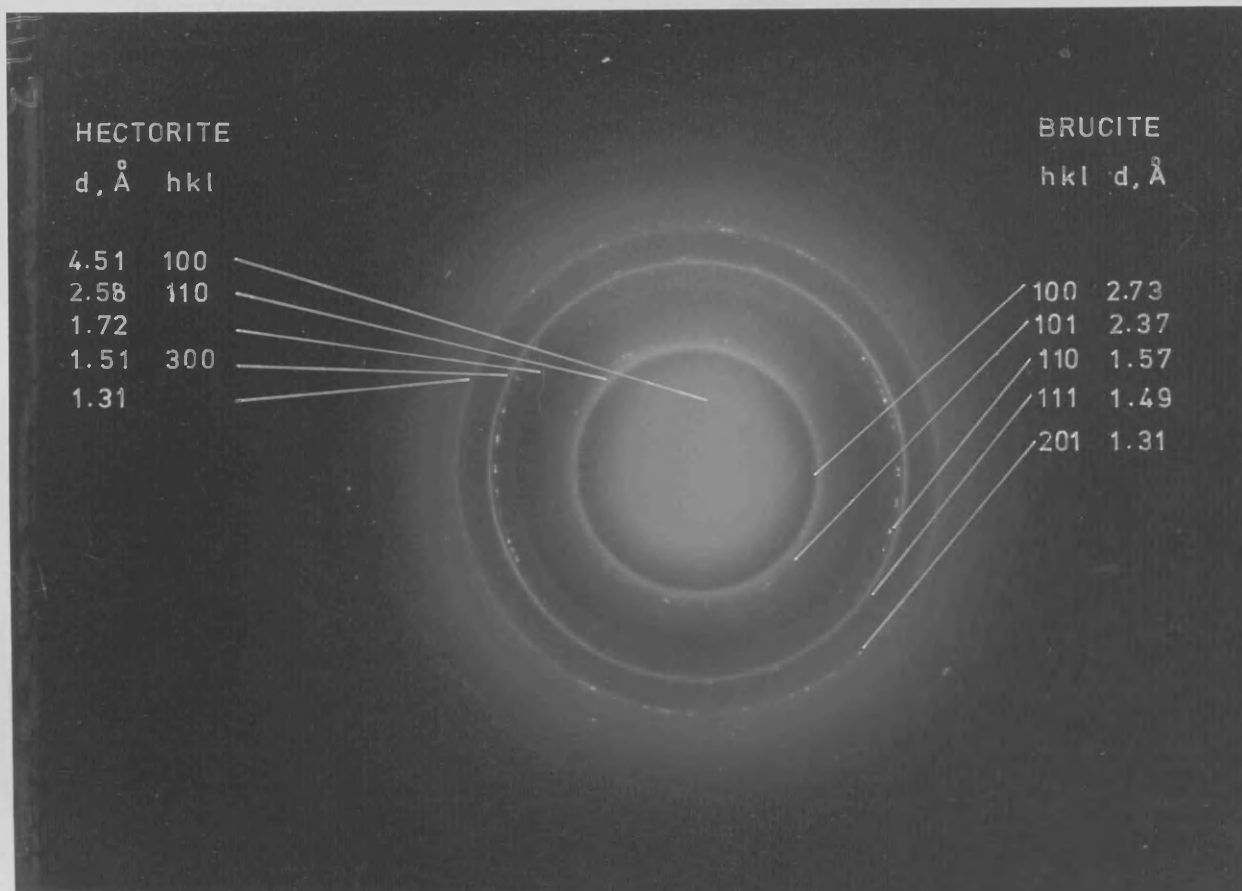
d, Å hkl

4.51 100
2.58 110
1.72
1.51 300
1.31

BRUCITE

hkl d, Å

100 2.73
101 2.37
110 1.57
111 1.49
201 1.31



CHAPTER 3. TOBERMORITE.

3.01 Introduction.

The product expected from reaction of $\text{Ca}(\text{OH})_2$ with silica gel at reflux temperatures is a Calcium Silicate Hydrate Gel (C-S-H gel) similar in structure to the natural mineral Tobermorite. (Appendix I). In the series of experiments described below, it was attempted to follow the same techniques as were applied in Chapter 2 in observing the reaction. Interference from atmospheric carbon dioxide was a serious hindrance in this case, however, and attempts to exclude CO_2 from the reaction mixture were made by a variety of methods outlined in the experimental section. The products of the reactions were shown by electron microscopy to vary widely in crystallinity, but exhibited a remarkable constancy of morphology, which was made the subject of section 3.05, where the relationships among the crystallinity, morphology and CO_2 -content of the gels are discussed.(23)

Monitoring the reactions by infra-red was complicated by the absorption of CO_2 , which continued after freeze-drying of the samples, and a smooth decay of the $\text{Ca}(\text{OH})_2$ O-H stretch could not be observed, in contrast to the results found for $\text{Mg}(\text{OH})_2$. Such conclusions as could be drawn from the spectra are discussed in section 3.03.

3.02 Experimental.

Two series of reactions were made:

(A) with Ca:Si = 5:6, to satisfy the formula of the natural Ballycraigy Tobermorite; and (B) with Ca:Si = 3:4, analogous with the Hectorite run.

Three type (A) experiments were performed.

In the first, run 6, no attempt to exclude CO₂ was made. Ca(OH)₂ was precipitated from calcium chloride solution with aqueous KOH, washed with saturated lime water to remove K⁺ and Cl⁻, freeze-dried and its residual water content estimated as before. The reaction was performed exactly as for Hectorite but no LiF was added. Samples were taken at the times shown in Table 3.01.

In the second, run 20, large crystals of Ca(OH)₂ were prepared by the diffusion method (24) in an attempt to avoid the sensitivity to CO₂ of the microcrystalline precipitate of run 6. A small amount of LiF was added to the reaction mixture. Samples, taken at the times shown in Table 3.01, were freeze-dried without washing and stored in tightly-stoppered sample tubes.

In the third, run 33, more stringent precautions against CO₂ were taken. A large quantity of distilled water was flushed with CO₂-free Nitrogen gas overnight at 90°C, and allowed to cool. This water was used for the preparation of the solutions for the precipitation of

TABLE 3.01.

Sample times for the C-S-H Gel runs.

Time (min.)	Run 6	Run 20	Run 26	Run 27	Run 33
0	6.02		26.00		
20		20.01			
55	6.03				
90			26.01		
115	6.04				
122		20.02			
180	6.05				
243	6.06				
312	6.07				
516		20.03			
362	6.08				33.00
415	6.09				
481	6.10				
485				27.01	
507		20.04			
535	6.11				
668	6.12				
907	6.13				
1352		20.05			
1360			26.02		
1383				27.02	
1442	6.14				
1663		20.06			
1689	6.15				
2833				27.03	
2892	6.16				
4309	6.17				
5148	6.18				
5725		20.07			
6989			26.03		
7363				27.04	
7513	6.19				
8535	6.20				

of microcrystalline $\text{Ca}(\text{OH})_2$ and its subsequent handling. The reflux was performed with a drying tube filled with "Sofnolite". No samples were taken, the reaction being stopped after 6 hours, which was judged on the basis of run 6 to be a suitable time for the formation of a well-crystallized product. Subsequent handling of the product is described in section 3.05.

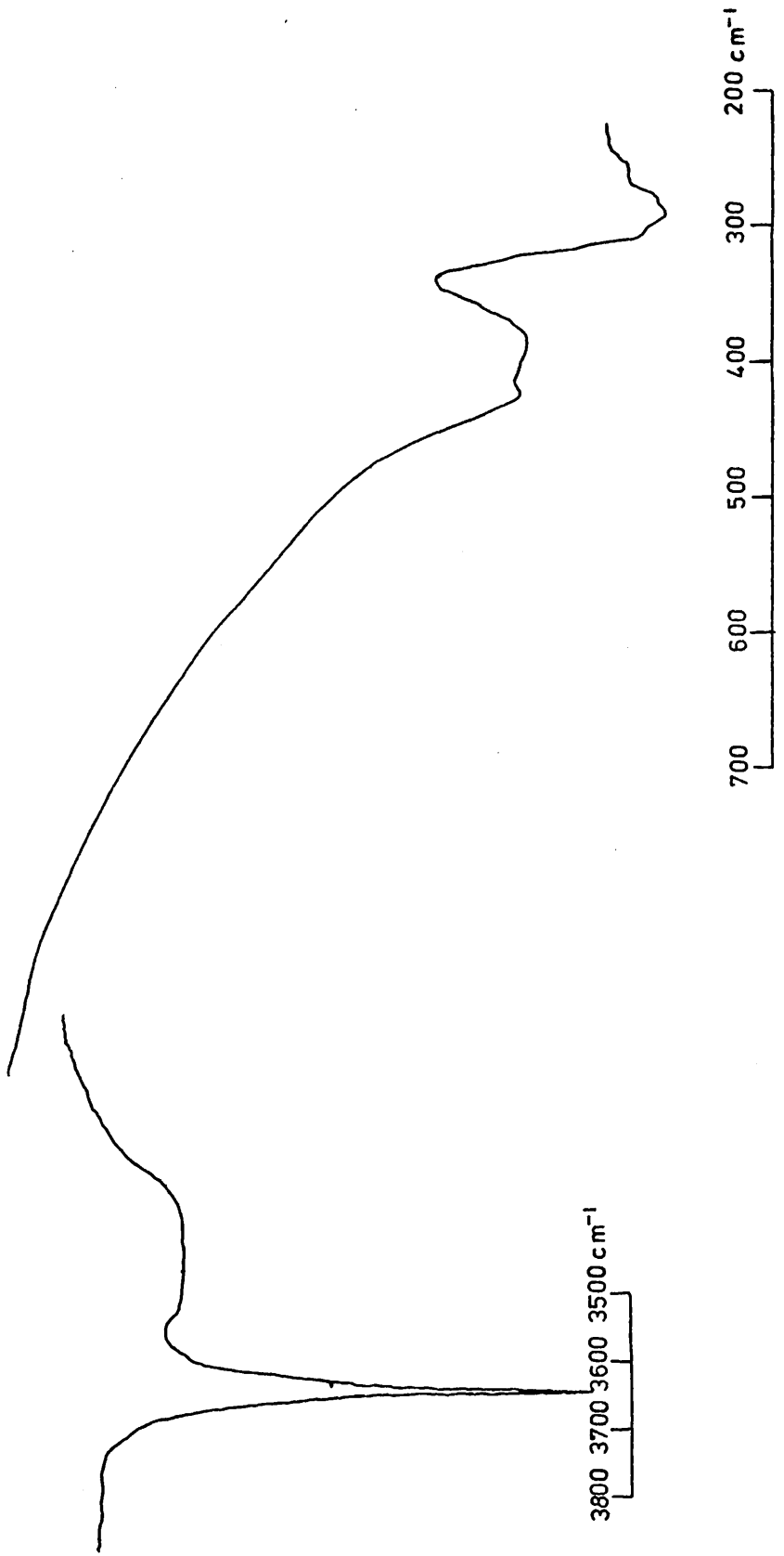
Two type (B) reactions were investigated. Run 26 was identical with run 33 except that samples were taken at the times shown in table 3.01. In run 27, the reflux technique was abandoned and portions of the feed mixture were sealed in 5 ml. glass ampoules and heated in an oil bath at 80°C . The ampoules were shaken at intervals and were opened and worked up at the times shown in table 3.01.

3.03 Results and Discussion - Series A.

The infra-red spectrum of $\text{Ca}(\text{OH})_2$ shows a sharp O-H stretch band at 3645 cm^{-1} . This band, shown in figure 3.01, was, however, not always observed in early samples of the runs, and its decay during silicification was impossible to estimate. The band is extremely sensitive to CO_2 absorption and was not found in samples of bulk commercial grade $\text{Ca}(\text{OH})_2$. A better appreciation of the rate of the reaction could be obtained from electron micrographs of the samples. Thus, in run 6, the unheated feed mixture, sample 6.02, showed the presence of large areas of

Figure 3.01

I.R. Spectrum of Ca(OH)_2



low particle-size material (plate 3.01) similar to C-S-H gel, and the strongest tobermorite reflection, at 3.07 \AA , could be picked up in SAD. After six hours at reflux, sample 6.08, the SAD pattern showed the hk0 rings of a tobermorite, and crumpled-sheet regions of the sample, typical of a tobermorite-like C-S-H gel, predominated. Plate 3.02 shows a good example of this morphology, which persisted unchanged until sample 6.20, by which time the SAD pattern had disappeared and intense absorption near 1450 cm^{-1} in the infrared showed the presence of large amounts of carbonate ion. The subsequent fate of sample 6.08 is described in section 3.05, but for the moment it may be taken as a typical tobermorite-like C-S-H gel.

The spectrum of sample 6.08 in the Si-O region is shown in figure 3.02. It reveals the presence of two distinct Si-O stretch frequencies, at 1020 and 980 cm^{-1} . These bands develop very rapidly, as seen in figure 3.03, in which both can be distinguished in the spectrum of sample 6.03, after 55 mins. at reflux. The 1020 cm^{-1} band appears to reach maximum intensity before the 980 cm^{-1} band, which increases irregularly in intensity throughout the run. It seems that the two bands indicate the presence of two differently-ordered silicate structures, The 1020 cm^{-1} band indicating a disordered or poorly-ordered

Figure 3.02
Sample 6.08

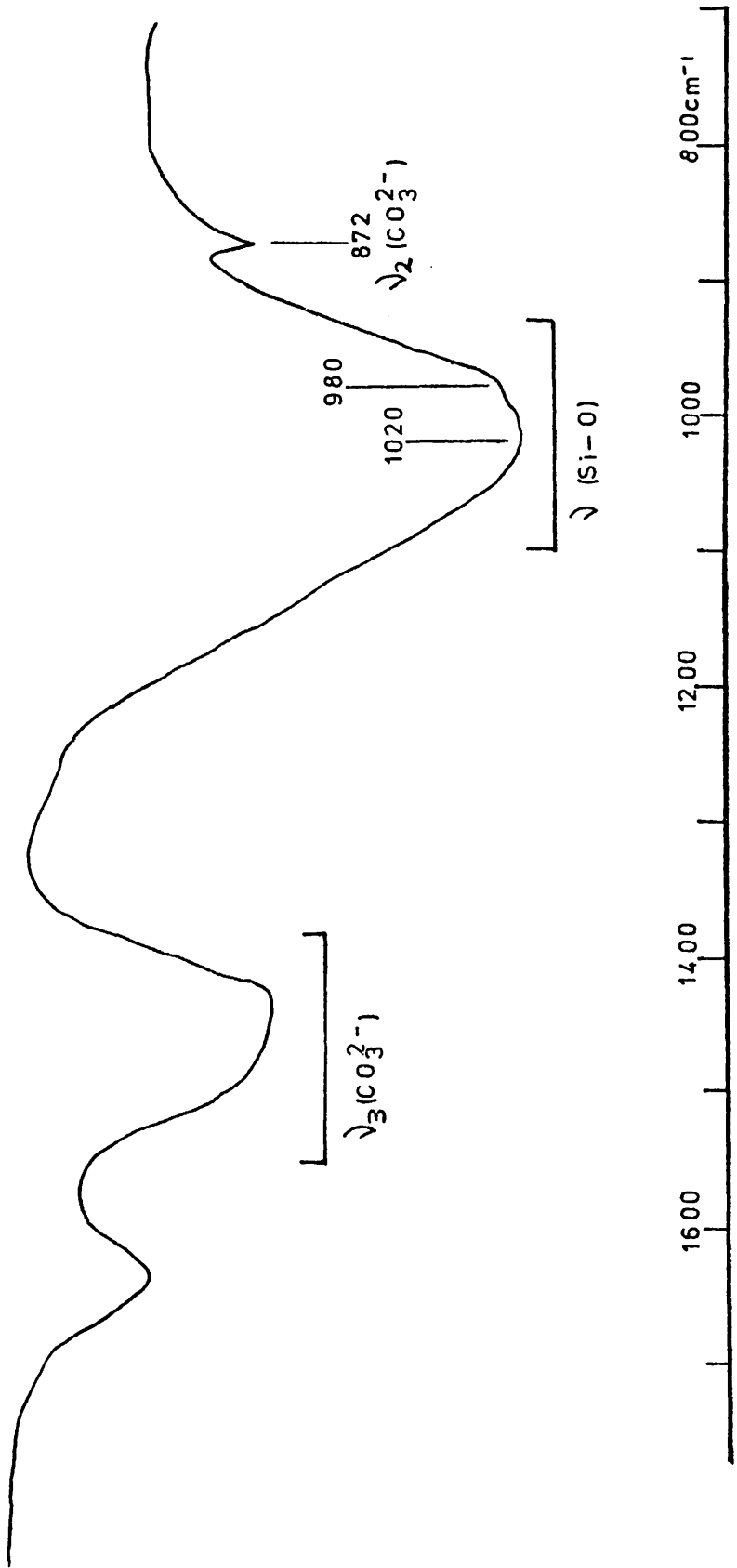
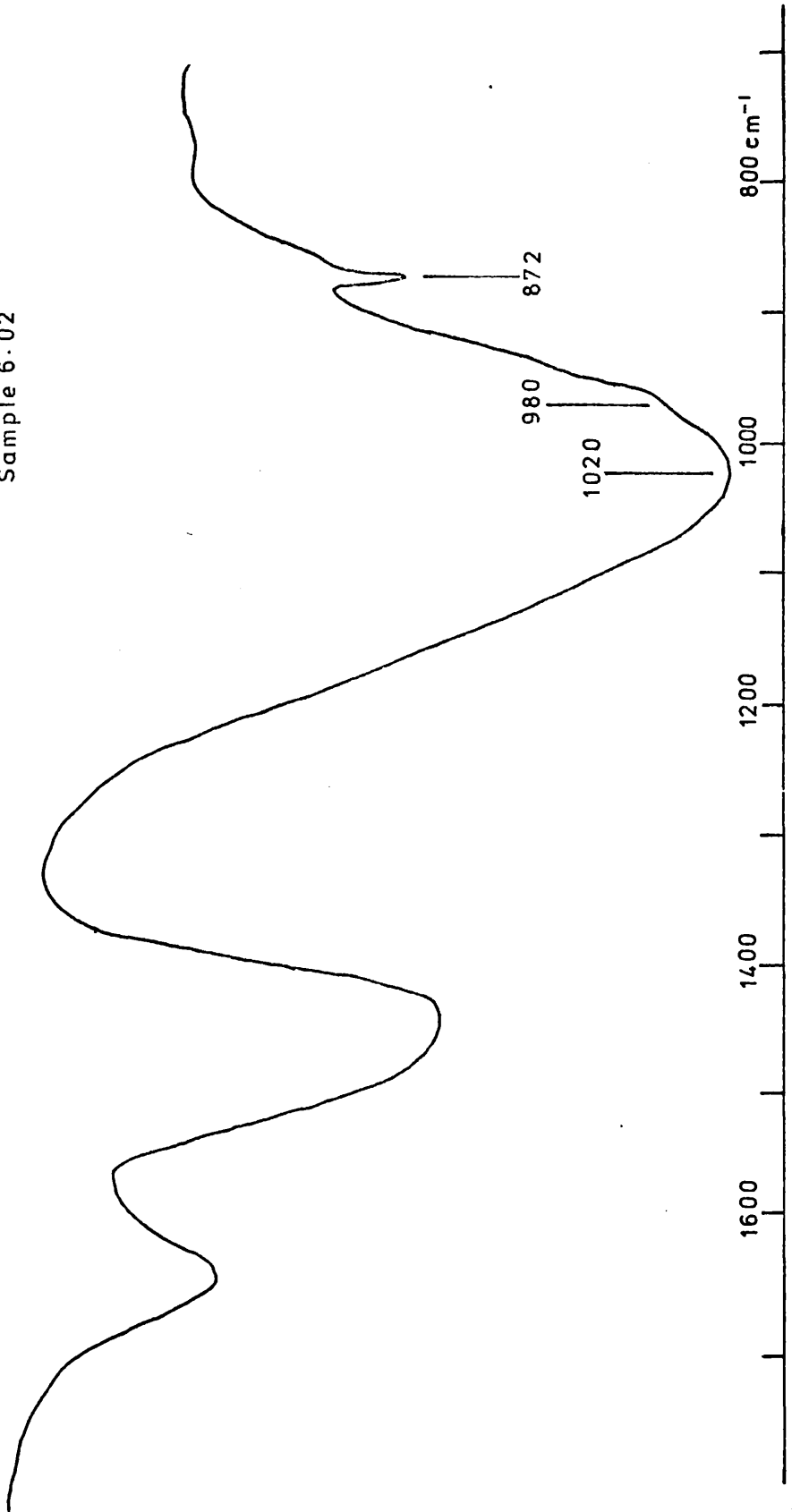


Figure 3.03

Sample 6.02

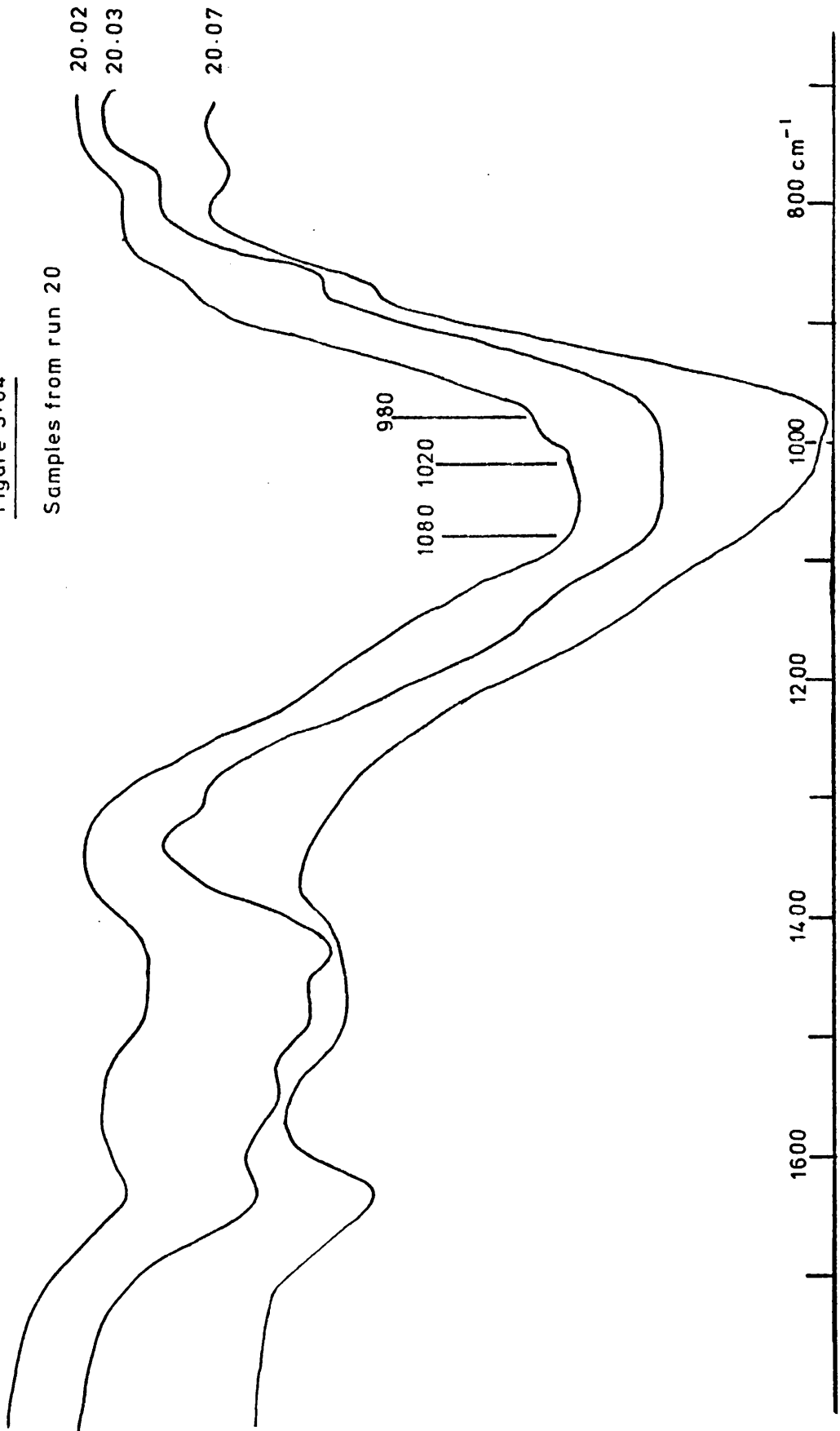


adsorbate, while the 980 cm^{-1} band resulted from the 'dreierketten' structure of Tobermorite chains. No region of the sample could be found in EM which might correspond with the disordered adsorbate, however. Crystals of Calcite, Aragonite and Calcium Hydroxide were the only phases apart from the crumpled foils which could be distinguished in the EM of early samples from run 6, and in later samples only crumpled foils were observed.

Attempts to isolate the system from CO_2 were only partially successful. Figure 3.04 shows spectra obtained from samples from run 20. Of these, 20.03 shows significant contamination but 20.02 and 20.07 have only traces of CO_3^{2-} . Sample 20.02, after 20 min. at reflux, shows the appearance of both the new Si-O bands, and in addition the O-H stretch at 3640 cm^{-1} is still present. By sample 20.07 the 980 cm^{-1} band is more intense than the 1020 cm^{-1} band, which is however still clearly recognisable. The development of a material recognisable from its SAD pattern as a Tobermorite-like silicate was seen in run 6 to occur within six hours of reflux. The development of the 980 cm^{-1} band, however, appears from run 20 to take much longer, up to 96 hours for sample 20.07. It began to appear that the presence of even small amounts of carbonate seriously hinders the formation of a well-crystallized Tobermorite having its principal Si-O stretch

Figure 3.04

Samples from run 20



frequency below 1000 cm^{-1} .

The aim of run 33 was to produce, in six hours, a material recognisable as Tobermorite, in the absence of carbonate. This was found to be possible, and it was discovered that the sample, 33.01, had a much sharper 980 cm^{-1} band than hitherto, and that the 1020 cm^{-1} band was much less intense than usual. Spectrum A of figure 3.05 is that of the product, while spectrum B is that of the material derived from it by deliberate carbonation with CO_2 gas, the consequences of which are discussed in section 3.05.

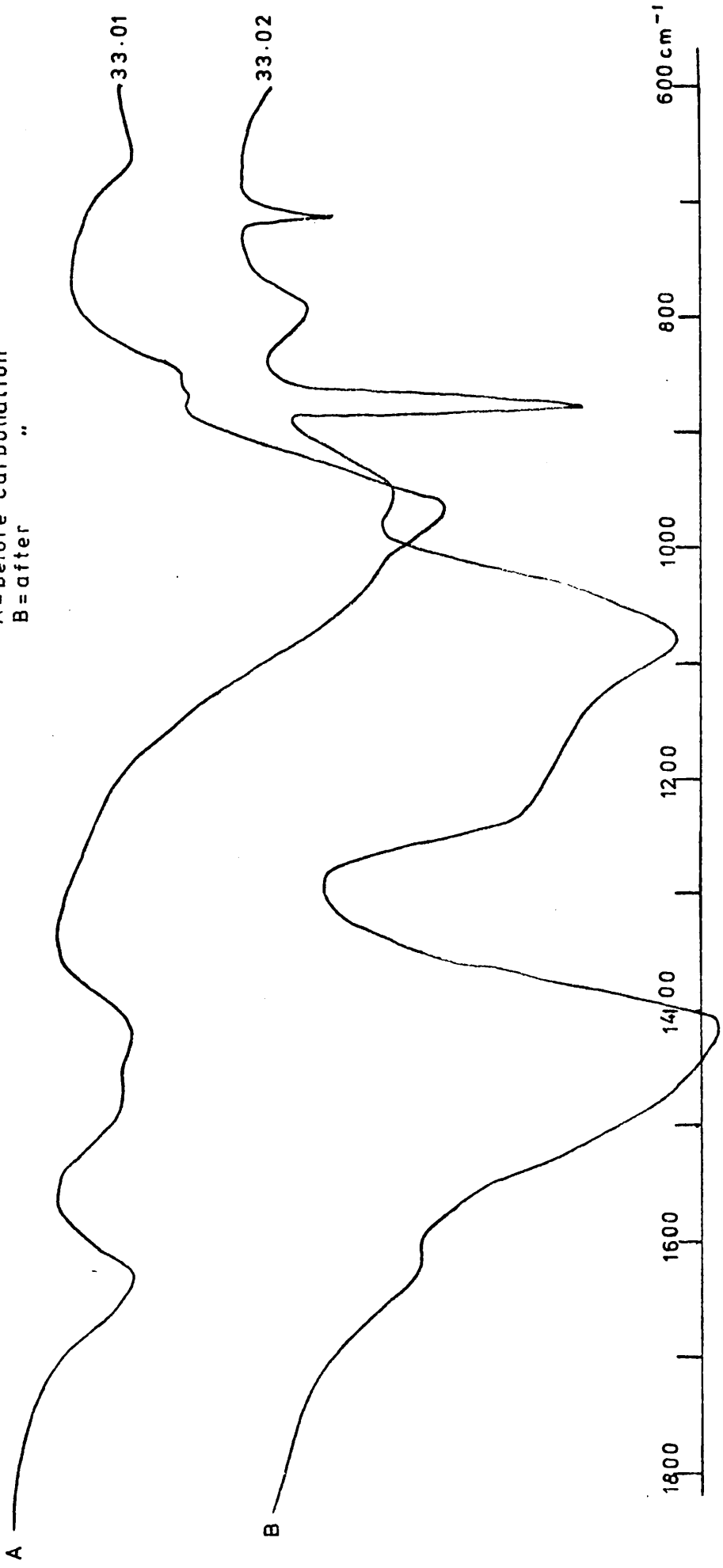
Plate 3.03 shows a typical region of sample 33.01, the SAD pattern of which is shown in plate 3.04. The sheet-like material is very similar to sample 6.08, but shows fewer randomly-crumpled regions; lath-like arrangements of the sheets are observed.

3.04 Results and Discussion - Series B.

Tobermorite-like calcium silicates are known to form within a wide range of compositions from $\text{Ca:Si} = 0.8$ to $\text{Ca:Si} = 1.2$. As was therefore expected, the Series B reactions yielded very similar products to those from series A. Runs 26 and 27 both gave good Tobermorite-like material. Run 26 showed progressively the disappearance of the O-H stretch band and the appearance of both the new Si-O bands by sample 26.01, the disappearance

Figure 3.05

Product from run 33
A = before carbonation
B = after carbonation



of the 1020 cm^{-1} band by sample 26.02, and a good Tobermorite was formed somewhere between one and twenty-three hours. Run 27, at 80°C , was similar but slower, the 1020 cm^{-1} band remaining evident until sample 27.03, after 47 hours, and disappearing by sample 27.04.

Morphological differences in the products were slight, the foils showing a tendency to form "asters" rather than laths, an example of which is shown in plate 3.05.

3.05 Morphology, crystallinity and CO_2 -uptake.

Plate 3.02 shows a typical example of sample 6.08, the diffraction data of which are given in table 3.02. The morphology is very similar to that shown by Gard, Howieson and Taylor (25), and consists of an irregular pile of thin sheets of material much folded in drying down onto the grid. The reference data in table 3.02, taken from the A. S. T. M. Powder Diffraction File, refer to:

- (a) 6-0005. A natural 14 \AA Tobermorite from Crestmore (26)
- (b) A natural 11.3 \AA Tobermorite from Ballycraigy, Co. Antrim (27), 10-0373
- (c) 6-0010. Data for poorly-crystallized mixed hydrates (26).

The absence in sample 6.08 and reference 6-0010 of any of the $00l$ spacings associated with natural Tobermorites suggests that these

TABLE 3.02

Sample	6-0005	10-0373	6-0010	6.08	33.01
hkl	d	d	d	d	d, $\overset{O}{A}$
002	14.0	11.3			
201	5.53	5.55	5.3	5.27	5.27
006	4.65				
205	3.95	3.57			
008	3.51				
220	3.07	3.11	3.07	3.14	3.07
222	2.98	2.99			
400	2.81	2.83	2.80	2.86	
209	2.72	2.29			
00.12	2.32				
22.10	2.08	2.10	2.1	2.14	2.17
040	1.83	1.85	1.83	1.67	1.84
620	1.67	1.676	1.67	1.69	1.66
00.18	1.550				
440	1.532	1.547	1.53		1.53
800	1.405		1.40	1.44	1.40
---		1.220		1.24	1.20
260			1.17	1.15	1.13
640	1.117		1.11		
10.20	1.07		1.07	1.09	

A. S. T. M. Reference Patterns:

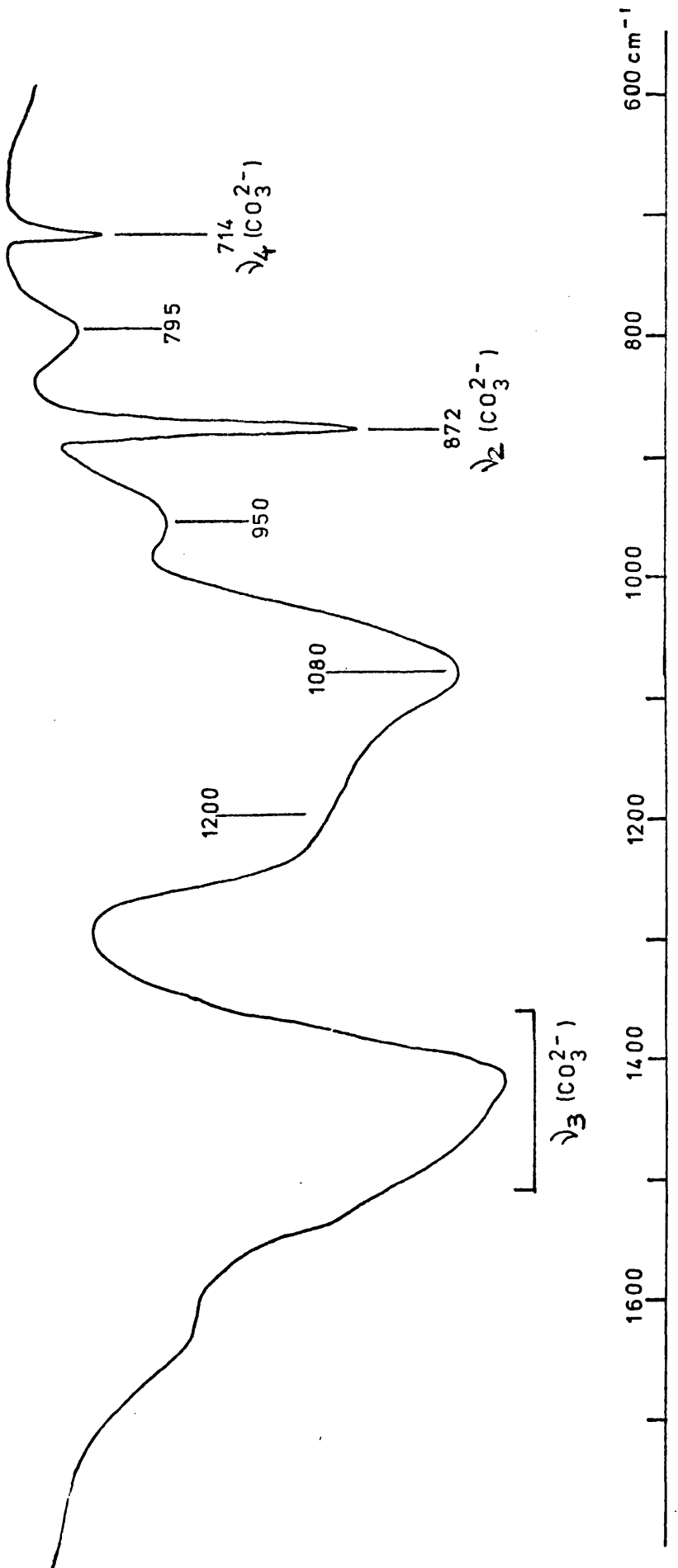
- 6-0005 - Tobermorite from Crestmore, California.
- 10-0373 - Tobermorite from Ballycraigy, N. Ireland.
- 6-0010 - Poorly crystalline, mixed hydrates.

C-S-H gels possess no c-axis ordering, while the predominance of hk0 spacings in 6.08 confirms the "crumpled sheet" theory of the structure.

Plate 3.06 shows a similar region of the same sample photographed two years later, during which time the sample had been stored, dry, in an unsealed glass sample tube with a screw cap. Although no difference in morphology is apparent, diffraction patterns such as were obtainable from the area in plate 3.06, and from all regions of the sample on the grid, were now typical of amorphous material.

Infra-red spectra of sample 6.08 were recorded after one week (figure 3.02) and after two years (figure 3.06). The sample had already begun to absorb CO_2 in one week as shown by the band at 1440 cm^{-1} in figure 3.02. The Si-O stretch shows a maximum at 1015 cm^{-1} and a shoulder around 950 cm^{-1} . This is formally similar to the spectrum of natural Tobermorite recorded by Henning and Gerstner (28) but bears little resemblance either to that of Henning's crystalline hydrothermal product or to that of the 14 \AA material from Creatmore described by Farmer et al. (29). In figure 3.06 the absorption around 1450 cm^{-1} due to CO_3^{2-} has become very intense and the Si-O bands at 800, 950, 1080 and 1200 cm^{-1} are now typical of an amorphous acidic silica gel, suggesting that there are no longer any

Figure 3.06
Sample 6.08



Ca-O-Si bonds in the structure. Analysis of sample 6.08 at this stage showed that it contained 6.36% carbon and 0.6% hydrogen (as H₂) by weight, corresponding to an approximate formula of 5CaO.6SiO₂.5.15CO₂.5.9H₂O.

The question remained as to whether the absorption of CO₂ caused the breakdown of the structure or was merely concomitant with it. A fresh sample (33.01) of C-S-H gel was prepared and stored in CO₂-free conditions under "Sofnolite" until infra-red and EM examinations had been made. It was then exposed to carbon dioxide (1 atm.) for three days and again examined. Sample 33.01 consisted of particles (plate 3.03) morphologically very similar to sample 6.08, having the diffraction pattern shown in table 3.02. After carbonation, no change in morphology was observed, but once again the sample was amorphous in electron diffraction. The infra-red spectra, figure 3.05, differ as before but that of 33.01 is now much closer to that of the Crestmore mineral of Farmer et al. (29), and contains very little carbonate. Analysis of the carbonated sample (33.02) yielded C = 5.75%, H₂ = 1.5%, corresponding to an approximate formula of 5CaO.6SiO₂.4.7CO₂.7.3H₂O.

Cole and Kroone (30) reported the products of carbonation of hydrated cements to be poorly-crystallized vaterite, calcite and

aragonite, and suggested that the process of carbonation was as follows: Cement minerals \longrightarrow siliceous residue + calcium hydroxide \longrightarrow vaterite + aragonite + poorly-crystallized calcite. Rashkovich (31) reported crush-strength and density data for samples of individual cement components before and after carbonation. He found that the crush strength of a hydrothermally synthesised Tobermorite increased from 175 to about 300 kg.cm^{-2} on carbonation. Asano et al. (32) examined the products of carbonation, under wet and dry conditions, of hydrothermally-synthesised Tobermorite and concluded that these consisted of "almost crystalline" calcite, and silica gel. Finally, Sauman (33) examined the changes on carbonation in an 11\AA Tobermorite of porous concrete and concluded that the products were, again, vaterite and calcite. He also reported, however, that the morphology of the original Tobermorite was preserved during the reaction. It seems clear from the work of these authors that the carbonation of a Tobermorite having a defined c-axis periodicity produces a mixture of the crystalline forms of calcium carbonate. In this work, however, no evidence of crystalline order in the product was found. Carbon dioxide was, nonetheless, absorbed in an amount equimolar with the CaO-content of the original gel, and is shown by the infra-red spectra to be present in the samples as CO_3^{2-} .

The CO_3^{2-} ion in calcite possesses D_3h symmetry and should thus have three infra-red active vibrational modes, $\nu_2(A_2'')$, $\nu_3(E')$, and $\nu_4(E')$, occurring at 874, 1429-1492, and 706 cm^{-1} , respectively (34). The bands attributable to CO_3^{2-} occur in figure 3.06 at 872, 1400-1500 and 714 cm^{-1} . Bearing in mind the errors likely to arise from the pressed-disc technique, it is safe to conclude that the ion has suffered no lowering of its symmetry such as would be evident with the formation of Aragonite. There is, however, no evidence for the presence of crystalline calcite. Such a situation might be expected of a carbonate ion in solution rather than of a solid. It seems probable that the carbon dioxide adsorbed reacts with the individual silicate sheets, displacing the silicate chains. The sheets have no regular stacking axis, so the carbonate ions cannot occupy the lattice positions which they would adopt in calcite. This process might occur with little migration of individual silicate tetrahedra and hence the silicate anion structure would be largely preserved, thus explaining the marked pseudomorphosis. The known occurrence of topotactic transformations among the calcium silicate hydrates (35,36) lends support to this view.

3.06. Conclusions.

The formation of a Tobermorite-like C-S-H gel under the conditions described, proceeds,

as has been postulated for Hectorite, in two distinct stages. In the first, lasting no longer than thirty minutes, adsorption of silicate ion on the crystal surfaces occurs, causing the removal of the hydroxyl groups of the $\text{Ca}(\text{OH})_2$ and the formation of Ca-O-Si linkages absorbing at about 1020 cm^{-1} in the infra-red. The adsorption is ordered, giving rise to a material showing at least some of the hk0 spacings of Tobermorite. Subsequently, in from 5 - 10 hours, formation of Si-O-Si bonds occurs and the new Si-O frequency at 980 cm^{-1} , typical of a well-ordered natural Tobermorite, appears. At this stage the product begins to show evidence of orientation of the initial sheets into more regular structures than are observed with the initial adsorbates, although c-axis ordering is not observed.

The presence of atmospheric CO_2 , while having little effect on the initial stage of the reaction, seriously hinders the formation of the dreierketten linkages. The c-axis aperiodic products are unstable in the presence of CO_2 , slowly decomposing to form a mixture of amorphous calcium carbonate and silica gel. This mixture shows strong pseudomorphosis with the original C-S-H gel.

The mechanism here suggested is very similar to that presented for the formation of Hectorite by Baird et al. (15). The absence of

of infra-red evidence for this view in chapter one may arise from the coincidence of the Si-O frequency of the initial adsorbate (about 1020 cm^{-1}) and of that frequency in Hectorite (1015 cm^{-1}).

PLATE 3.01

0.1 μ



PLATE 3.02

0.1 μ

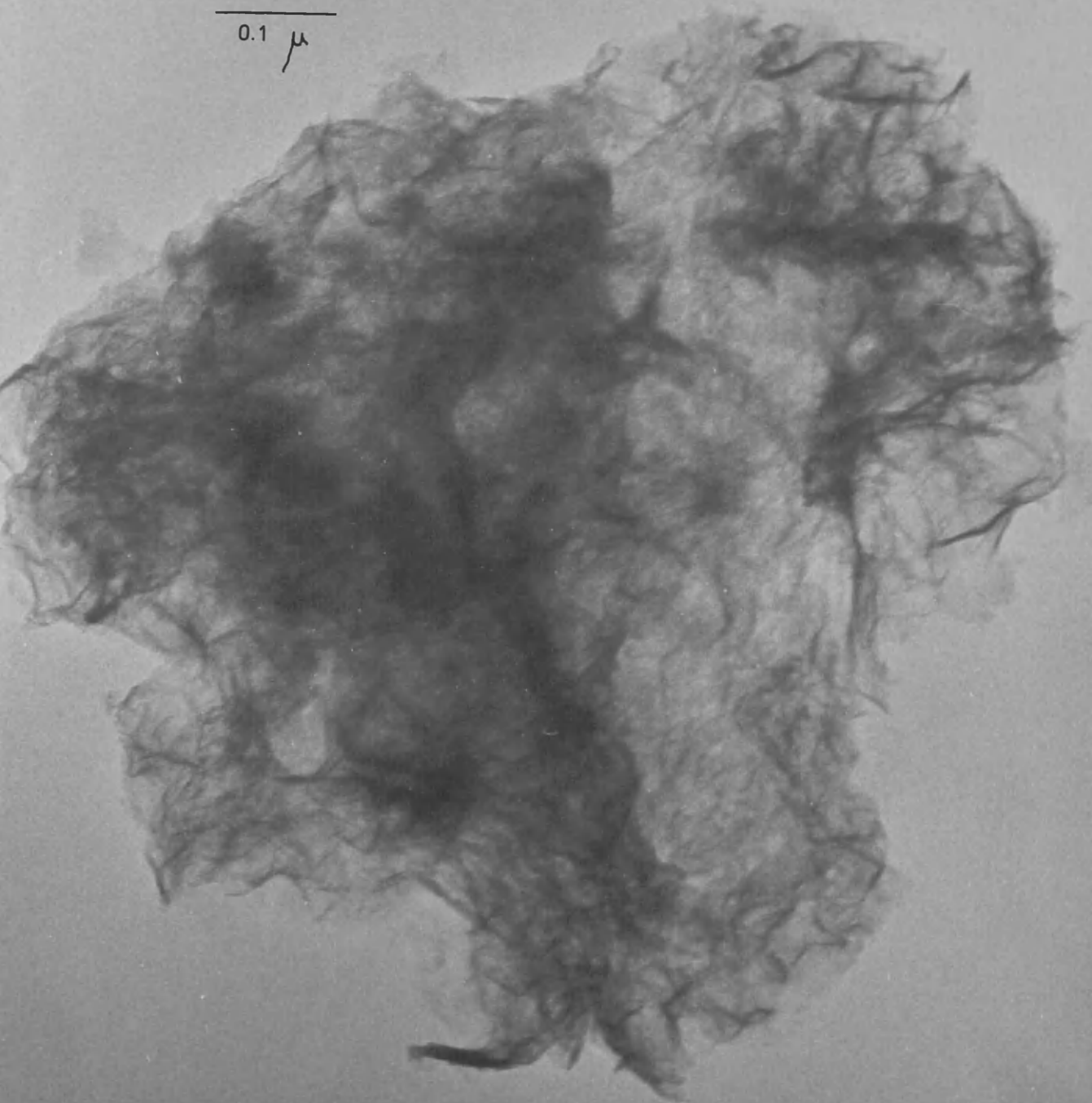


PLATE 3.03

0.1 μ

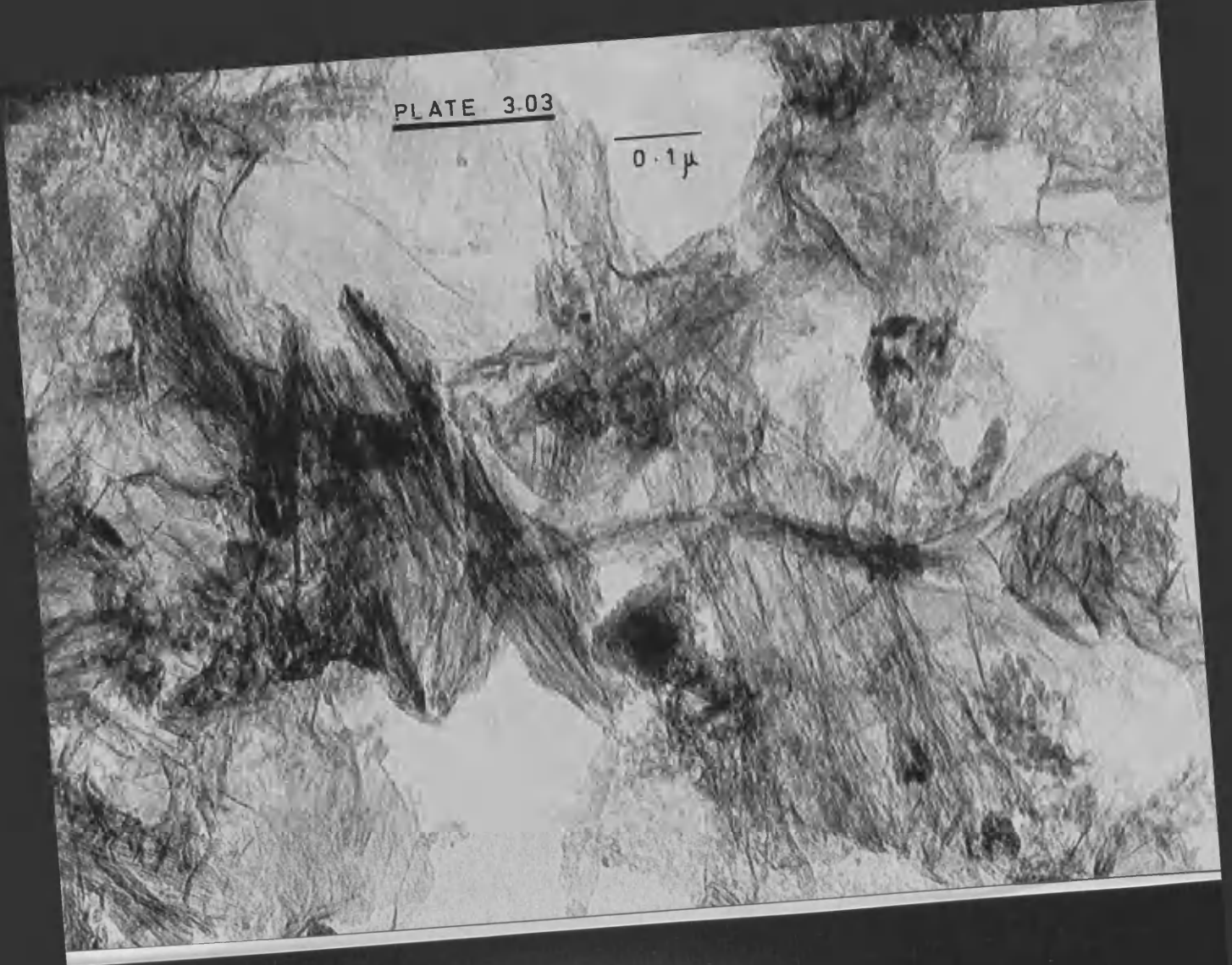


PLATE 3.04

Tobermorite — Sample 33.01

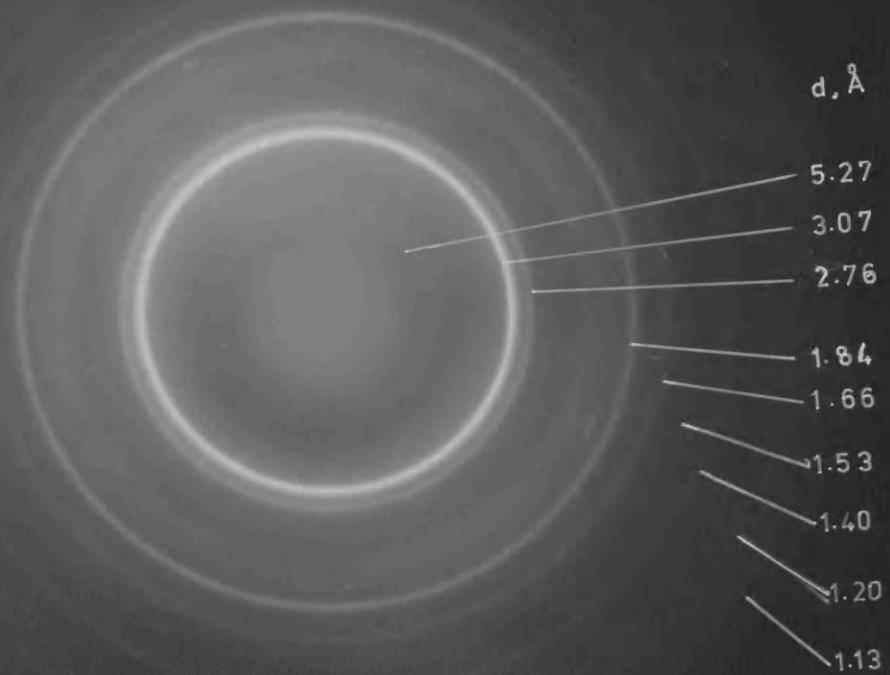
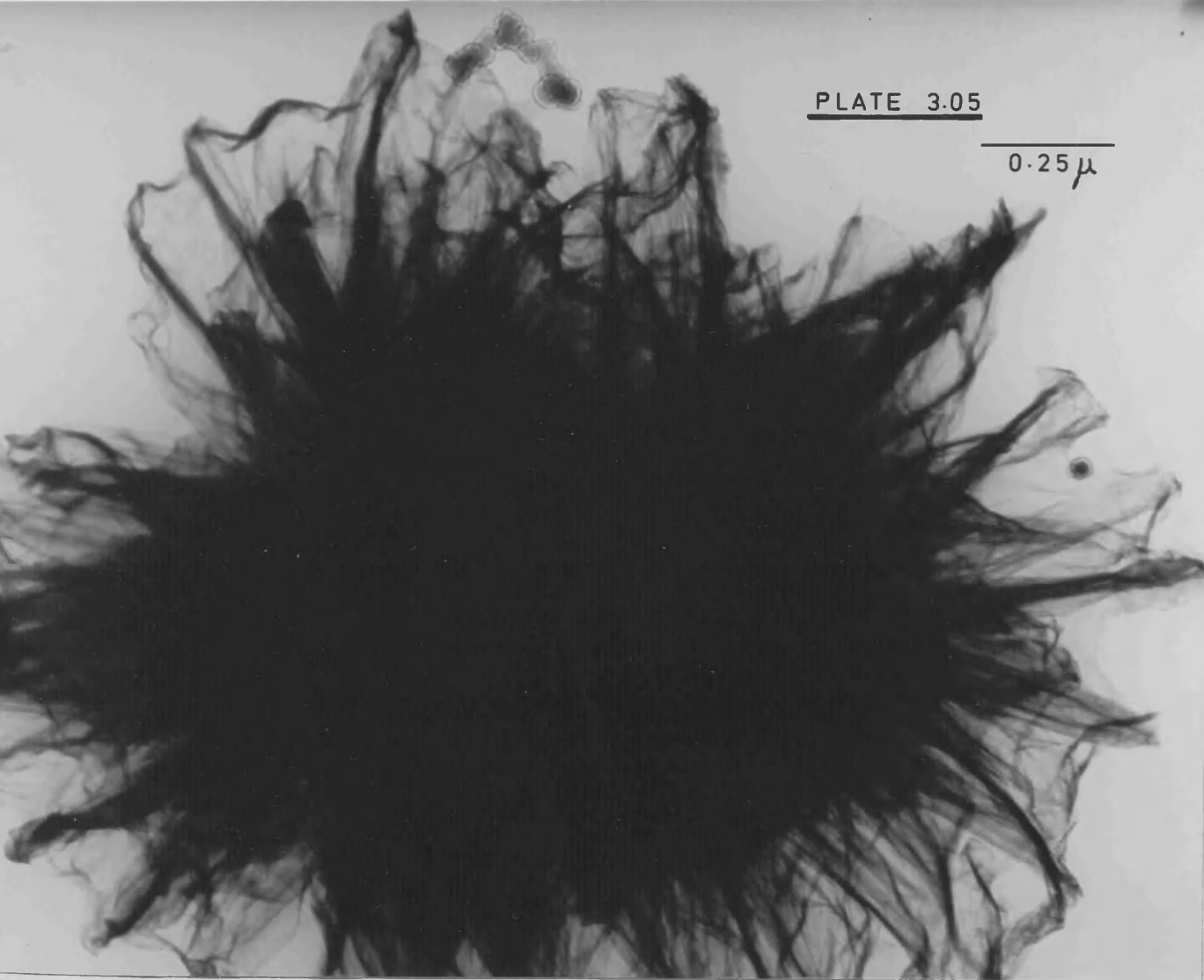
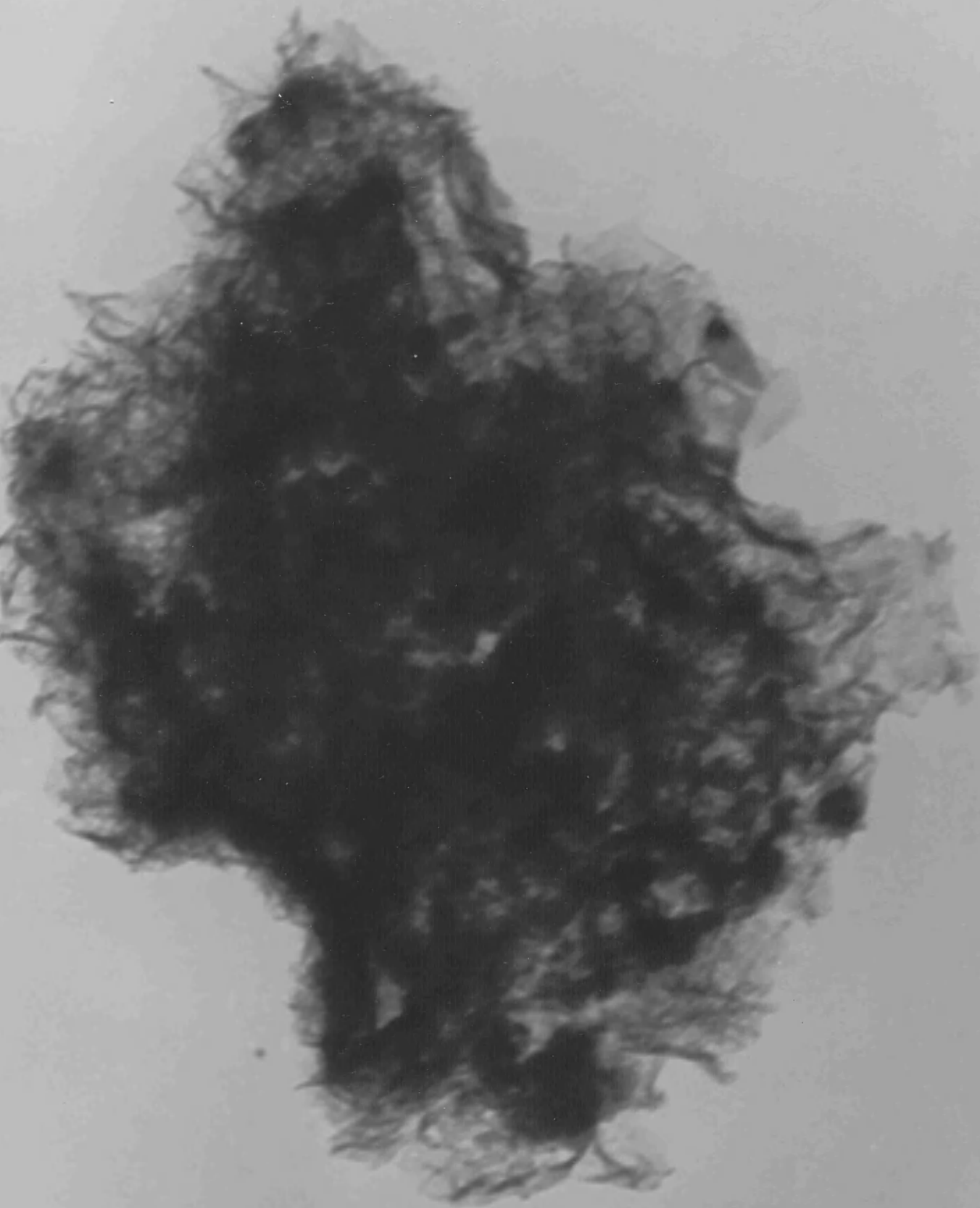


PLATE 3.05

0.25 μ





0.1 μ

PLATE 3.06

CHAPTER 4. CADMIUM HYDROXIDE.

4.01. Experimental.

Cadmium hydroxide was precipitated from cadmium iodide solution with potassium hydroxide solution, washed on the centrifuge and freeze-dried. The feed mixture was made up in the proportion Cd:Si = 3:4 for a theoretical product analogous with hectorite. The pH of the run (Run 18) was adjusted to 10 with solid lithium hydroxide. Samples were taken at the times shown in table 4.01, and were washed and freeze-dried.

DTA was performed on a Du Pont 900 Thermal Analyser, using a nitrogen atmosphere. 10 mg. samples were run, generally at a heating rate of 20°C per min., with a ΔT sensitivity of 1.0°C/inch.

4.02. Results and Discussion.

Figure 4.01 shows the infra-red spectrum of the cadmium hydroxide used, and figure 4.02 the spectra of samples taken during run 18. DTA traces from the $\text{Cd}(\text{OH})_2$ and the run samples are shown in figures 4.03 and 4.04 respectively. The spectrum of $\text{Cd}(\text{OH})_2$ is very similar to that of $\text{Mg}(\text{OH})_2$ and that of $\text{Ca}(\text{OH})_2$, showing a sharp O-H stretch band, in this case at 3615 cm^{-1} , and a broad band below 600 cm^{-1} arising from vibrations within the octahedral layer. In DTA, the dehydration to black CdO produces an endotherm centred at 260°C: at lower heating rates another endotherm, at 245°C, is apparent.

TABLE 4.01

Sample times for Run 18.

Sample No.	Time at Reflux min.	(dy)
18.00	0	
18.01	147	
18.02	1176	
18.03	1636	(1)
18.04	2690	(2)
18.05	3037	
18.06	7175	(5)
18.07	11676	(8)
18.08	17263	(12)

TABLE 4.02

Diffraction data from Run 18.

Cd(OH) ₂ *		18.00	18.08
d	hkl	d	d
4.7	001		
			4.22
3.03	100	3.04	
			2.85
2.55	101	2.53	2.58
2.34	002		
1.857	102	1.86	
1.748	110	1.75	
			1.68
1.513	200	1.51	
1.441	201		1.44
1.398	103		
1.274	202		
1.142	216	1.15	

* ASTM No. 13-0226.

d-spacings in Å.

Figure 4.01
IR Spectrum of $\text{Cd}(\text{OH})_2$

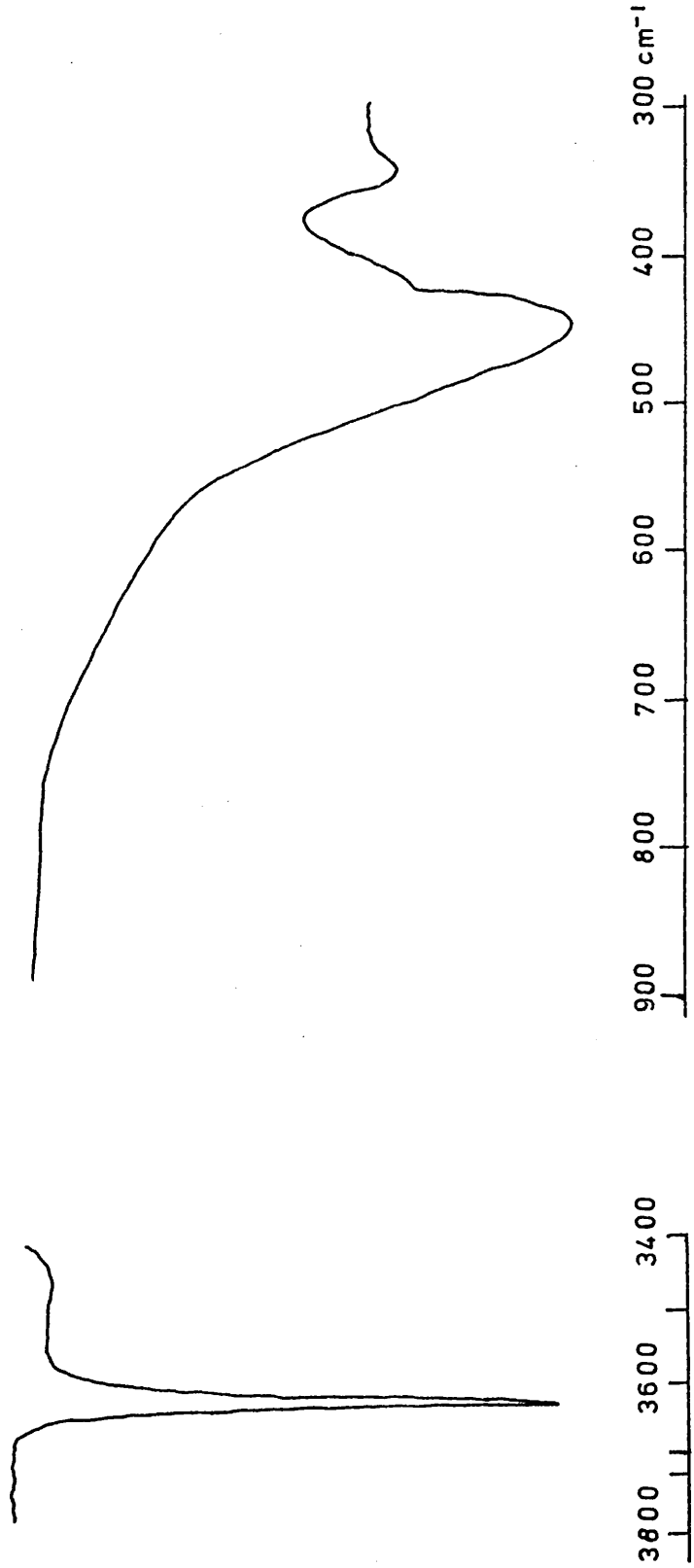


Figure 4.02
Samples from run 18.

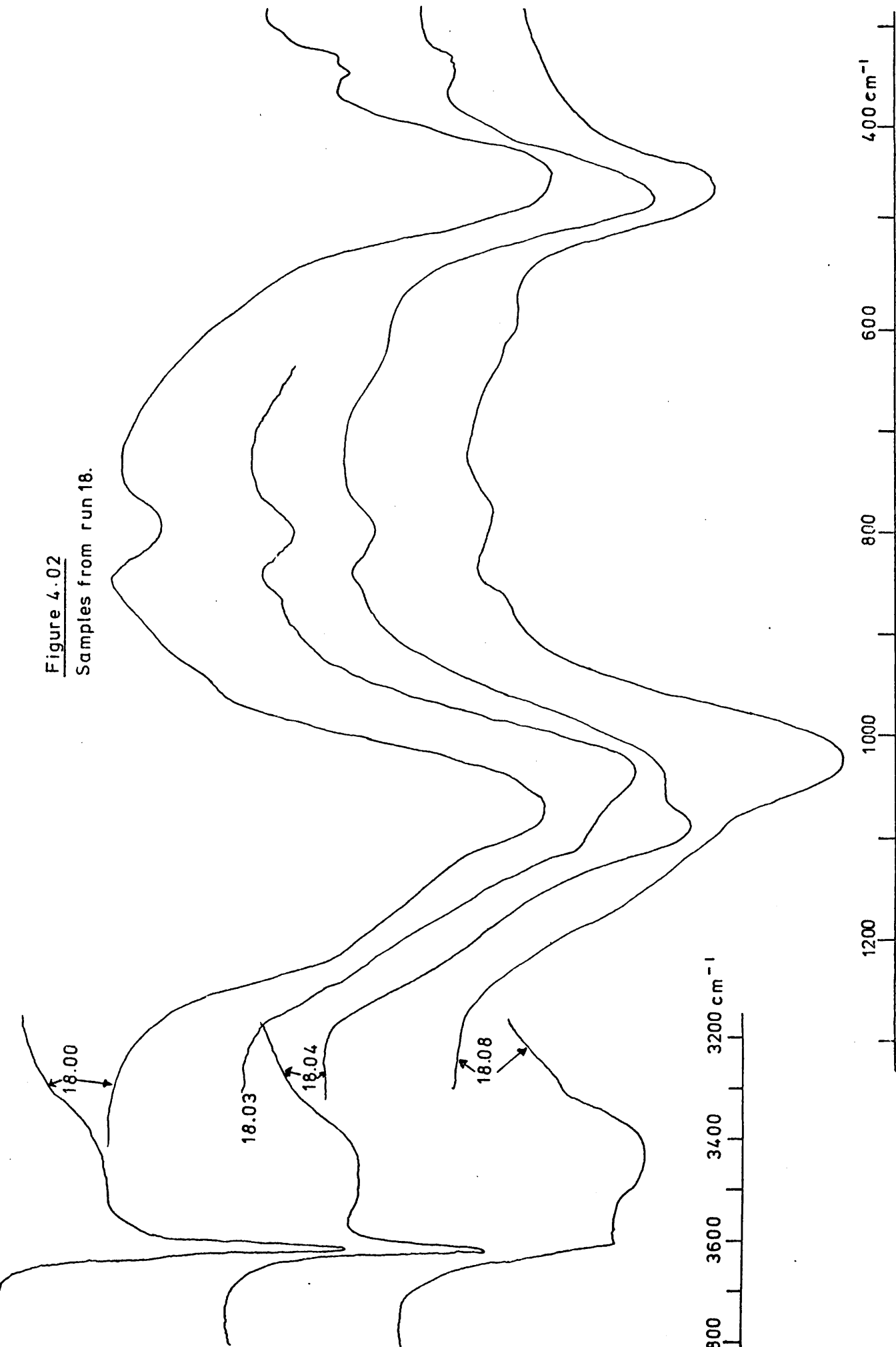


Figure 4.03
DTA of Cd(OH)₂

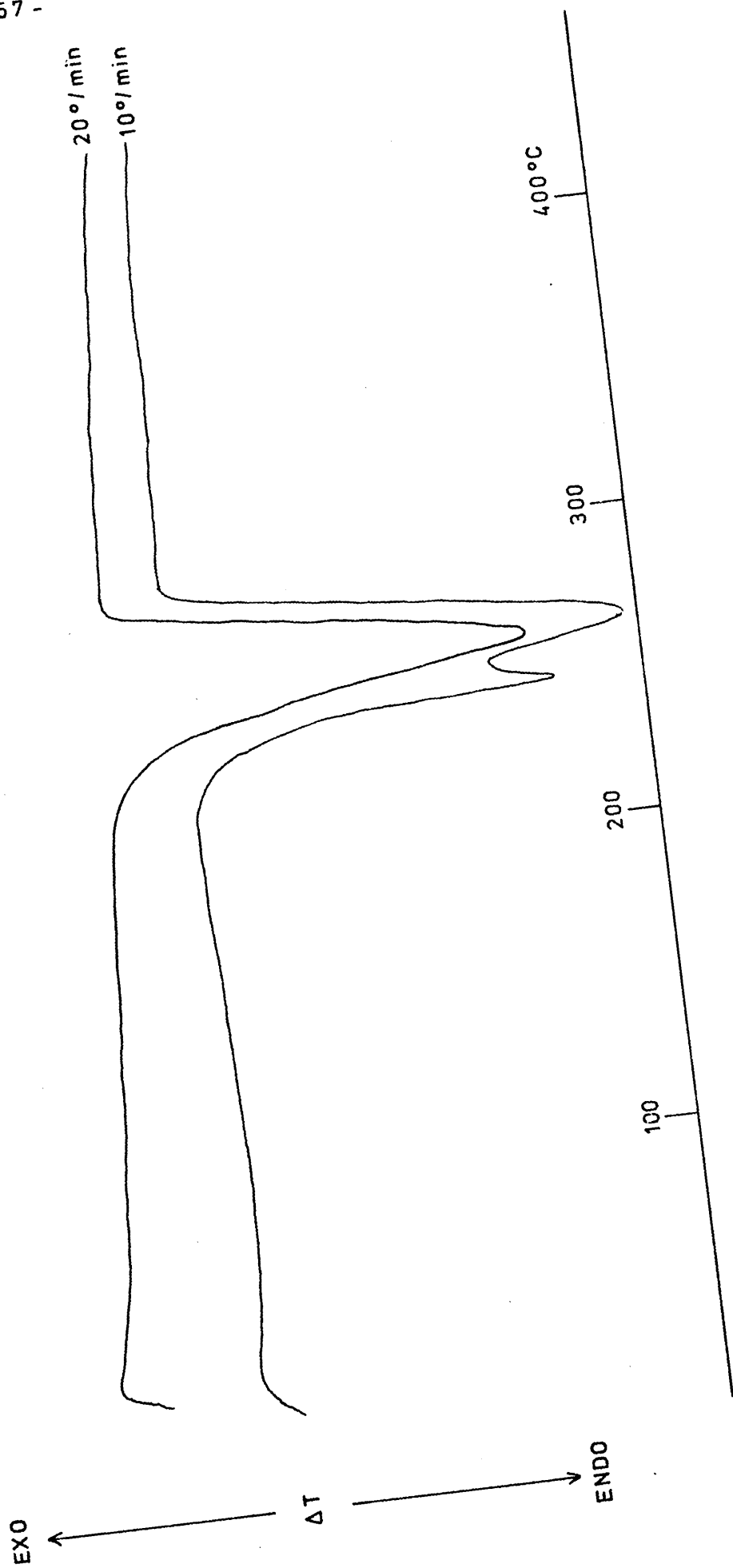
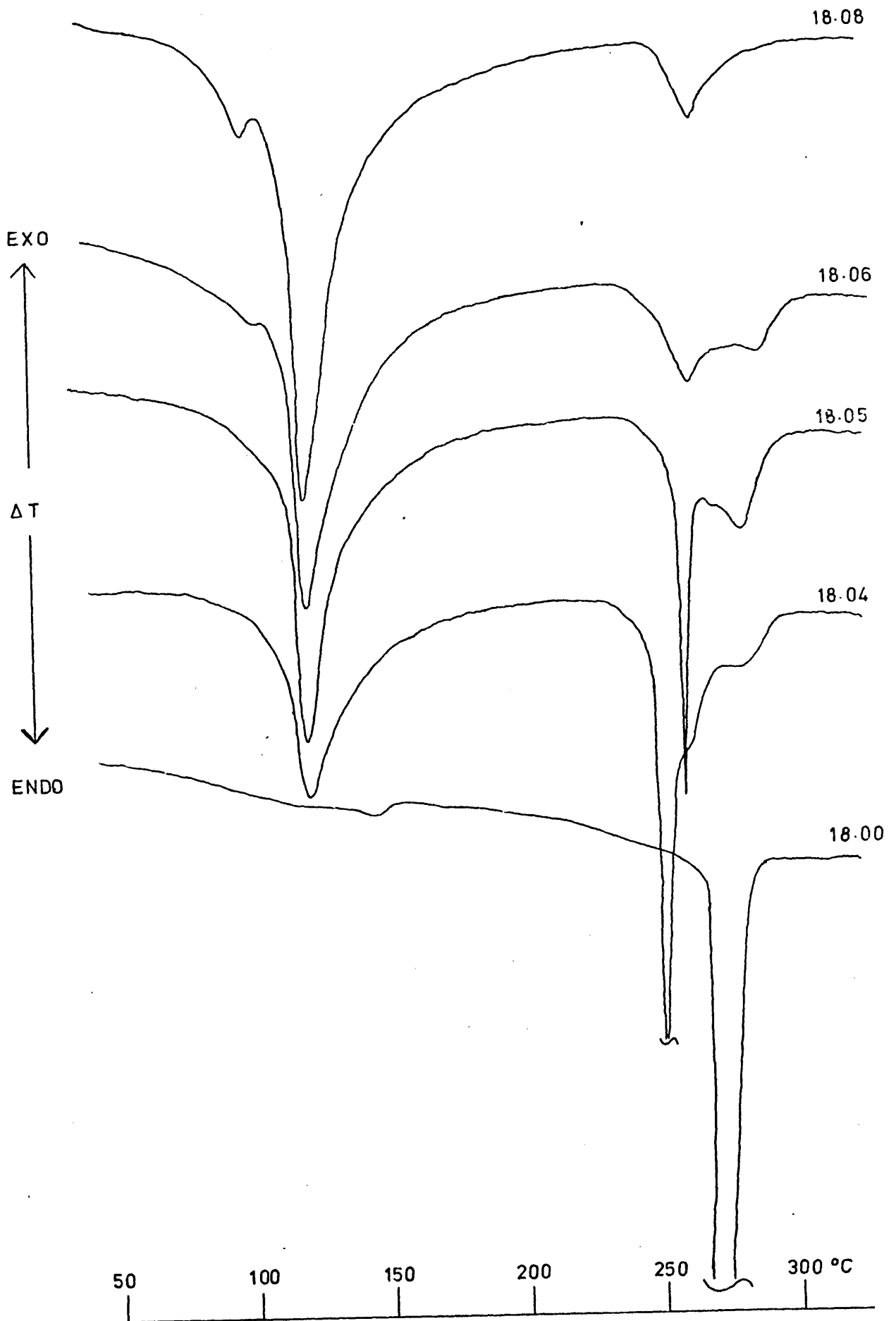


Figure 4.04

DTA of Samples from run 18.



The infra-red spectrum of the feed mixture, sample 18.00, shows the presence of $\text{Cd}(\text{OH})_2$ and amorphous silica gel, no reaction being apparent. The DTA of the mixture is, however, slightly different from that of $\text{Cd}(\text{OH})_2$, in that the dehydration endotherm is now much sharper, single, and centred on 255°C : considerable superheating was observed in early samples, the onset temperature for sample 18.00 being around 265°C .

As the reaction progresses, changes, similar to those observed in the early stages of Hectorite formation, occur in the spectra. The O-H stretch at 3615 cm^{-1} decays, although it never completely disappears, and a new Si-O stretch band appears around 1020 cm^{-1} , replacing the 1080 cm^{-1} band of the silica gel (Figure 4.02). The band progression is not regular, see sample 18.04. In DTA, the dehydration endotherm becomes less intense, and a new endotherm appears at 145°C . In later samples another endotherm appears at 100°C . The DTA of sample 18.08 is typical of that of a hydrated silicate, the endotherm at 100°C indicating the removal of small amounts of surface water, and that at 145°C being caused by the liberation of water molecules intercalated in the structure, either in pores or between layers. By sample 18.08 the residue, after heating to 450°C , was no longer black, but white.

Electron micrographs of the product, sample 18.08, reveal a remarkable morphology. Plate 4.01

appears to show round, or rounded hexagonal, particles, individuals of which (arrowed) are about 8 nm. in diameter. The apparent shape of the particles may be a phase contrast artefact, resulting from the slight defocus of the micrograph: in-focus, the circles vanish and not enough contrast remains to permit resolution of the particles.

The particles have a strong tendency to associate edge-to-edge, producing broad raft-like agglomerates (plate 4.02) which are extremely thin, the outlines of overlapping regions being clearly visible (arrowed). Attempts to shadow individual particles were unsuccessful because of the grain size of the shadowing materials. Attempts to shadow agglomerates revealed that the edges of the "rafts" curled up from the carbon film. No direct measurement of the particle thickness was thus possible.

The $\text{Cd}(\text{OH})_2$ used in the run, appears very similar to $\text{Mg}(\text{OH})_2$, consisting of small hexagonal platelets 0.1 - 0.2 μm across. In SAD, the CO_2 spots, initially present, fade rapidly in the beam, as is the case with $\text{Mg}(\text{OH})_2$. The measurable spacings correspond well with X-ray powder patterns of $\text{Cd}(\text{OH})_2$ (table 4.02). Sample 18.08, on the other hand, gave five diffuse rings in SAD, the spacings from which correspond to those of none of the Cadmium Oxides, Hydroxides or Silicates listed in the ASTM file.

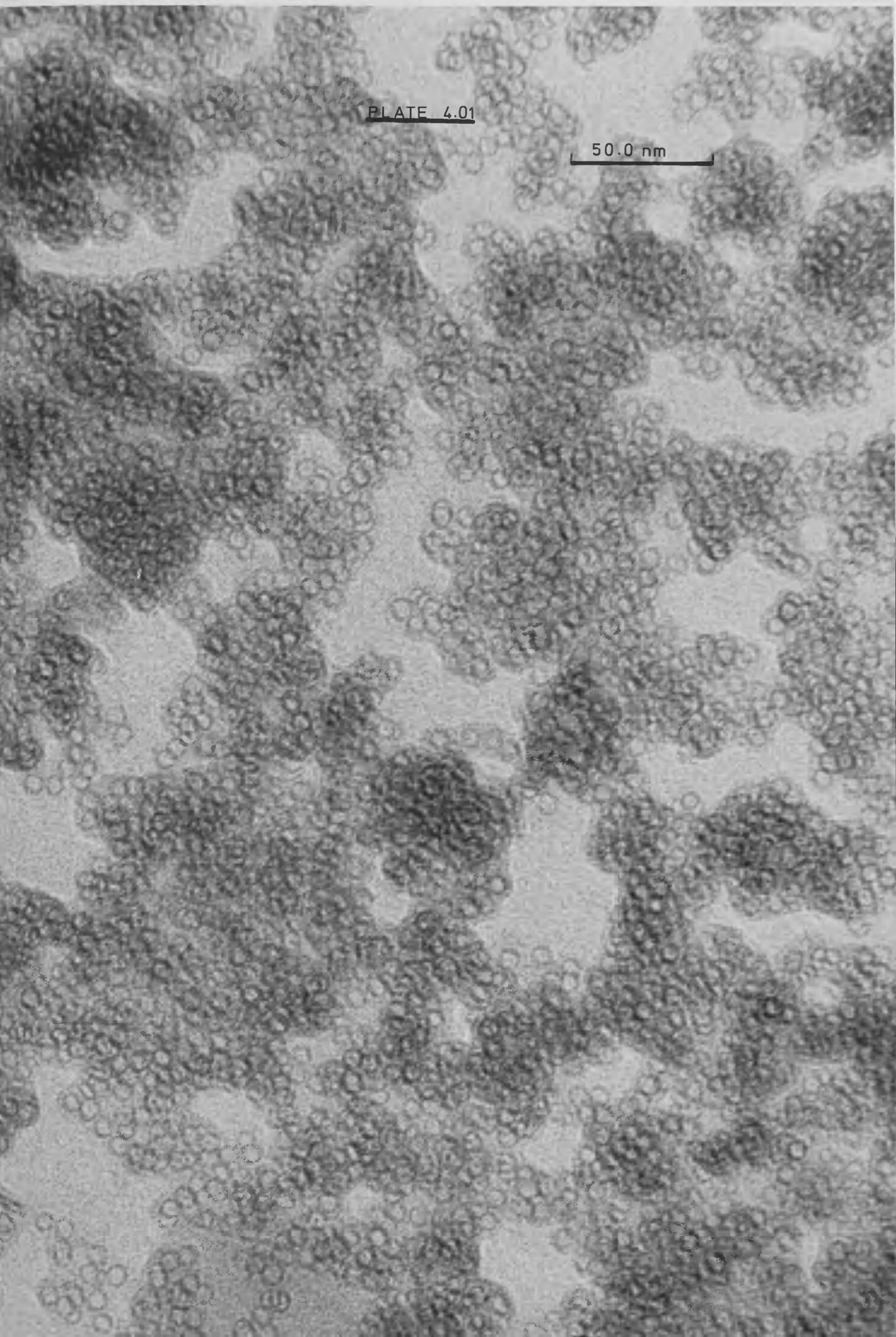
4.03 Conclusions.

Cadmium hydroxide appears to adsorb silicate ion from high pH slurries in the same way as Magnesium and Calcium hydroxides. The process is accompanied by a reduction in the particle size of the hydroxide crystallites, structural units between 5 and 10 nm. in diameter being formed. These units are thought to be plate-like rather than cylindrical, of the order of a few nm. thick, although no direct evidence of this is available. Both IR and DTA evidence suggest that there is some residual $\text{Cd}(\text{OH})_2$ present in the product, and it is suggested that this lies at the centre of the structural units. The product thus seems to have the characteristics of the "doughnut" structures observed in the formation of Hectorite (15), on a much smaller scale. The Si-O stretch band, centred near 1020 cm^{-1} , which was discussed in chapters 2 and 3, appears in the product, and again is taken to indicate the presence of silicate units adsorbed on the surfaces of the hydroxide layers in a poorly-ordered pattern.

On the question of whether the adsorbate formed resembles Tobermorite rather than Hectorite, no conclusions have been formed.

PLATE 4.01

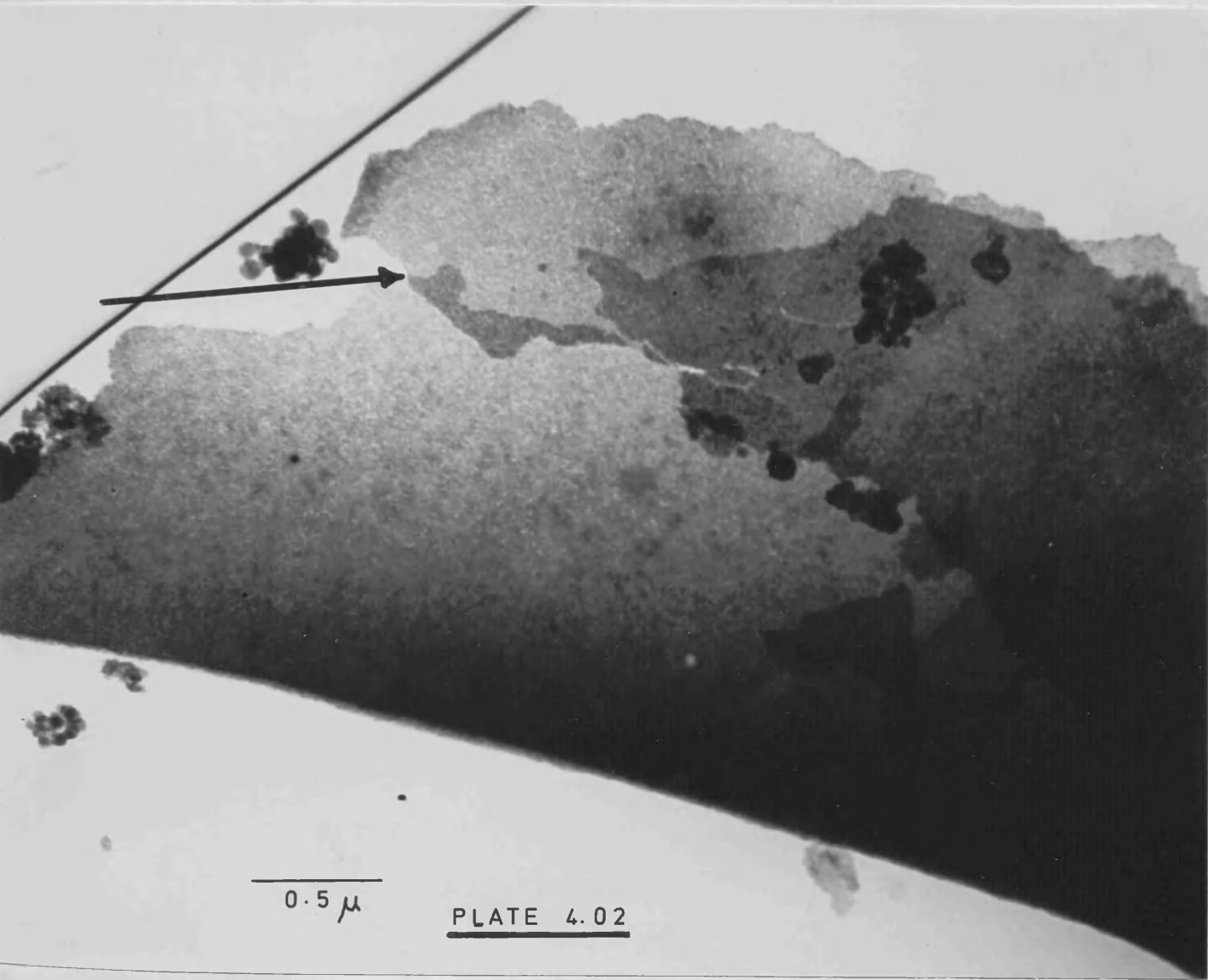
50.0 nm



CHAPTER 4. SUPERCONDUCTIVITY

4.01. EXPERIMENTAL

$\text{Cu}(\text{OH})_2$ was prepared by adding a solution of copper sulfate to a solution of sodium hydroxide. The precipitate was washed with water and dried at room temperature.



The micrograph shows the morphology of the precipitate. The dark region is irregular in shape and has a granular texture. The lighter material surrounding it appears to be the matrix. The scale bar indicates that the size of the features is on the order of 0.5 micrometers. The text "PLATE 4.02" is printed at the bottom of the image.

CHAPTER 5. COPPER HYDROXIDE.

5.01 Experimental.

$\text{Cu}(\text{OH})_2$ may be precipitated from aqueous solutions of copper salts with KOH solution, if the base is always in excess, at temperatures below 5°C (37). If Cu^{2+} is in excess, copper basic salts are formed, while at higher temperatures excess OH^- causes oxidation of the precipitate.

Copper sulphate solution ($\sim 0.1\text{M}$) was added slowly to 0.1M KOH solution, cooled in an ice bath. The resulting dark blue precipitate of $\text{Cu}(\text{OH})_2$ was washed on the centrifuge with ice-cold distilled water and freeze-dried.

As a comparison, the procedure was reversed, the KOH being added slowly to cooled copper sulphate solution. The pale blue precipitate thus formed, when washed and freeze-dried, had the infra-red spectrum shown in figure 5.01. This spectrum agrees well with that described by Tarte (38) for the compound $\text{CuSO}_4 \cdot 3\text{Cu}(\text{OH})_2$. The DTA of this compound, at two heating rates, is shown in figure 5.02.

The dark blue $\text{Cu}(\text{OH})_2$ precipitate was mixed with Mallinkrodt Silicic Acid in the proportions $\text{Cu}:\text{Si} = 3;4$, and made up into a 10% slurry with distilled water. The pH was brought up to 9 with solid LiOH and the mixture dispersed ultrasonically before being refluxed in the usual way. Samples from the reflux (Run 21) were taken at the times shown in table 5.01. The run was stopped at sample

Figure 5.01.

Ppt. from xs. Cu^{2+}

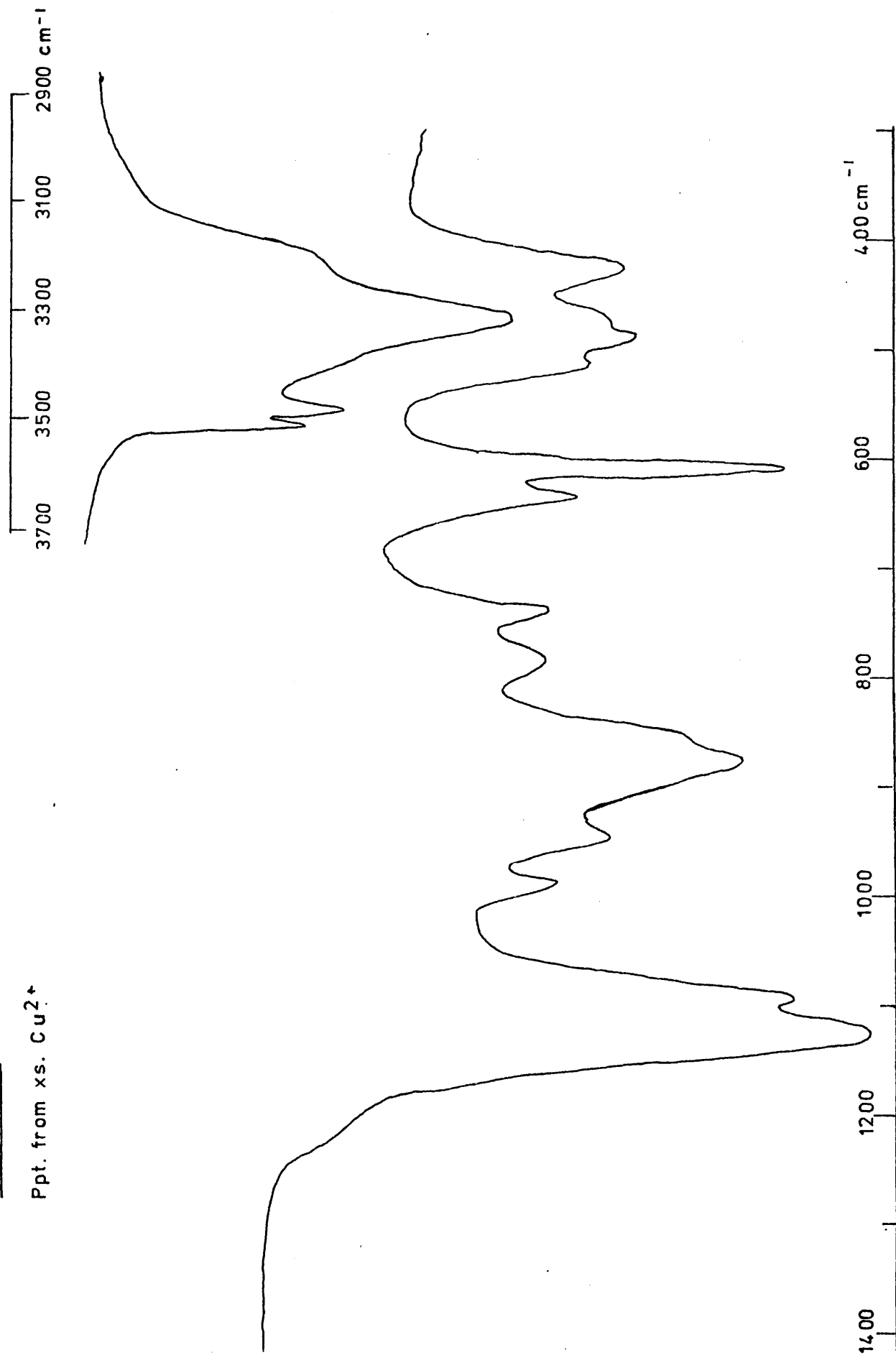


Figure 5.02

DTA of ppt. from xs. Cu^{2+} .

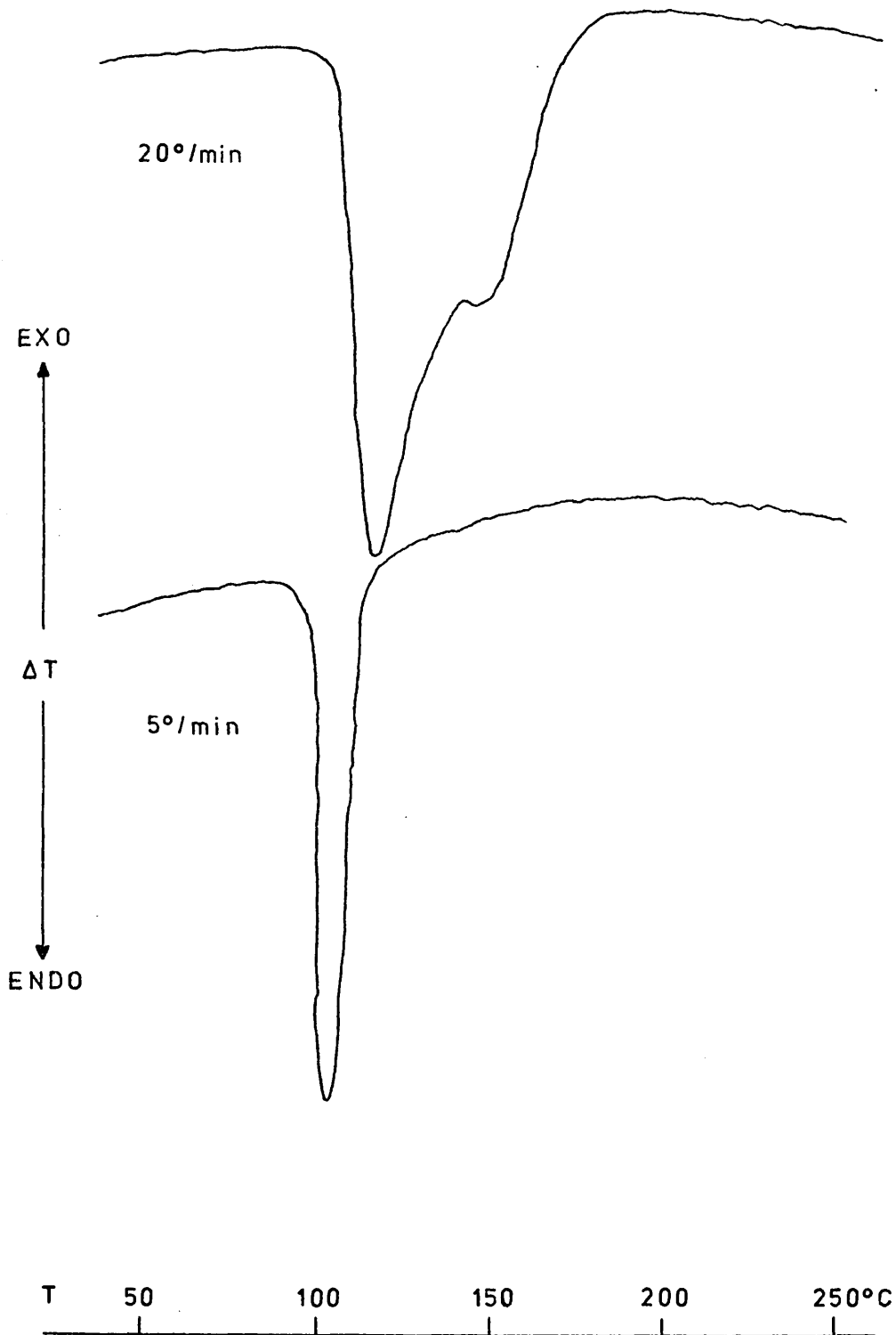


TABLE 5.01.

Sample Times For Run 21.

Time (mins)	Sample Number
0	21.00
51	21.01
144	21.02
265	21.03
354	21.04
464	21.05
1463	21.06
2072	21.07
2822	21.08 ----- 21.12
3812	21.13
5167	21.14
5917	21.10
6627	21.15
7540	21.11
8027	21.16
9827	21.17

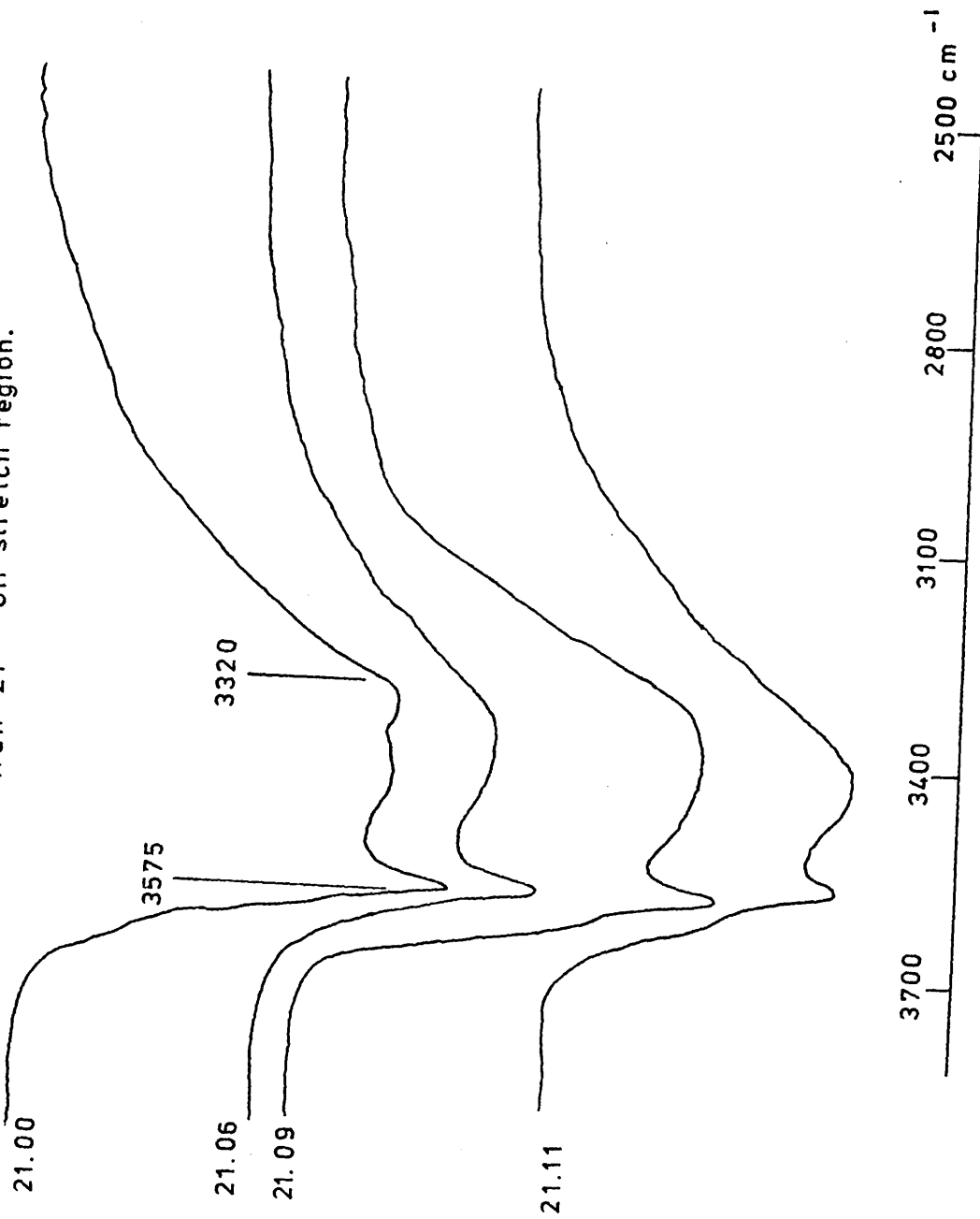
21.11, examination of which indicated that silicate formation, although occurring, remained incomplete: an attempt was made to improve the crystallinity of the product by restarting the run at a higher pH, beginning with sample 21.08. Samples 21.12 to 21.17 were taken from this restarted run.

5.02 Results and Discussion.

Infra-red spectra (figures 5.03 and 5.04) and DTA traces (figure 5.08) of samples from the earlier part of the run, are presented. The feed mixture, sample 21.00, shows infra-red bands (besides those of the silica) at 3575, 3400 and 3320 cm^{-1} in the O-H stretching region (figure 5.03) and at 680 and 420 cm^{-1} (figure 5.04). The band at 3575 cm^{-1} is assigned by Carbannes-Ott (39) to stretching of the non-hydrogen-bonded (intra-layer: see figure 1.02) OH groups, while that at 3320 cm^{-1} corresponds to stretching of hydrogen-bonded (inter-layer) OH groups. The band at 680 cm^{-1} is the δ - deformation of the intra-layer hydroxyls, while that at 420 cm^{-1} is a vibration of the distorted octahedral double layer. The band at 915 cm^{-1} reported by Ott, the δ - deformation of the inter-layer hydroxyls, is not observed in any of the spectra.

EM examination of sample 21.00 revealed, besides amorphous silica, flat, irregular crystals (plate 5.01) with the diffraction pattern of $\text{Cu}(\text{OH})_2$, recorded in table 5.02. These crystals quickly became

Figure 5.03
Run 21 — OH stretch region.



21.00

21.06

21.09

21.11

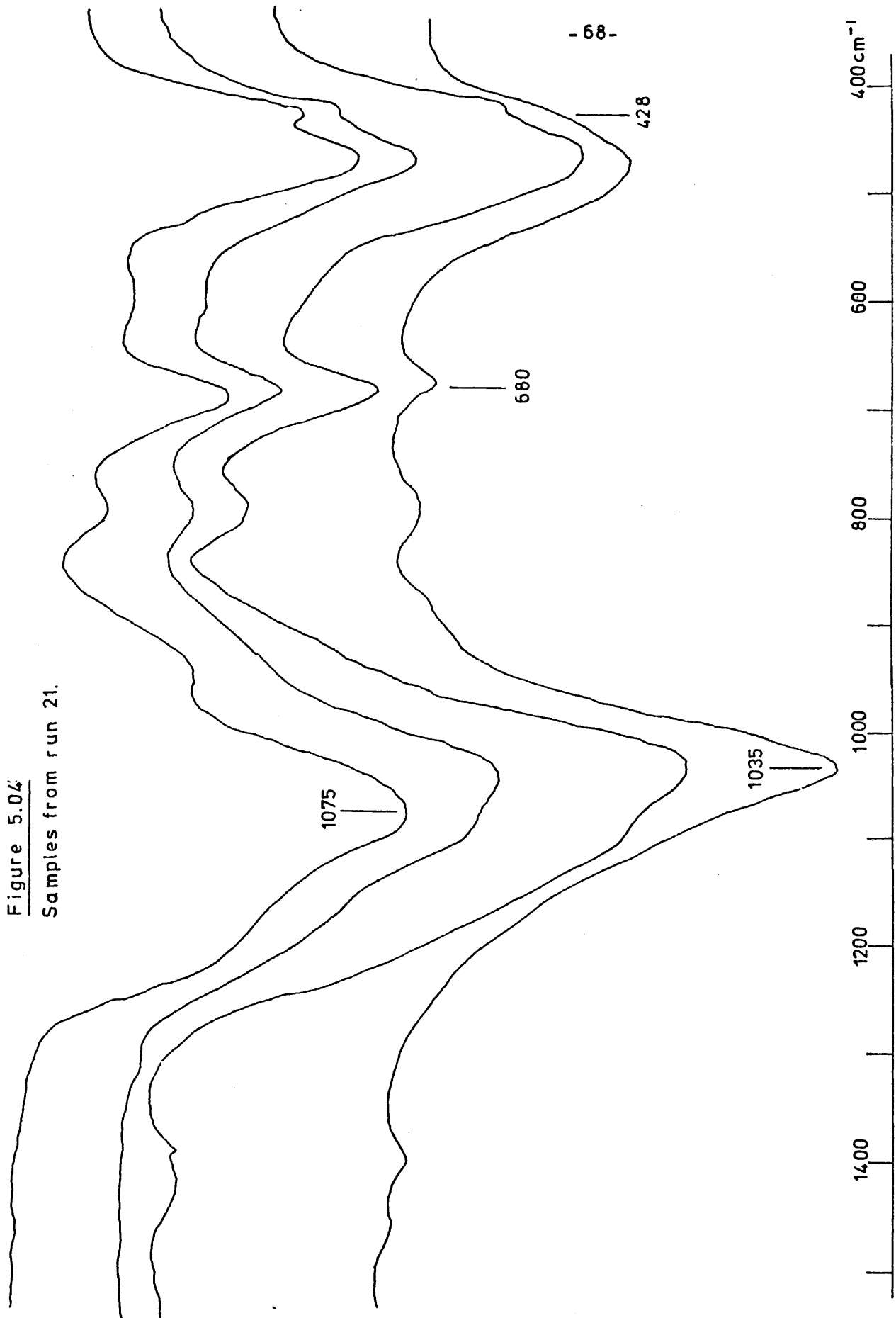


Figure 5.04
Samples from run 21.

Figure 5.08

DTA of samples from run 21.

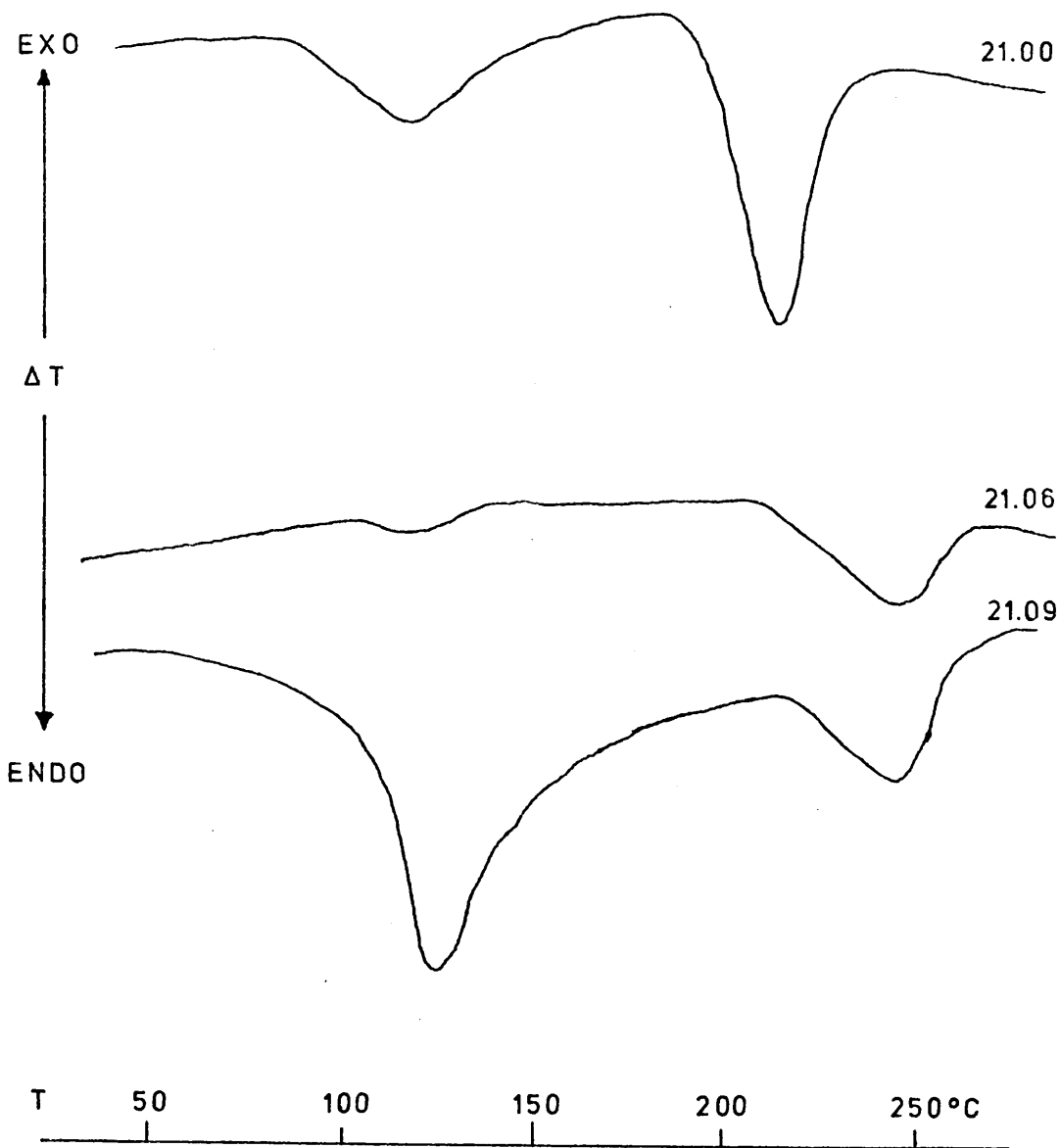


TABLE 5.02.

d-spacings from SAD of sample 21.00.

1 d, Å	2 d, Å I	3 d, Å	4 d, Å I	5 d, Å I	6 d, Å
5.12			5.30 90		
	3.03 w			3.020 9	
2.64			2.63 70		
	2.48 vs			2.465 100	
	2.12 m			2.135 37	
		2.09			2.088
		1.81			1.808
	1.72 vw			1.743 1	
1.53			1.49 6		
	1.51 m			1.510 27	
1.32			1.32 4		
1.28	1.28 w	1.28	1.29 6	1.287 17	1.278
		1.09			1.090

- 1 - Pattern from unheated crystals.
- 2 - Pattern from pitted crystals after heating in electron beam.
- 3 - Pattern from copper formed on melting of crystals.
- 4 - ASTM 13-420, $\text{Cu}(\text{OH})_2$.
- 5 - ASTM 5-667, Cu_2O , Cuprite.
- 6 - ASTM 4-836, Cu, Copper metal.

pitted in the electron beam, and dehydrated to form Cu_2O , cuprite, which was also identifiable by its diffraction pattern. Further heating in the beam melted the Cu_2O crystallites, which were then reduced to metallic copper, again identifiable by a characteristic diffraction pattern. The formation of CuO , tenorite, was not observed in the electron microscope.

The feed mixture shows two endotherms in DTA, both at higher temperatures than the single endotherm given by the copper basic sulphate. The endotherm at 220°C from sample 21.00 represents initial decomposition to tenorite: no higher-temperature effects are observed up to 500°C , at which point the residue was black.

During the reflux, the blue colour of the samples became progressively paler, and once again a new Si-O stretch band appeared in the infrared, this time at 1035 cm^{-1} . The intra-layer O-H stretch, 3575 cm^{-1} , remains unchanged until sample 21.09, as do the 680 and 420 cm^{-1} bands. The inter-layer O-H stretch at 3320 cm^{-1} appears to decrease in intensity, although it is difficult to be certain of this because of the masking of the overlapping H_2O band at 3400 cm^{-1} . In DTA, the lower-temperature endotherm disappears, and is later replaced by another, larger one at slightly higher temperature. The decomposition endotherm at 220°C remains present throughout, but its onset is delayed as the reaction proceeds. The

residues, after heating to 500°C, were in all cases black.

EM of sample 21.09 showed agglomerates of short fibres, apparently occurring in pairs (plate 5.02, arrowed). A higher resolution micrograph (plate 5.03) showed that these are in fact complete or nearly complete tubes, estimates of the diameters of which gave values ranging from 3.7 to 6.5 nm. It is not known whether these tubes are hollow or or filled with material fairly transparent to electrons, such as silica gel. The agglomerates gave only one diffuse ring in SAD, at $d=4.21 \text{ \AA}$.

It appears that sample 21.09 is an exfoliative adsorbate of copper hydroxide and silicate ion, the tubes being formed by peeling off of the double octahedral layers of the copper hydroxide after adsorption of silicate units. The decay of the interlayer OH stretch band in the infrared, while the intralayer bands remain constant, suggests that the exfoliation occurs with little disruption of the double octahedral layer. The new endotherm at 145°C in DTA is typical of the loss of intercalated water from an hydrated silicate. The adsorption appears to stabilise the hydroxide to dehydration, successive samples decomposing at higher temperatures. This has also been claimed to occur with $\text{Fe}(\text{OH})_2$ (17).

Later samples from the run seemed to be inhomogeneous, sedimentation revealing a pale blue heavy fraction and a blue-white colloidal suspension.

The spectrum of sample 21.11 shown in figures 5.03 and 5.04 is that of the heavy fraction. The colloidal fraction spectrum is shown in figure 5.05. The OH stretch at 3575 cm^{-1} has been replaced by a weak band at 3610 cm^{-1} , a shoulder is visible at 880 cm^{-1} and the 680 cm^{-1} band is now very weak. SAD examination of this material gave eight faint fine-grained rings (table 5.03).

In an attempt to improve the crystallinity of this colloidal product, the run was restarted as described above. Samples 21.12 to 21.17 were obtained from this part of the run. 21.12 was amorphous in electron diffraction, but the crystallinity of successive samples increased until 21.15, which gave a diffraction pattern similar to that of 21.11. No fractionation of the samples was observed in this part of the run. The morphology of the product shows little change (plate 5.04, sample 21.16); "tubes" were, however, not observed. Decomposition of the samples in the electron beam still occurred, beads of copper (identifiable by its diffraction pattern) being formed on the fibres (plate 5.05, arrowed). No copper (I) oxide was formed in the beam, however, as was the case with the feed mixture.

A comparison of the electron diffraction pattern with the X-ray patterns of various copper compounds is shown in figure 5.06, in which, in addition to the compounds named in the figure, the following patterns are presented:-

Figure 5.05

Sample 21.11, colloidal fraction.

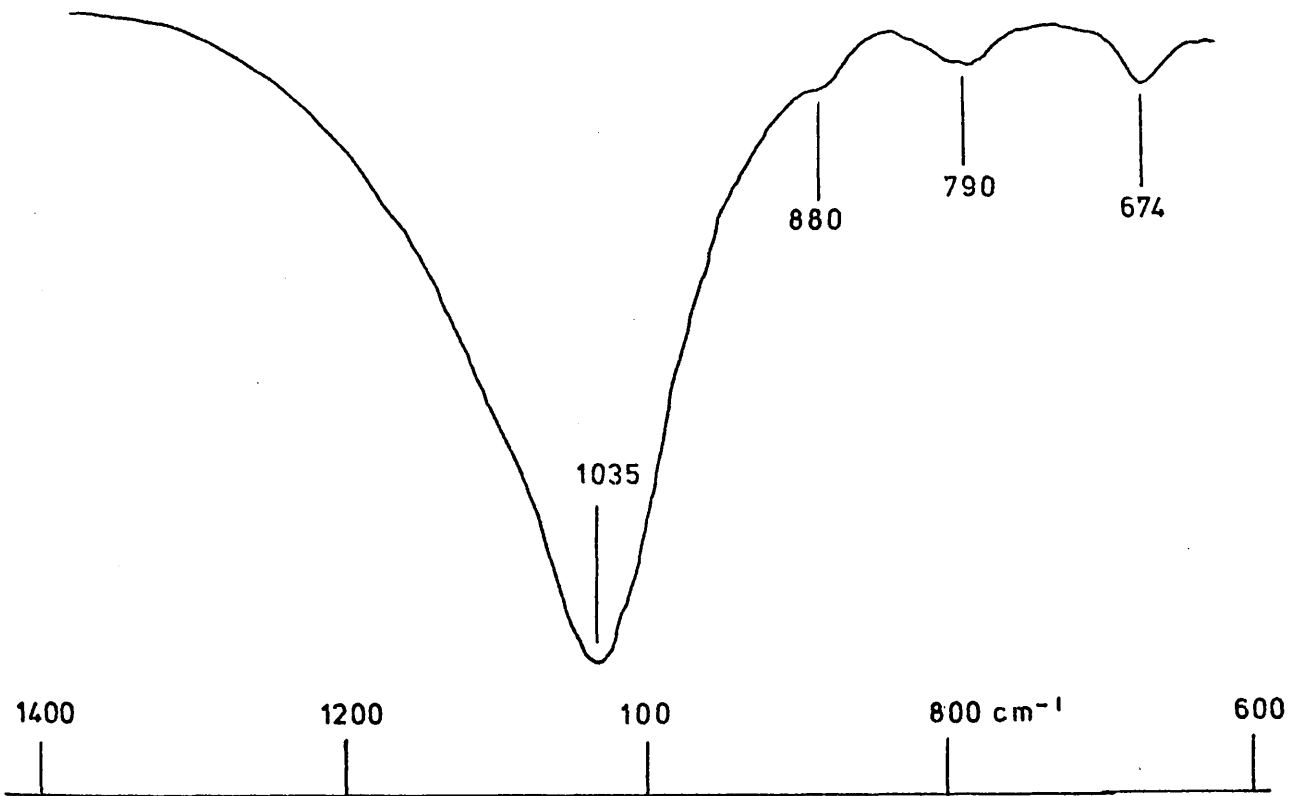
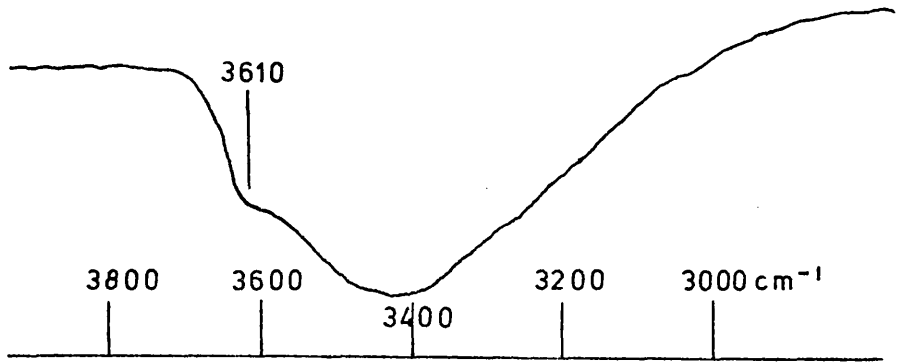


TABLE 5.03

d- spacings from samples from Run 21.

Natural Chrysocollas. (Ref. 38)	ASTM 11-322	21.11	21.15	21.16
17.7 - 18				
12.4 - 13.3				
7.5 - 8	8.3			
	5.72			
4.14 - 4.46	4.43	4.19	4.21	4.22
	3.57	3.32		
2.79 - 2.92	2.92	2.86	2.90	
		2.66		
2.49 - 2.63	2.49	2.48	2.47	2.49
			2.08*	
1.60 - 1.63	1.638	1.64	1.63	
1.474-1.496	1.494		1.48	
	1.334	1.38	1.31	
		1.26?		
	0.957			
	0.879			

ASTM 11-322, Chrysocolla from Belgian Congo.

* Copper (111), d= 2.088.

Spacings in Angstroms.

Figure 5.06

Diffraction patterns of Copper Oxides and Silicates.

Ref:-
Sample:
21.16

21.15

21.11

ASTM:
5-667 Cuprite

5-661 Tenorite

4-836 Copper

7-172 Dioptase

11-322 } Chrysocolla
3-219 }

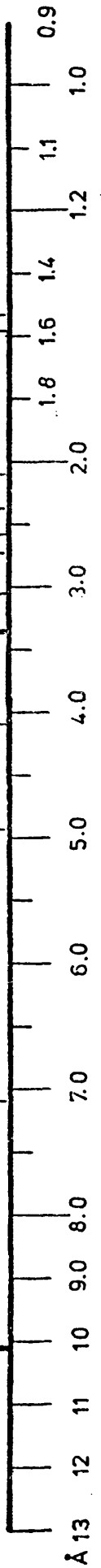
See text:
20-356

13-507

13-501

††

11-248



ASTM - No.	Compound
20-356	: Shattuckite, $\text{Cu}_5(\text{SiO}_3)_4(\text{OH})_2$
13-507	: Shattuckite, $3\text{CuSiO}_3 \cdot \text{H}_2\text{O}$
*13-501	: "Plancheite", $\text{Cu}_6\text{Si}_5\text{O}_{16} \cdot 2\text{H}_2\text{O}$
+++	: Plancheite, reference (40).
11-248	: Plancheite, $3\text{CuSiO}_3 \cdot \text{H}_2\text{O}$

From figure 5.06 tenorite, cuprite, copper and diopside may be ruled out as candidates for the identity of the product of run 21. The agreement in the literature patterns attributed to chrysocolla is poor, particularly in intensities; nonetheless, reflections near 4.5, 2.9, 2.5 and 1.7 Å are common to both, and a similar pattern of 4.2, 2.8, 2.5 and 1.7 Å occurs in the products. The possibility of shattuckite-like structures seems to be excluded by the lack of strong reflections near 4.9, 3.5, 3.3 and 2.8 Å. A similar lack of spacings above 4.5 Å seems to exclude plancheite-like structures. A description of the literature on the plancheites and shattuckites is given in appendix III.

The infrared spectra of chrysocolla, diopside, shattuckite and plancheite, as described by Tarte (42), are given alongside that of the colloidal fraction of sample 21.11 in table 5.04. A reasonable correspondence between 21.11 and chrysocolla is again observed.

A structure for chrysocolla was described by Van Oosterwyck-Gastuche (43), "intermediate

* This sample was certainly a shattuckite: see Guellemin and Pierrot, (41).

TABLE 5.04.

Infrared Spectra of Copper Silicates.

1	2	3	4	5
3620 vw		3600 vs	3610 w	~3610 w
3450 s	3368 s	3300 vs	3380 m	3410 s
	3210 w	3220 m		
1640 m				1645 m
		1100 vw	~1140 w	
		1077 w		
1030 vs		1045 vw	~1035 vs	1035 vs
	1000 vs	1019 vs		
	960 s	962 m	~950 m	
	939 m	925 vw		
		905 vw		
	888 s	870 m	880 w	880 vw
			842 w	
785 w	781 m		765 vw	790 w
	727 vw		735 vw	
675 m	676 vw	660 m	660 m	674 w
	611 vw	630 vw	630 vw	

1 - Chrysocolla

2 - Dioptase

3 - Shattuckite

4 - Plancheteite (spectrum 'B')

5 - Sample 21.11 colloidal fraction.

} from Tarte, P., (42).

Band frequencies in wavenumbers.

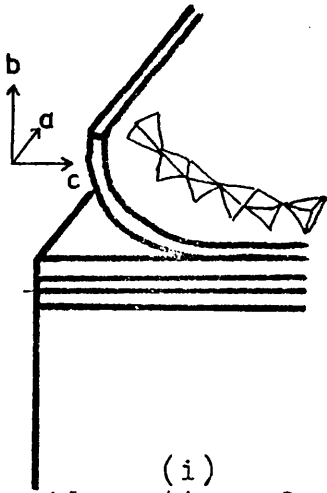
between a layer structure and a simple chain structure". In this work, the range of X-ray spacings given for natural chrysocolla samples was as follows:-

d, Å	I	hkl
17.7 - 18	s	010
12.4 - 13.3	vs	---
7.5 - 8	s or w	001
4.14- 4.46	s or w	040
2.79- 2.92	s	060
2.49- 2.63	m or s	070
1.600- 1.625	w	0.11.0
1.474- 1.496	vs	0.12.0,

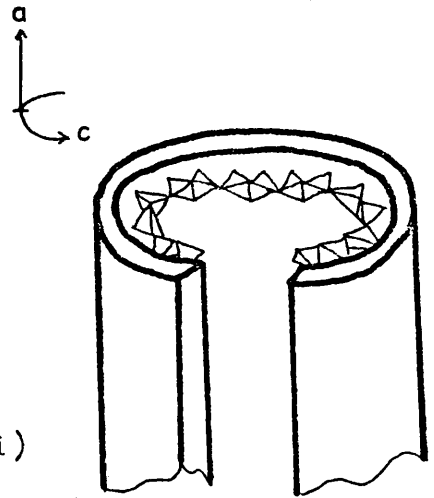
the indices corresponding to unit cell dimensions in the range $a=4.92-6.16$, $b=8.85-8.91$, $c=6.4-8.6$ Å. The structure is described as involving "chains of four silicate tetrahedra pointing alternately up and down, bound to chains formed of four copper atoms hexa-coordinated to oxygen atoms, hydroxyls and water molecules".

It is possible to derive such a structure from the exfoliative adsorbate postulated for sample 21.09, by the transformations outlined schematically in figure 5.07. This approach, however, requires that, at least initially, adsorption occurs on only one side of the $\text{Cu}(\text{OH})_2$ layers, thus causing curling by the misfit between the octahedral layer and the developing silicate chains. Coverage of only one side gives a Si:Cu ratio of 0.5 (see figure 1.02, top of unit layer of $\text{Cu}(\text{OH})_2$ structure). To obtain the expected Si:Cu ratio of 1.0 (43), the other side of the $\text{Cu}(\text{OH})_2$ layer must become covered, and, if the scheme outlined in figure 5.07 is correct, must detach

Figure 5.07

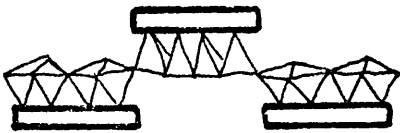


(i)
Adsorption of
silicate ion
chains on (010)
face of $\text{Cu}(\text{OH})_2$.
Initial (010)
cleavage.



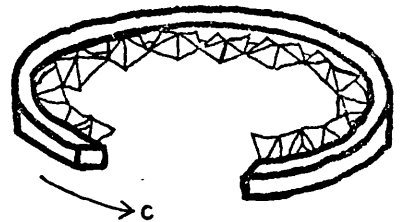
(ii)
Adsorbate tubes:
sample 21.09:
original double
octahedral layer
intact.

(100)
cleavage.



(iv)
Chrysocolla-
like chains.

(001)
cleavage.
 180° rotation
in blocks of 4
silicons.



(iii)
Double octahedral layer
must now break up, by
further adsorption or
by a solution process.

itself from the top half before the (001) cleavage and rotation takes place. The same result would be obtained if the bottom half of the double octahedral layer dissolved away from the adsorbate and recrystallized as $\text{Cu}(\text{OH})_2$, between stages (ii) and (iv) of figure 5.07.

5.03 Conclusions.

The changes in morphology, electron diffraction and infrared spectra which take place during the reaction can be interpreted as due to the formation of a chrysocolla-like copper silicate of low crystallinity. The reaction can be described as a sequence of adsorption and cleavage steps, outlined in figure 5.07.

The formation of chain silicates rather than phyllosilicates appears to occur with the hydroxides of larger cations (Ionic radii: $\text{Ca}^{2+}=0.99$, $\text{Cd}^{2+}=0.98$, $\text{Cu}^{2+}=0.72 \text{ \AA}$). True phyllosilicates form from hydroxides of smaller cations ($\text{Mg}^{2+}=0.66$, $\text{Fe}^{3+}=0.64$, $\text{Al}^{3+}=0.51 \text{ \AA}$). Distortion of the symmetry of the octahedral layer is related to cation radius, since the radius of the octahedral hole in an hexagonal close packed oxide lattice is 0.61 \AA : cations of larger radii disturb the close-packing.

PLATE 5.01

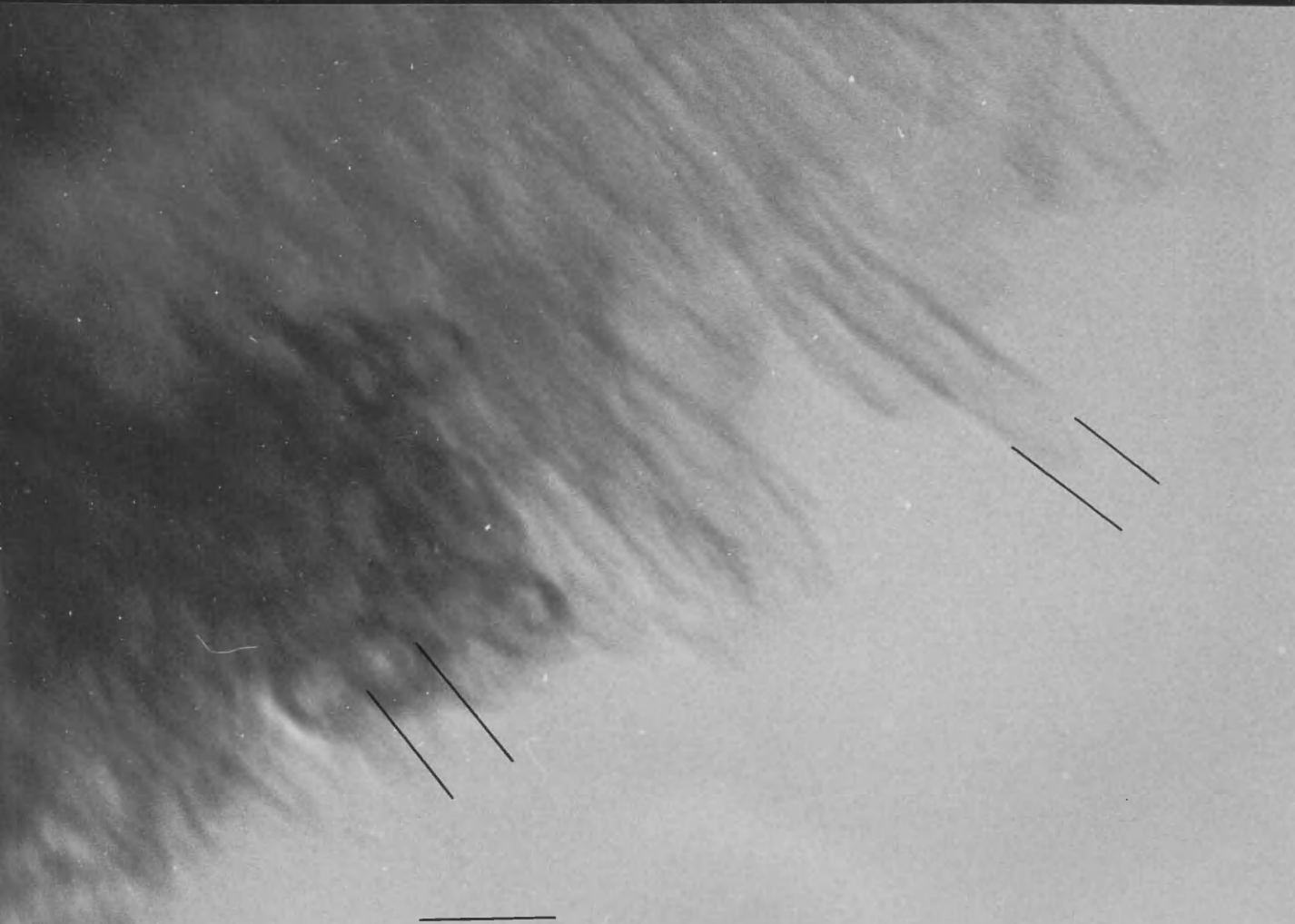
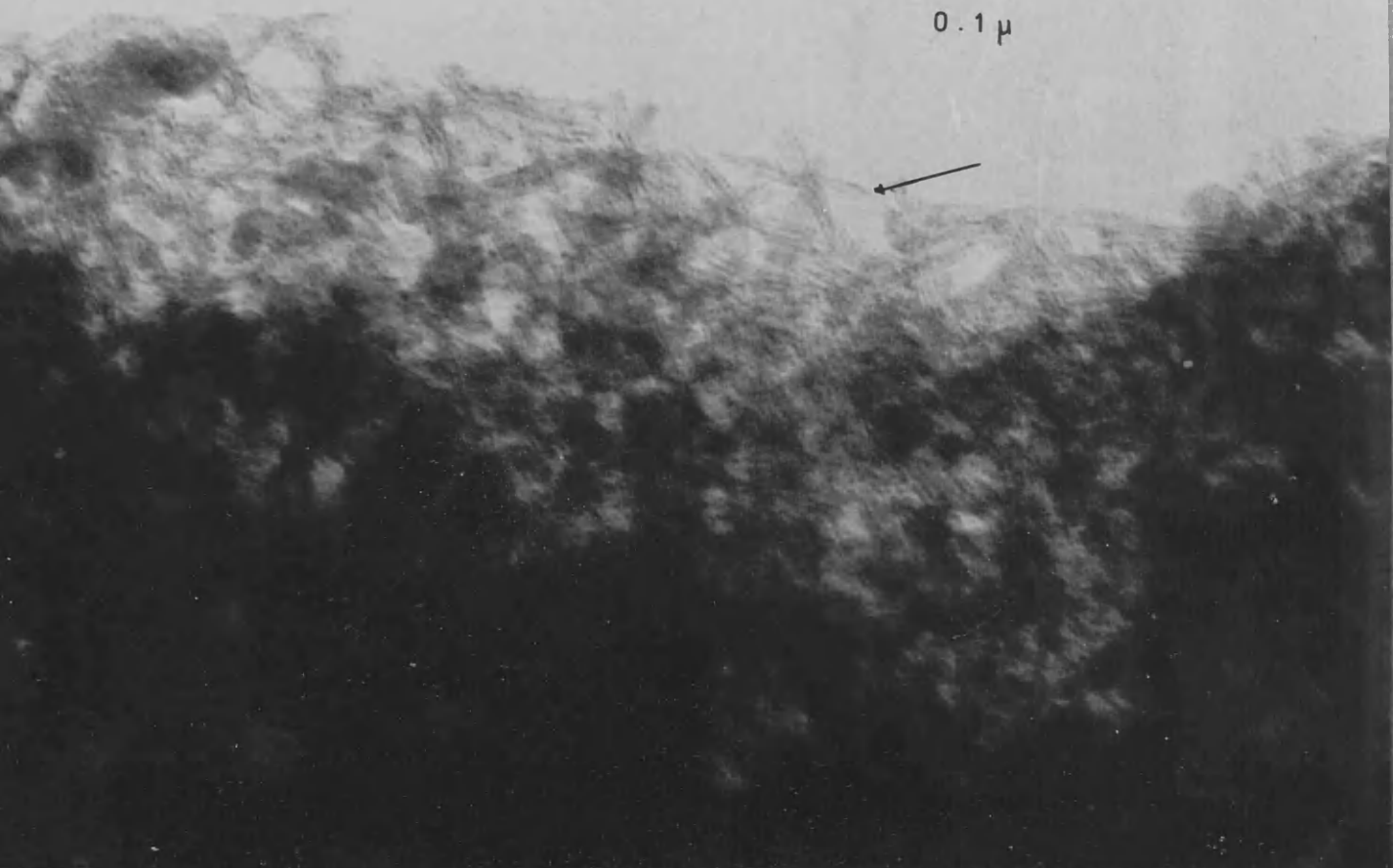
PLATE 5.01

0.1 μ



PLATE 5.02

0.1 μ



10.0 nm

PLATE 5.03

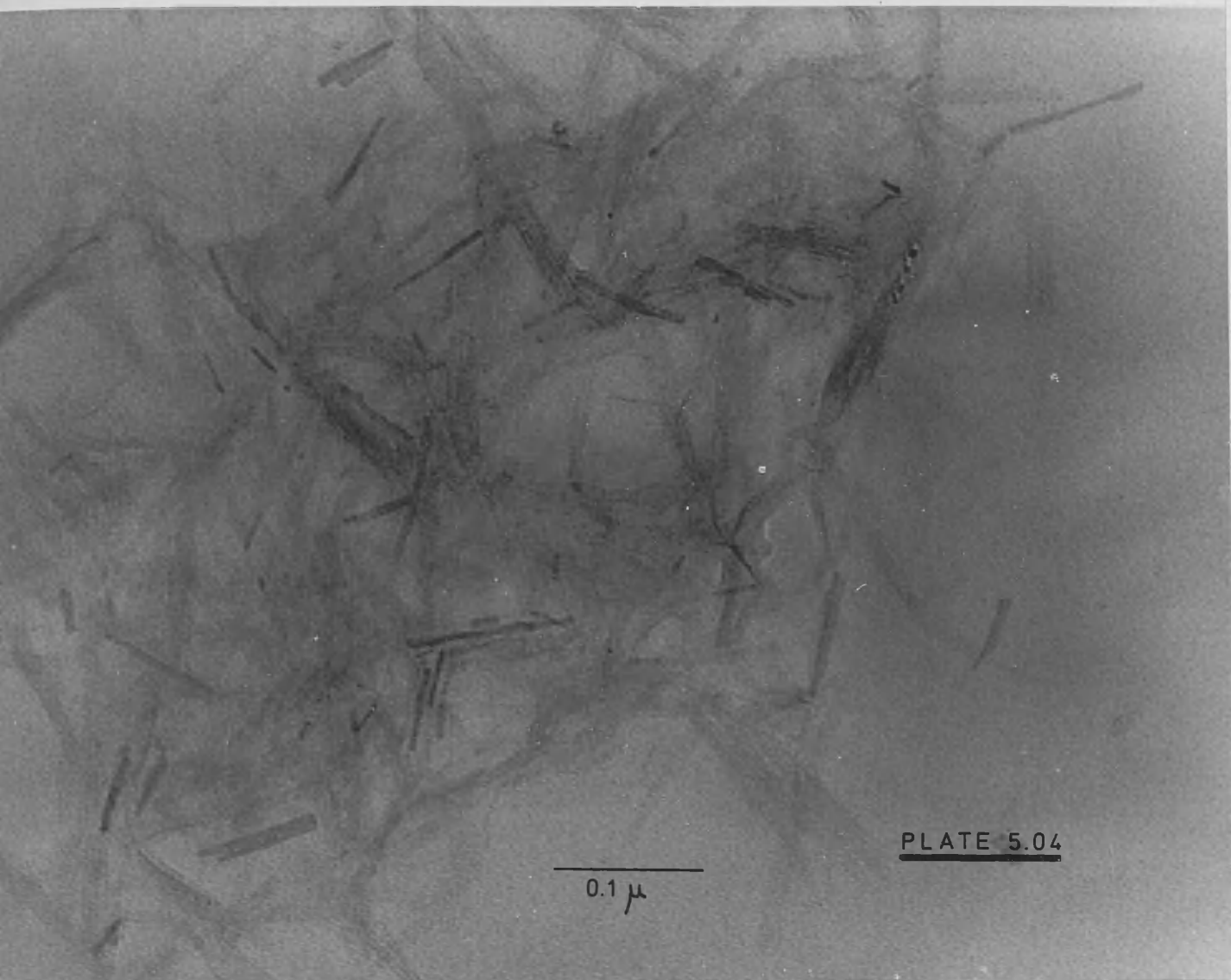


PLATE 5.04

0.1 μ

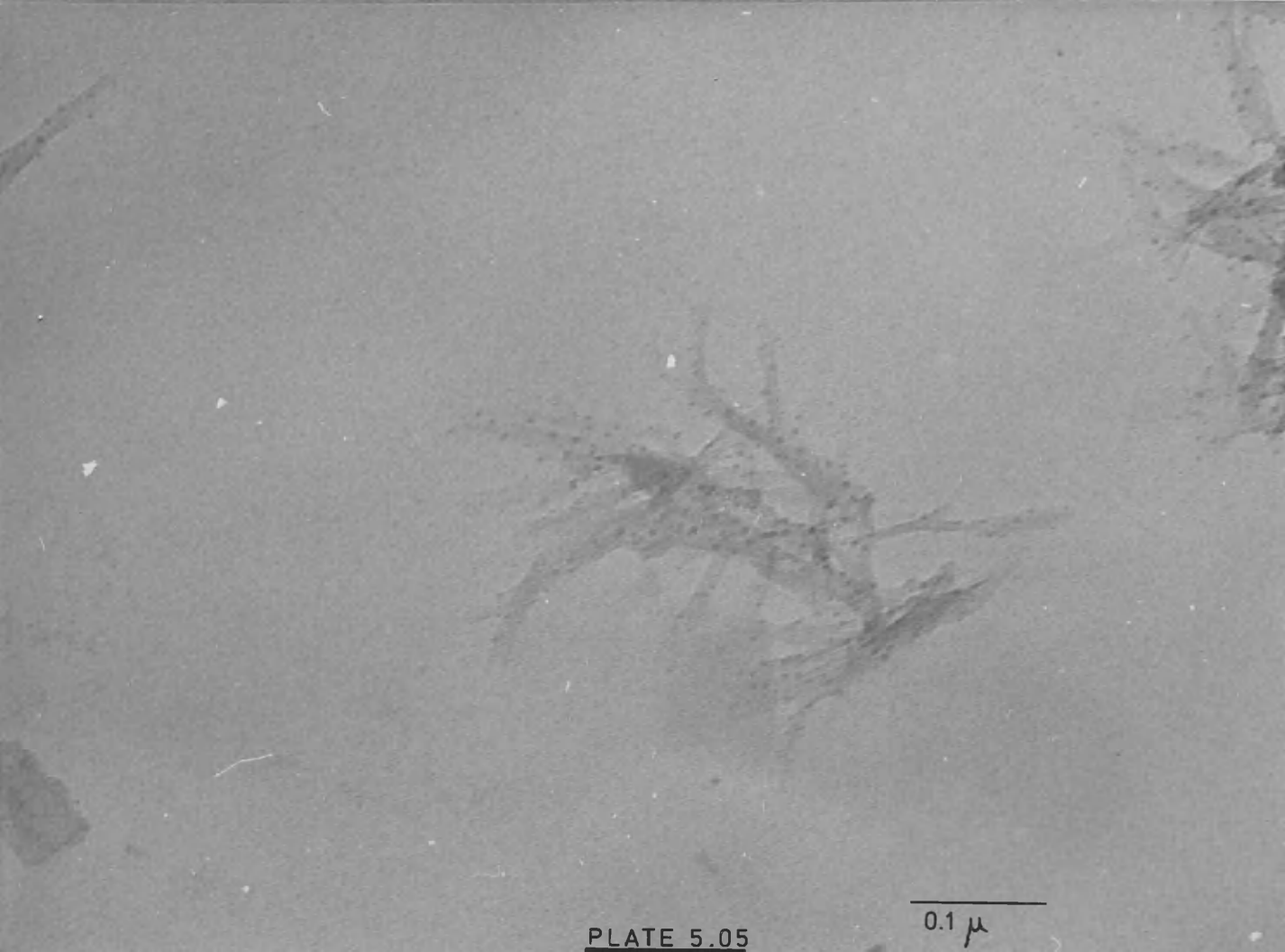


PLATE 5.05

0.1 μ

CHAPTER 6. BERYLLIUM AND ZINC HYDROXIDES.

6.01 Experimental

The precipitation of beryllium hydroxide from beryllium sulphate solution with ammonia solution yields an amorphous gel which will age in contact with the mother liquor to the metastable α - $\text{Be}(\text{OH})_2$. In the absence of ammonium ion, aging leads to the thermodynamically stable β - form, very slowly at room temperature but in only a few hours at 150°C . (44). It was expected, then, that in an attempt to bring about reaction of amorphous (am-) $\text{Be}(\text{OH})_2$ with silica gel, rapid aging of the hydroxide to β - $\text{Be}(\text{OH})_2$ would occur.

Am - $\text{Be}(\text{OH})_2$ was precipitated from BeSO_4 solution by adding the stoichiometric amount of 0.880 s.g. ammonia solution. The white gelatinous precipitate was washed with distilled water until free of NH_4^+ and freeze-dried. A 10% slurry was made up with Mallinkrodt silica gel in the proportions $\text{Be}:\text{Si} = 0.75$, the pH adjusted to 10 by adding solid LiOH , and the run refluxed. This was run 23: sample times are given in table 6.01.

There are five polymorphs of zinc hydroxide, designated α , β , γ , δ , and ϵ , of which the last is thermodynamically stable, the others being metastable (8). The metastable varieties are difficult to prepare in macro-crystalline form (8), while the ϵ -polymorph can be crystallized slowly from dilute sodium zincate solutions, in the absence of atmospheric carbon dioxide (45), large

TABLE 6.01

Sample times for the Zinc and Beryllium runs.

Time (mins)	Sample Nos.		
	Run 23	Run 35	Run 36
0	23.00	35.00	
80			36.01
120		35.01	
144	23.01		
248	23.02		
260		35.02	
280			36.02
636	23.03		
740		35.03	
1130			36.03
1200		35.04	
1290	23.04		
1575		35.05	
1706	23.05		
2615			36.04
2895		35.06	
4030			36.05
4225		35.07	
5500			36.06
5605		35.08	
7056	23.06		

crystals being obtained. Unit cell dimensions have been reported for all the polymorphs (8), but the structures of only the ϵ - (46,47) and δ - (48) forms are known.

Precipitation of zinc salt solutions with alkalis is very complex. Zinc sulphate solution with excess of sodium or potassium hydroxide gives zinc oxide, and with ammonia gives a zinc hydroxide sulphate, the composition depending on the solution concentrations and amounts. Zinc nitrate solution with the stoichiometric amount of ammonia gives a mixture of amorphous and metastable hydroxides. Excess ammonia dissolves the precipitate by formation of zinc ammine complexes. The possibility of the formation of a zinc hydroxide nitrate also exists.

Attempts to prepare pure zinc hydroxide samples were made as follows:-

Analar zinc nitrate solution was precipitated with ammonia, and the precipitate washed and dried in a vacuum oven at 30°C over P_2O_5 . This precipitate was then redissolved in 5% aqueous ammonia and crystallized by withdrawing the ammonia in a desiccator over conc. sulphuric acid. In one day a large batch of white crystals formed, which was filtered off, washed, and dried under vacuum at 30°C .

Recrystallization of the same precipitate from 0.880 s.g. ammonia gave, in four days, a batch of transparent pyramidal crystals formed on the base and sides of the flask. These were similarly treated.

The first batch was found to consist almost entirely of small needle-shaped crystals of δ - $\text{Zn}(\text{OH})_2$ (Plate 6.01), most of them lying, in the EM, on the

(100) face, together with a small amount of amorphous $\text{Zn}(\text{OH})_2$. The crystals from the second crystallization proved to be the stable ϵ - $\text{Zn}(\text{OH})_2$, as found by Dietrich and Johnston (49).

Runs 35 and 36 were set up with δ - and ϵ - $\text{Zn}(\text{OH})_2$ respectively, as 10% slurries with $\text{Zn}:\text{Si} = 0.75$, the proportions being thus chosen to provide an excess of silica for the formation of hemimorphite or willemite, and enough for the formation of an hypothetical 2:1 phyllosilicate. Refluxing and sampling were done as before, sample times being shown in table 6.01.

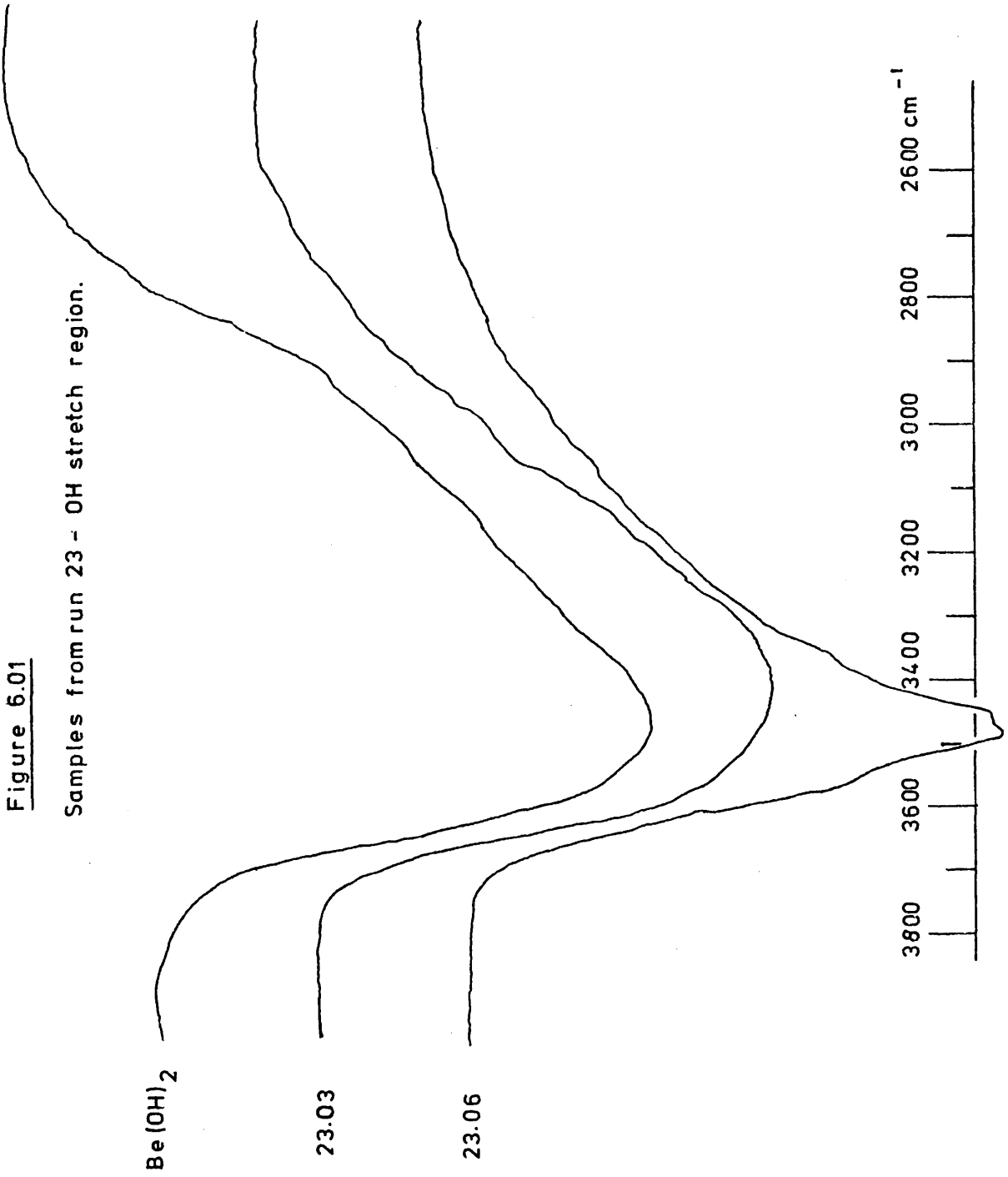
X-ray powder diffraction patterns were recorded on threads of "Durofix"-embedded sample, using $\text{Cu K}\alpha$ radiation with a nickel filter, and a Phillips 57.3 mm radius camera.

6.02 Results and discussion.

The infrared spectra of the freshly-precipitated $\text{Be}(\text{OH})_2$ and of samples 23.00, 23.03 and 23.06 are shown in figures 6.01 and 6.02. The spectra of am-, α -, and β - $\text{Be}(\text{OH})_2$ were reported in some detail by Bear et al. (44). Table 6.02 gives a comparison of the main features of the spectra of samples 23.00 and 23.06 with those of am- and β - $\text{Be}(\text{OH})_2$. It is evident from the shifting and narrowing of the bands from the run 23 samples, that aging of the amorphous hydroxide precipitate is proceeding unhindered by the presence of the silica gel, β - $\text{Be}(\text{OH})_2$ being formed. There is no change in the

Figure 6.01

Samples from run 23 - OH stretch region.



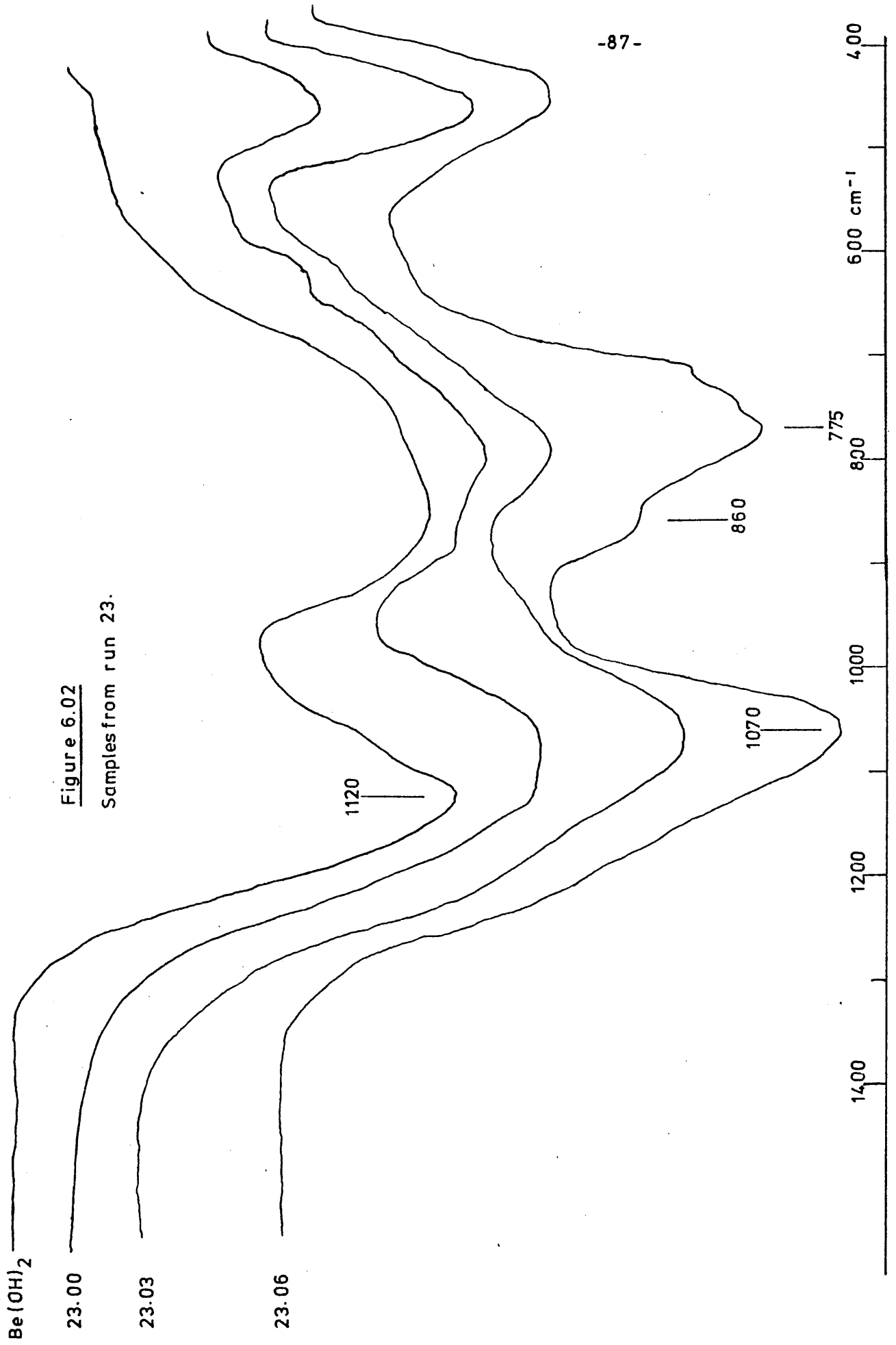


Figure 6.02
Samples from run 23.

$\text{Be}(\text{OH})_2$

23.00

23.03

23.06

1120

1070

860

775

4.00

600 cm^{-1}

800

1000

1200

1400

TABLE 6.02

Infrared bands from run 23 - comparison with $\text{Be}(\text{OH})_2$.

1 23.00	2 23.06	3 $\text{Am-Be}(\text{OH})_2$	4 $\beta\text{-Be}(\text{OH})_2$
	3570 sh		3615 sh
	3485 s		3590 sh
3470 vb, s	3460 s	3470	3505 sh
3400 vb, s	3370 b, sh		3495
			3450
1130 vb, sh		1125	
1070 vb, s	1070 s, b		1070
880 b, s	865 m, b		880
800 vb, s	775 s, b	845	780
	750 sh	725	755
	715 sh		720
			685
			610

$\text{Be}(\text{OH})_2$ spectra - ref. 50

b = broad
s = strong
m = medium
sh = shoulder

frequencies in cm^{-1} .

position of the main Si-O stretch band at 1080 cm^{-1} . It can be concluded that no intrastructural adsorption of silicate ion takes place in the time elapsed to sample 23.06. X-ray diffraction of sample 23.06 gave three of the four strongest reflections of β -Be(OH)₂.

X-ray powder data for the starting materials of runs 35 and 36 are recorded in table 6.03, and infrared spectra in table 6.04. Good correspondence is observed for γ -Zn(OH)₂ and ϵ -Zn(OH)₂.

Syntheses from dilute solutions of zinc ion with sodium silicate solutions were reported to yield hemimorphite at pH 10 - 12 and willemite at pH 6.5 - 8.5 (50,51). It was therefore expected that the final product, if any, of runs 35 and 36 would be hemimorphite.

Infrared spectra of samples from run 35 are shown in figure 6.03. The silica gel Si-O stretch band at 1080 cm^{-1} is replaced by a new band at 1010 cm^{-1} by sample 35.05, and this in its turn is gradually replaced by the bands, marked 'H', of the spectrum of hemimorphite (52). Sample 35.05 was found to consist of very small particles with a fine-grain, weak, diffuse polycrystalline diffraction pattern (Plate 6.02) with spacings similar to, but not identical with, hemimorphite. By 35.06, small crystals of hemimorphite were visible (Plate 6.03) among the earlier material. These were identified as hemimorphite by electron diffraction in two different zones (Plates 6.04 and 6.05): the (220) lattice spacing (3.30 \AA) was resolved (Plate 6.06).

TABLE 6.03

Diffraction data for the zinc hydroxides.

$d, \text{\AA}^1$	I	$d, \text{\AA}^2$	I	$d, \text{\AA}^3$	I	$d, \text{\AA}^4$	I
7.50	s	7.56	40				
		5.74	20				
5.54		5.50	30	4.44	vs	4.41	100
		3.98	40	4.22	s	4.26	80
3.80	vs	3.83	90			3.54	50
		3.75	80	3.23	vs	3.28	100
3.28	vs	3.27	100	3.19	s	3.19	80
		3.26	100	2.72	s	2.71	80
3.03	vs	3.03	90			2.57	50
		3.02	90	2.46		2.45	80
		2.938	90			2.35	50
2.88		2.873	80	2.28	s	2.28	80
		2.761	60	2.21	s	2.20	80
2.71		2.688	10	2.14		2.14	80
2.54		2.527	60			2.01	30
2.46		2.431	20	1.74		1.74	80
2.33		2.328	70	1.64		1.64	80
2.22	s	2.220	90	1.59		1.57	80
		2.015	30	1.55		1.55	80
2.00		1.991	30	1.53		1.53	80
1.71		1.725	60				
1.65	s	1.646	90				
1.61	s	1.610	90				

- 1 - Run 35 starting material.
- 2 - ASTM 20-1437, γ - Zn(OH)₂.
- 3 - Run 36 starting material.
- 4 - ASTM 12-479, ϵ - Zn(OH)₂.

TABLE 6.04

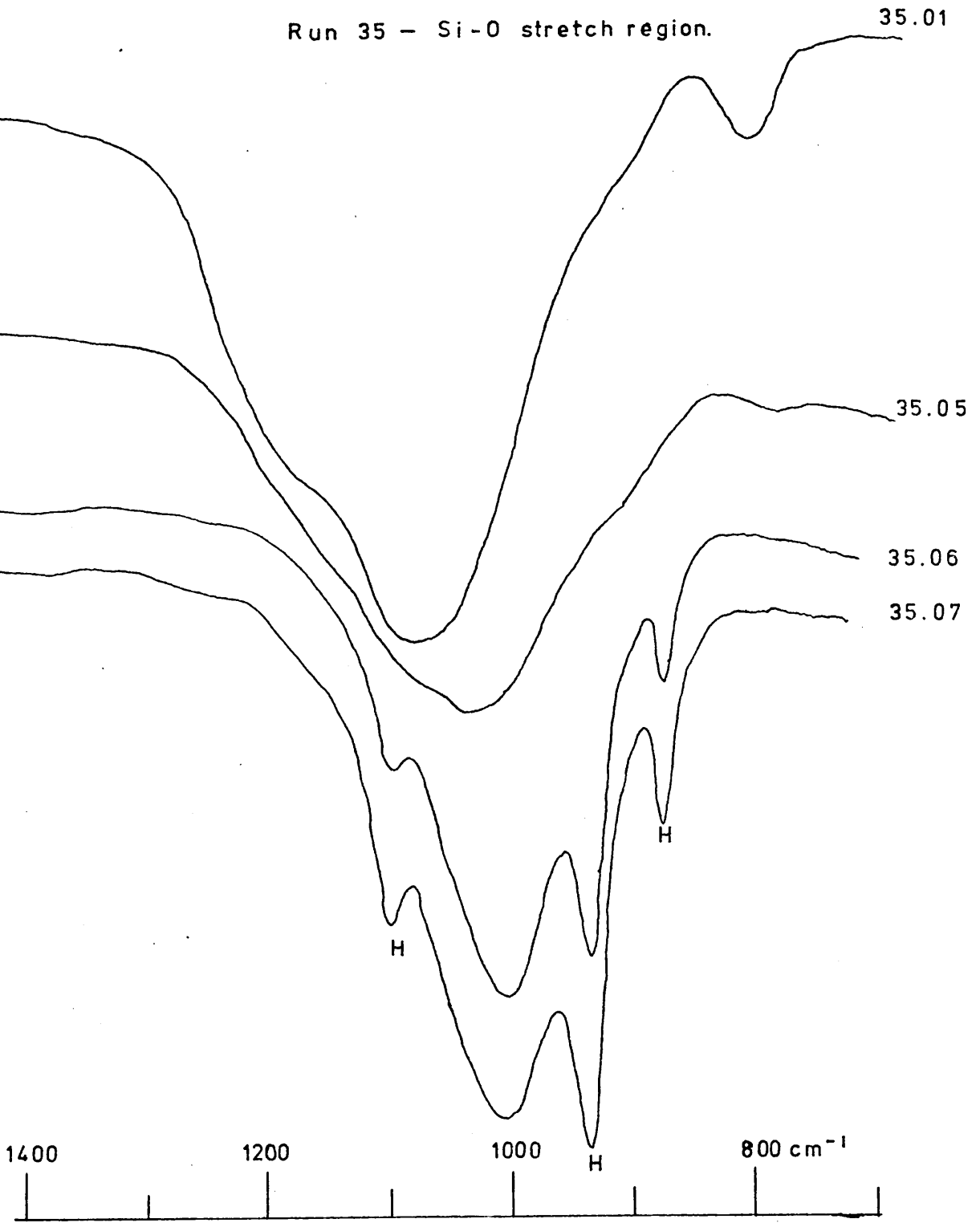
Infrared data for the zinc hydroxides.

ϵ - Zn(OH) ₂		γ - Zn(OH) ₂	
Frequency (cm ⁻¹)	Intensity (est.)	Frequency (cm ⁻¹)	Intensity (est.)
3260	vs, b	3275	vs, b
		1388	m
		1169	s
1094	s	1105	s, sh
1047	s	1090	s, sh
		1070	s, sh
		1049	s
		1000	vW
850	m	860	s, b
		810	s
775	m	750	vW
722	s	702	m
550	m, sh	572	s
518	s	545	s
490	s	490	w
		451	s
		428	m, sh
410	s		
374	s	380	s
		365	s

b = broad
sh = shoulder

Figure 6.03

Run 35 - Si-O stretch region.



H — hemimorphite bands

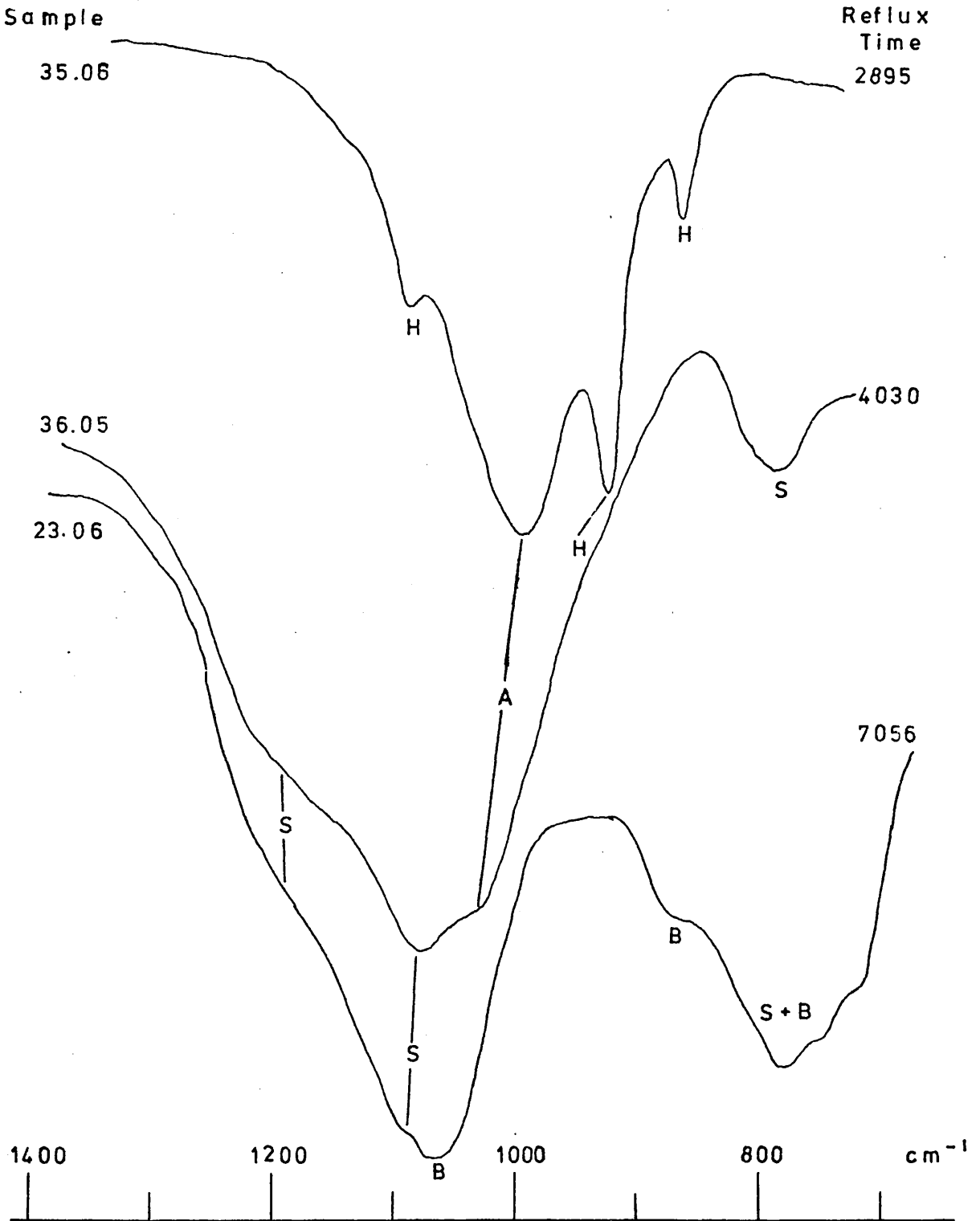
By contrast, the spectrum of sample 36.05, later than 35.06 by nineteen hours, shows none of the hemimorphite bands, and the 'adsorbate' Si-O stretch is only of medium intensity. No hemimorphite crystals were found in the EM, and the low-particle-size fraction of the sample had only a veryweak, diffuse electron diffraction pattern with no measurable rings. Adsorbate formation from $\epsilon - \text{Zn}(\text{OH})_2$ was very much slower than from $\gamma - \text{Zn}(\text{OH})_2$.

The spectra of samples 35.06, 36.05 and 23.06 are shown together in figure 6.04 (Si-O stretch region). The structures of $\gamma - \text{Zn}(\text{OH})_2$ and of hemimorphite (53) are shown schematically in figures 6.05 and 6.06. No obvious adsorption-and-cleavage pathway, such as was suggested for chrysocolla in chapter 5, is evident between the two structures. The adsorbate must therefore dissolve and recrystallize for hemimorphite to be formed.

6.03 Conclusions.

$\gamma - \text{Zn}(\text{OH})_2$ forms an adsorbate with silicate ion which recrystallizes to form hemimorphite. The reaction is fairly rapid, recrystallization of the adsorbate commencing after about 36 hours at reflux. $\epsilon - \text{Zn}(\text{OH})_2$ reacts similarly, but much more slowly, the adsorbate being only partially formed after 90 hours, by which time no recrystallization to hemimorphite is observed. No evidence for the formation of an adsorbate with $\beta - \text{Be}(\text{OH})_2$ was found after 118 hours at reflux.

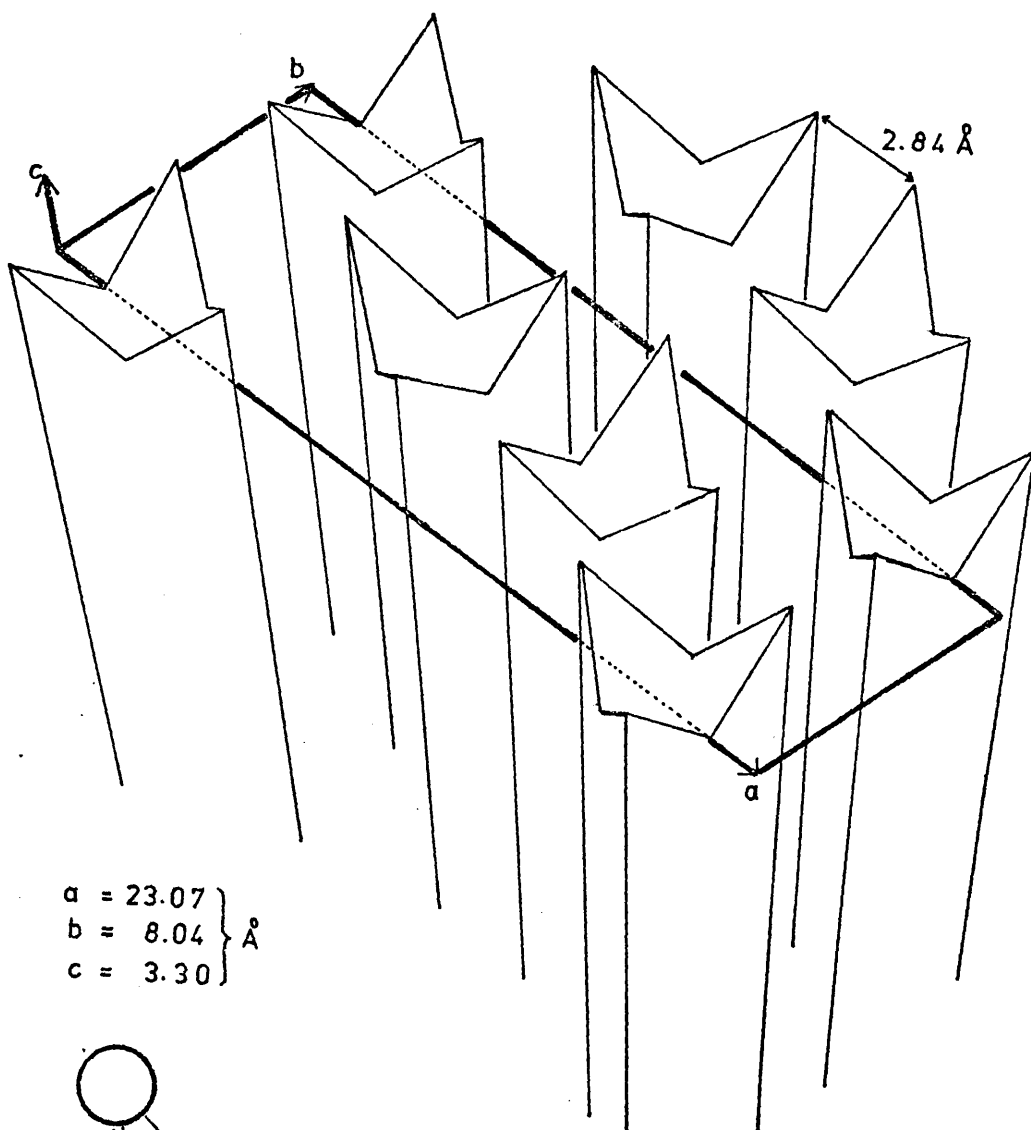
Figure 6.04



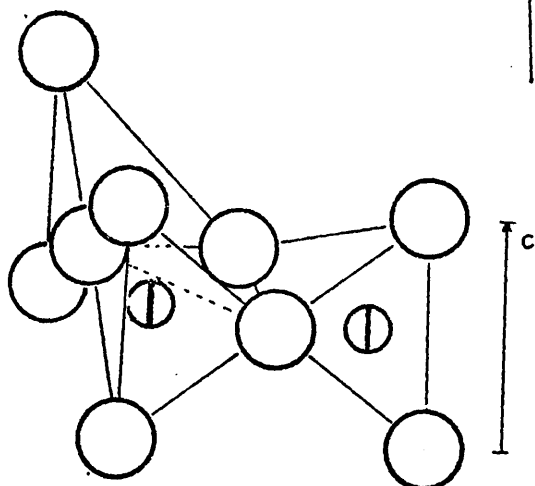
- H - hemimorphite
- B - β -Be(OH)₂
- S - amorphous silica
- A - silica-hydroxide adsorbate

Figure 6.05

Structure of γ -Zn(OH)₂



$\left. \begin{array}{l} a = 23.07 \\ b = 8.04 \\ c = 3.30 \end{array} \right\} \text{Å}$

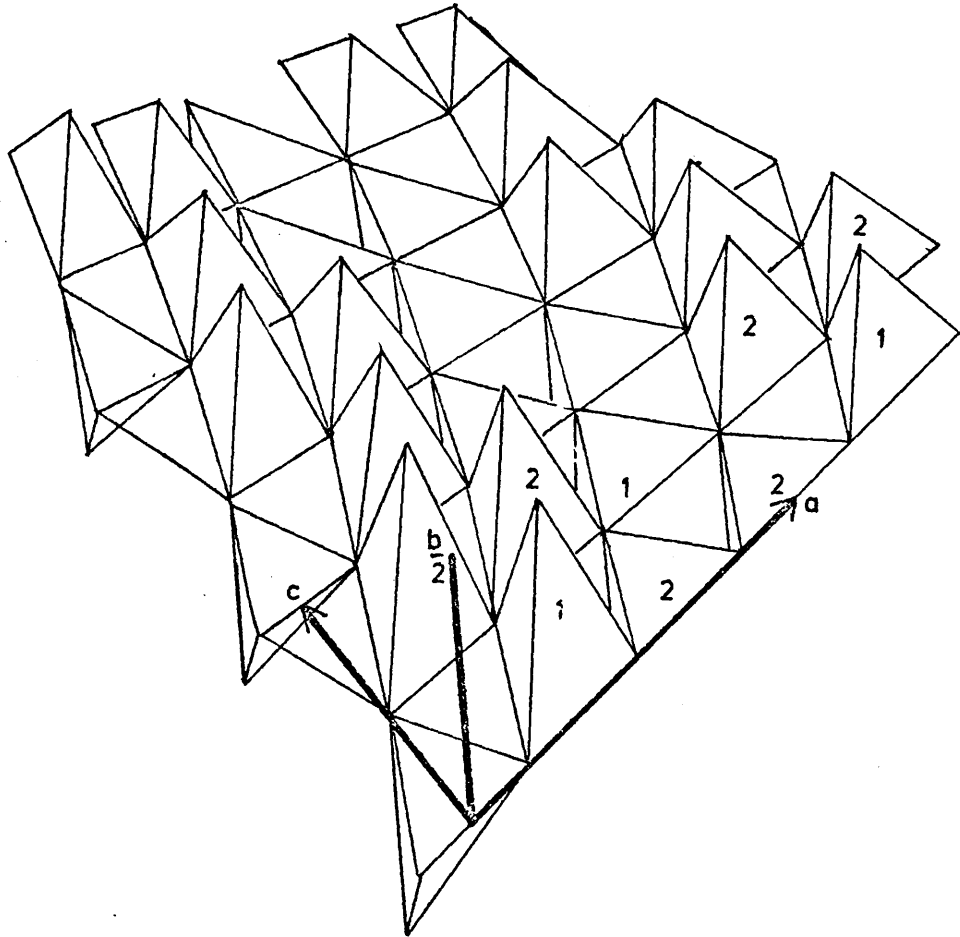


⊕ Zn(3)
 ○ OH(6)

Arrangement of atoms in c-axis repeat unit.

Figure 6.06

The hemimorphite layer.

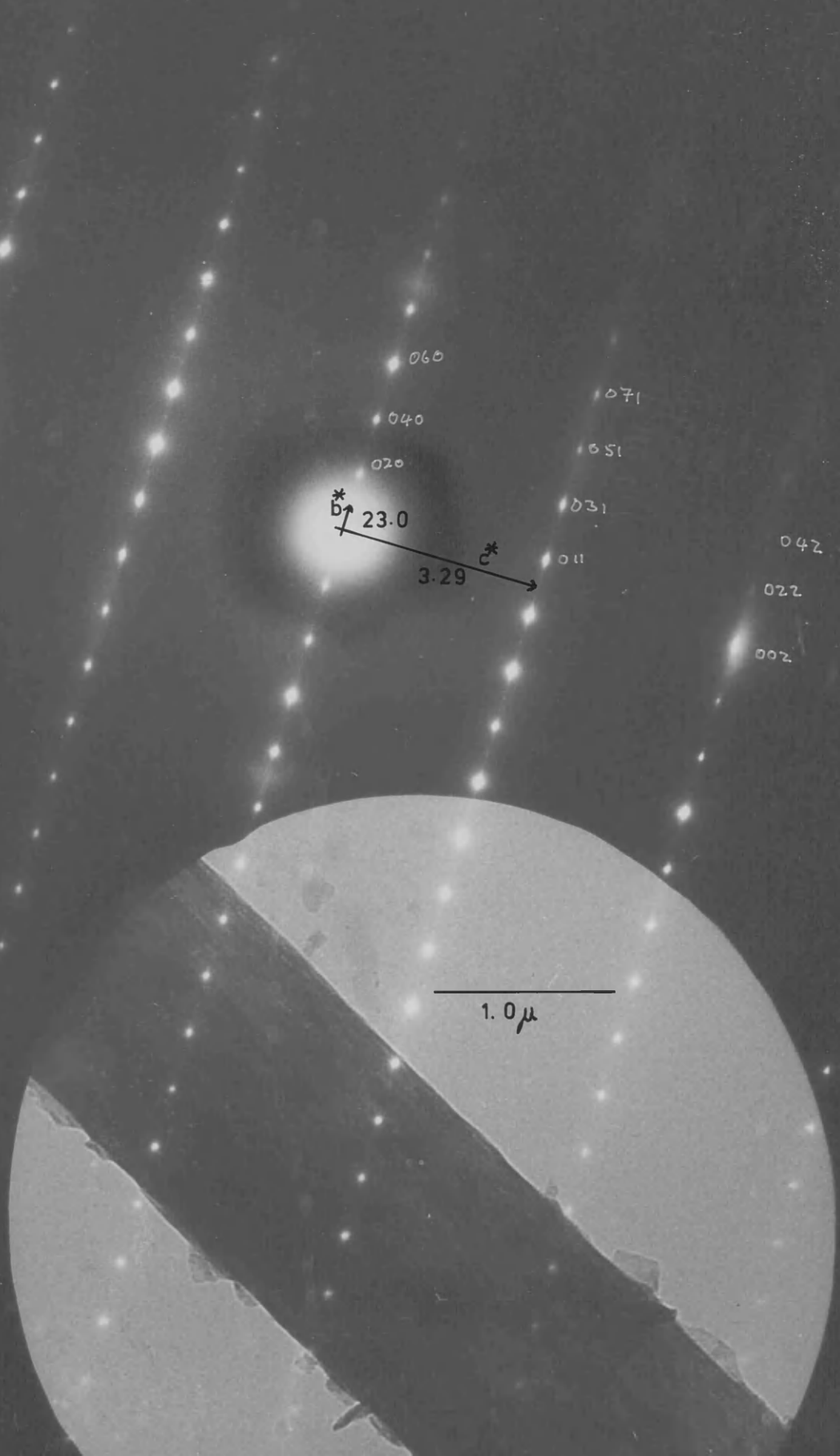


$$\left. \begin{array}{l} a = 8.370 \\ b = 5.360 \\ c = 5.120 \end{array} \right\} \text{ \AA}$$

- 1 — SiO₄ tetrahedra
- 2 — ZnO₄ "

PLATE 6.01

γ -Zn(OH)₂ - (100) r.l.p.



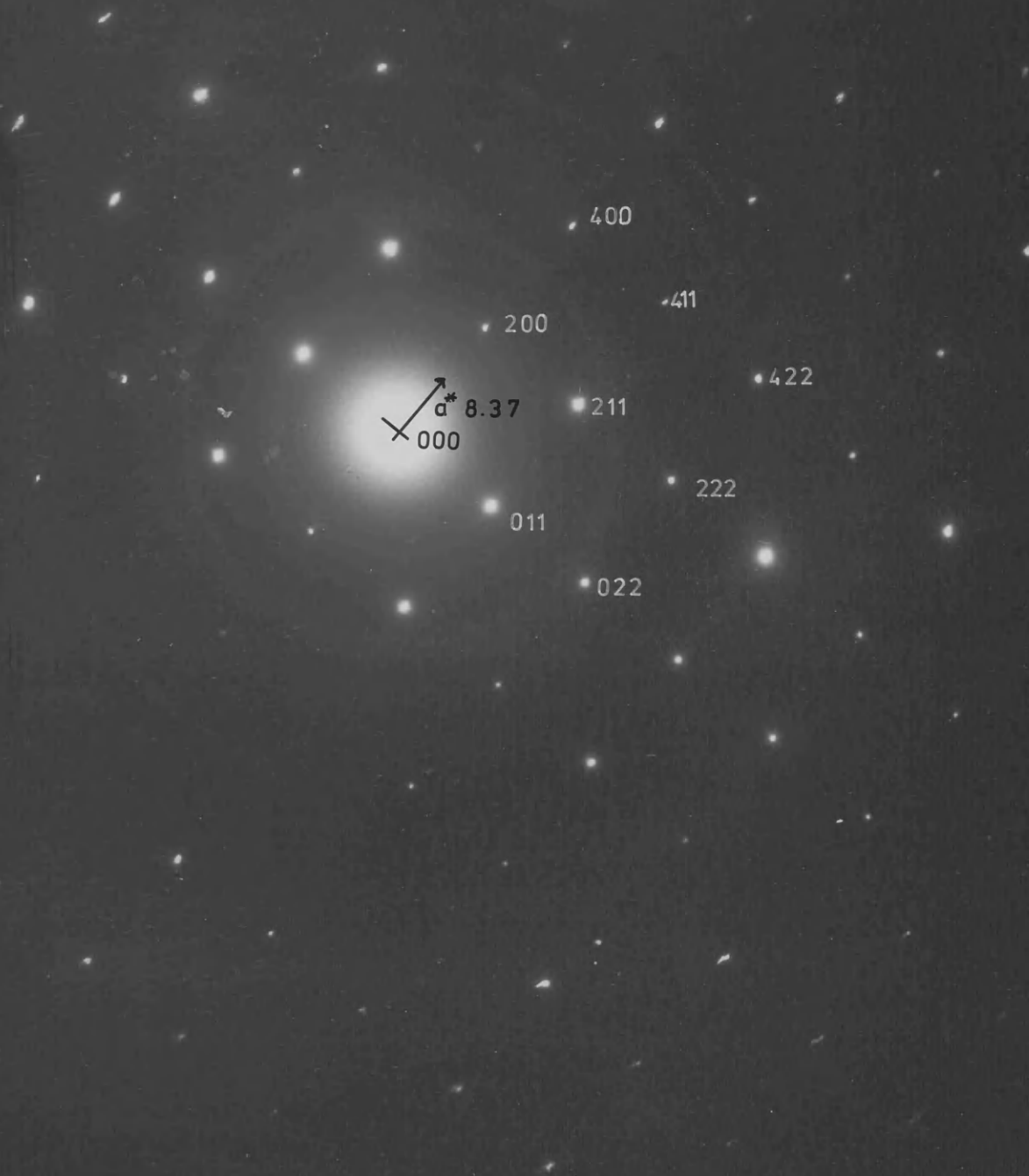
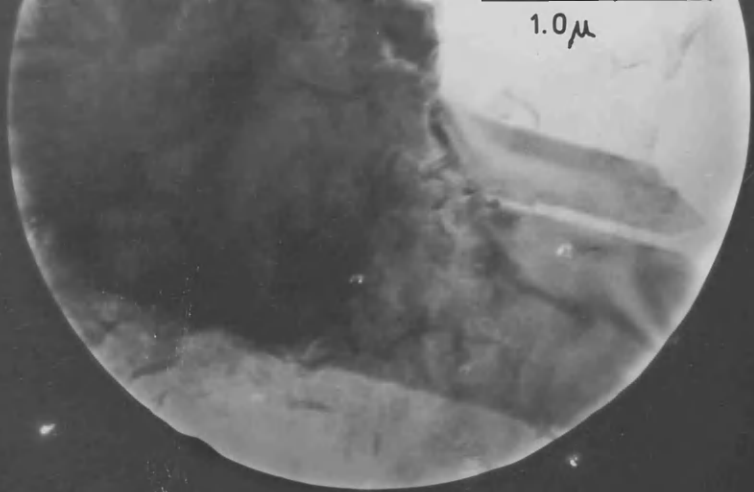


PLATE 6.04

Sample 35.06

Hemimorphite - (011) r.l.p.

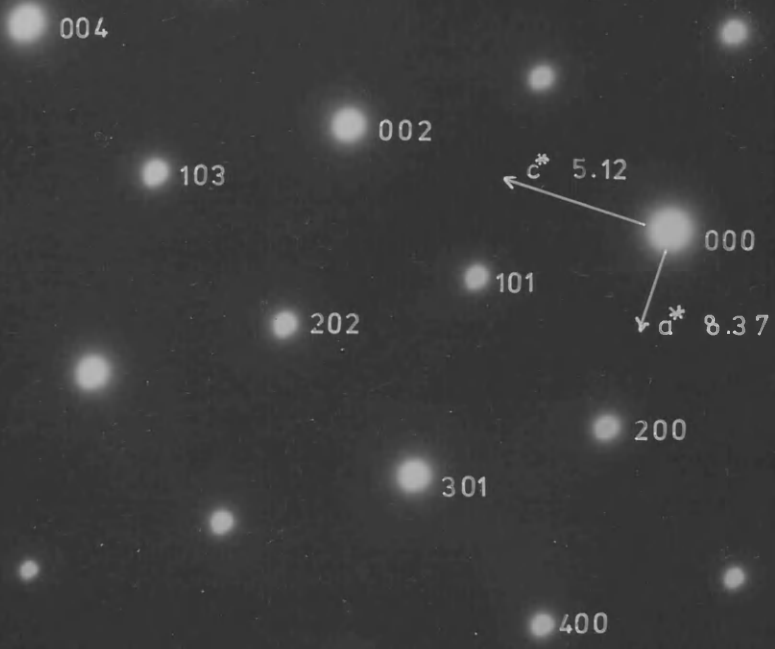


PLATE 6.05

Sample 35.06
Hemimorphite - (010) r.l.p.

PLATE 6.06

 3.3 Å

CHAPTER 7.

Magnesium Hydroxide -- Higher temperature work.

7.01 Introduction.

Besson, Caillère and Henin reported (18) the synthesis of a phlogopite-like magnesium silicate by repeated evaporation and dissolution, in Pyrex flasks, of saturated potassium carbonate solutions containing solid magnesium hydroxide. The X-ray powder pattern obtained from the product identified it as a phlogopite.

The use of boiling saturated potassium carbonate solution as the reaction medium provides a reflux temperature of about 115° at atmospheric pressure, and a pH above 13. Silicate ion leaches from Pyrex glass quite rapidly under these conditions. Removal of the silicate ion from the solution by adsorption onto a metal hydroxide should lower the silicate ion concentration below saturation, and the Pyrex should dissolve smoothly until silicification of the hydroxide is complete, after which the rate of dissolution should decrease and polymerisation of the silicate ion to silica gel should occur.

In this trial of the method, it was decided to reflux the reaction mixture rather than to follow the evaporation and dissolution cycle described by Besson, Caillère and Henin. This gave better constancy of temperature and pH.

7.02 Experimental.

1.5 g of the magnesium hydroxide described in chapter 2 was added to 100 ml. of saturated (108g/100ml.) potassium carbonate solution, in a 250 ml. Pyrex conical flask equipped with a reflux condenser and a teflon-coated magnetic stirrer. The mixture was refluxed with gentle stirring in an oil bath for eight days (run 15), samples being taken at the times shown in table 7.01. The samples were washed several times with distilled water to remove potassium carbonate and freeze-dried. The total yield of freeze-dried sample was about 4.2 g.

Infrared spectroscopy and electron microscopy were performed as before. Powder X-ray diffraction patterns were recorded using Cu K_{α} radiation (Ni filter), in a Phillips camera of radius 57.3 mm. A diffractometer X-ray trace was obtained for sample 15.08, on which an X-ray fluorescence analysis was also performed. Wet analysis for SiO_2 was carried out on each sample.

7.03 Results and Discussion.

Infrared spectra of the samples are shown in figures 7.01 and 7.02. The Si - O stretch band appears at 1000 cm^{-1} and increases in intensity during the run (fig. 7.01). Later samples show some absorption at 1080 cm^{-1} , indicating the presence of amorphous silica gel.

Sample 15.07, on examination in the E.M., was found to consist of hexagonal or rounded hexagonal crystallites

TABLE 7.01

Sample times for run 15.

Sample	% SiO ₂	Time at reflux, min.	(hours)
15.01	3.5	142	2
15.02	22.7	1478	25
15.03	22.6	1840	31
15.04	24.7	2069	34
15.05	30.8	2810	47
15.06	37.5	3163	53
15.07	49.4	7428	124
15.08	50.3	11653	194

Figure 7.01

Samples from Run 15
Si-O Stretch region.

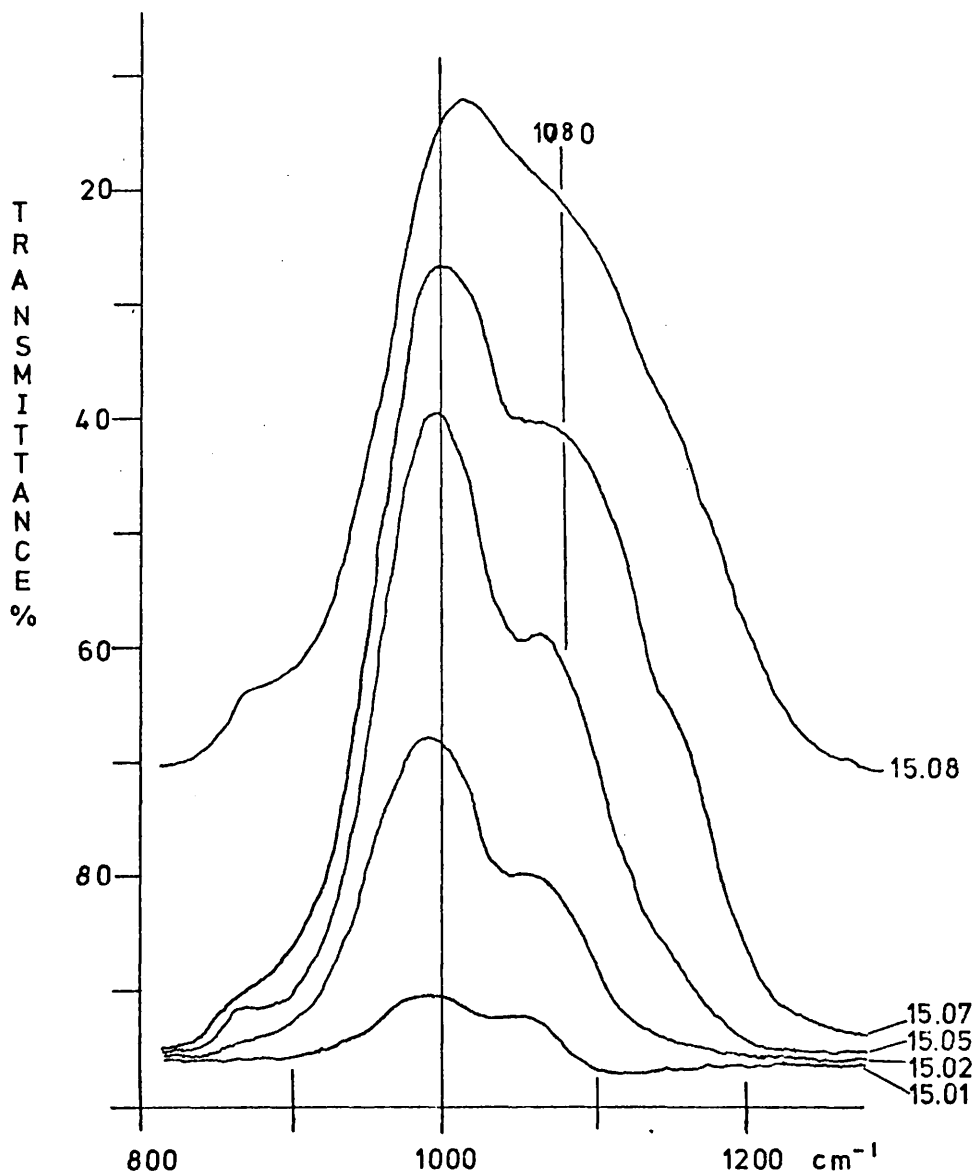
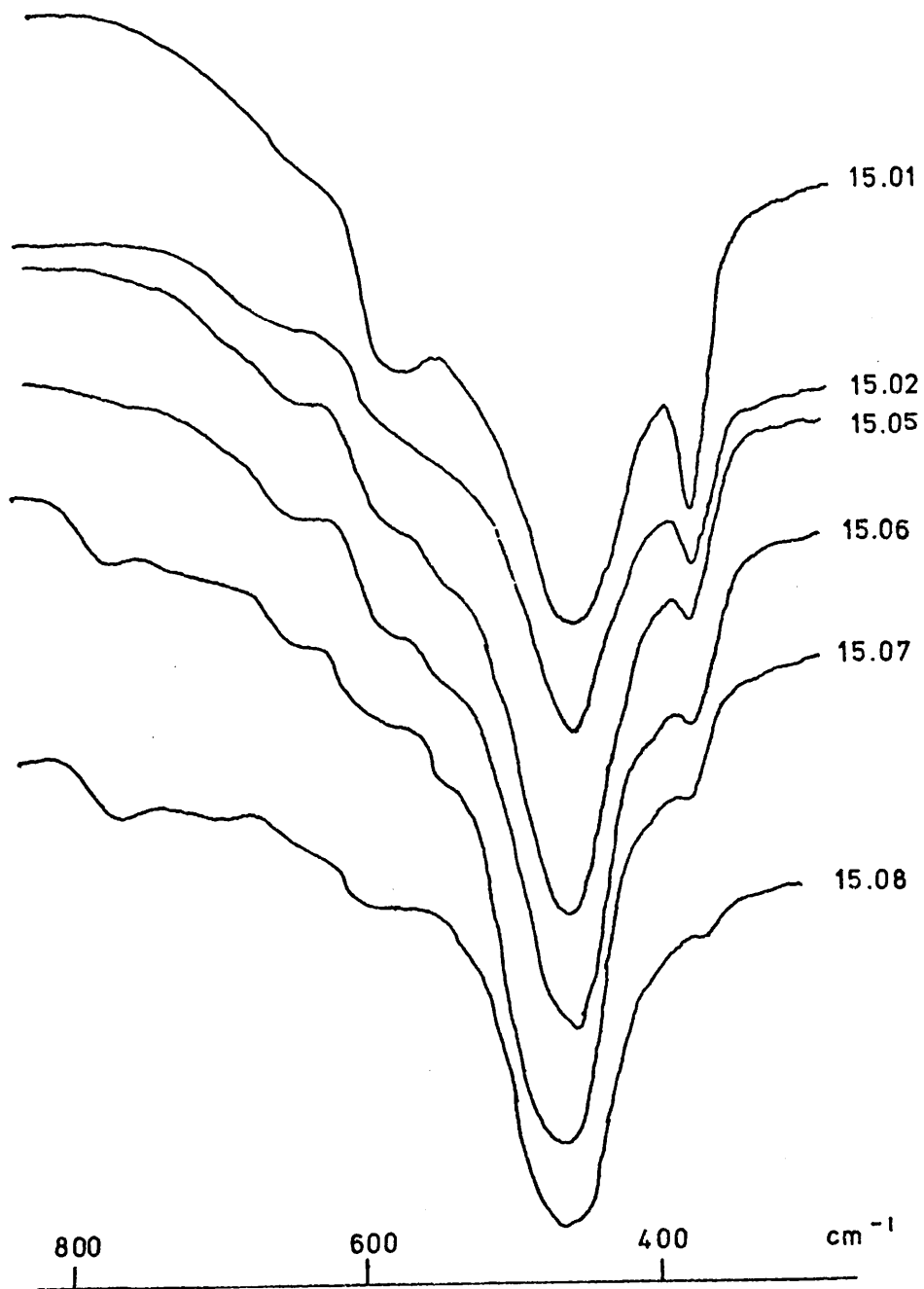


Figure 7.02

Run 15. M—O bend region.



with an easily-resolved 16\AA lattice fringe image normal to to the main cleavage plane (plate 7.01). Diffraction data, summarised in table 7.02, were collected for samples 15.07 and 15.08, and single-crystal electron diffraction patterns were recorded for crystals lying on the main cleavage plane (plate 7.02).

The d-spacings observed can be indexed on an hexagonal unit cell with $a=18.2$ and $c=7.5\text{\AA}$. Reflections at 11.3 , 4.59 and 3.13\AA are due to a small amount of hectorite found, along with amorphous material and magnesium hydroxide, in sample 15.08. On this unit cell, plate 7.02 displays the (001) reciprocal lattice plane, which is also the main cleavage plane. Crystals in other orientations, although frequently observed, were rarely found alone and were usually too thick for good S.A.D. It appears that the crystals represent a new synthetic magnesium silicate phase.

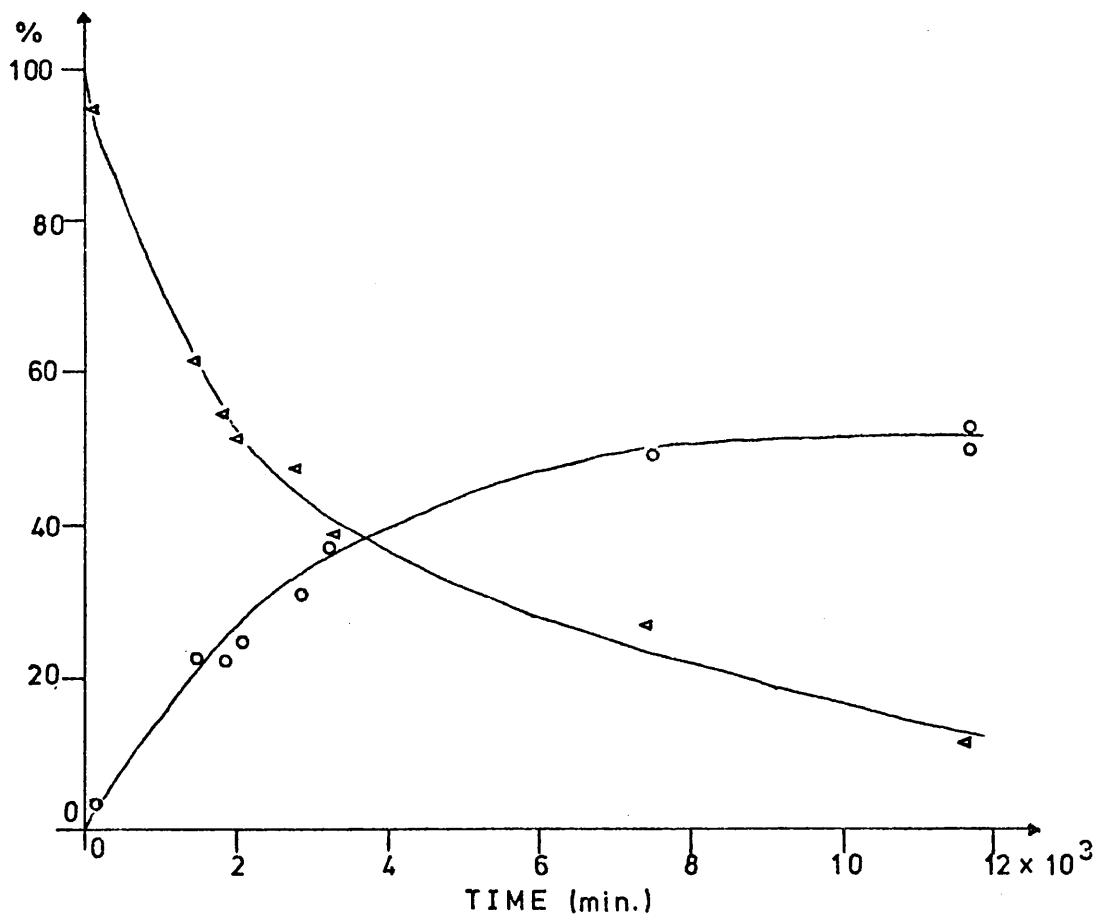
Analysis figures for SiO_2 for the samples are shown in table 7.01, and plotted against time at reflux in figure 7.03. X-ray fluorescence analysis of sample 15.08 gave the following results (above 100°C):-

$\text{Fe}_2\text{O}_3 = 0.07\%$, $\text{TiO}_2 = 0.05\%$, $\text{CaO} = 0.04\%$, $\text{K}_2\text{O} = 14.87\%$,
 $\text{SiO}_2 = 54.01\%$, $\text{Al}_2\text{O}_3 = 4.85\%$, $\text{MgO} = 15.05\%$, $\text{H}_2\text{O} = 9.42\%$.
 MnO and P_2O_5 were not detectable. B_2O_3 and Na_2O were not determined. Estimated amount of brucite remaining in sample 15.08 was 6%.

Decay of the O-H stretching and bending modes in the infrared took place as observed in the formation of hectorite. No new O-H stretch band appeared, and the new phase does not appear to contain hydroxyl groups, although

Figure 7.03

Analysis of samples from run 15.



▲ — Rel. absorbance of free O—H groups.

○ — SiO₂ analysis figures.

TABLE 7.02

Diffraction data for samples 15.07 and 15.08.

1	2	3	4	hkl	calc.*
15.6	15.5	15.63	15.6	100	15.78
11.5	11.5	11.5	-----	---	Hect.
-----	-----	-----	9.11	110	99.11
-----	-----	7.97	7.92	200	7.891
7.50	7.50	7.48	-----	001	7.48
-----	-----	-----	-----	011	6.75
5.97	5.97	5.98	6.01	210	5.965
-----	-----	5.72	-----	111?	5.782
-----	-----	-----	5.34	300	5.26
-----	-----	4.60	-----	---	Hect.?
4.55	4.55	4.55	4.54	220	4.55
-----	-----	4.37	4.40	310	4.367
3.90	3.90	3.90	3.96	400	3.945
3.64	3.64	3.64	3.66	320	3.620
3.27	3.26	3.26	-----	---	---
3.16	3.16	3.16	3.19	500	3.156
-----	-----	3.13	-----	---	Hect.?
3.05	3.05	3.05	3.07	330	3.037
-----	-----	-----	3.01	420	2.983
2.89	2.89	2.89	-----	222	2.891
2.64	2.64	2.64	-----	---	---
2.61	2.61	2.61	2.66?	600	2.605
-----	-----	-----	2.29	440	2.275

- 1 - 15.07
 - 2 - 15.08
- } Phillips camera films.
- 3 - 15.08, diffractometer trace.
 - 4 - 15.07, Single crystal electron diffraction.

Miller indices from plate 7.02.

Calculated spacings on unit cell with $a = 18.22$ and $c = 7.48$ (hexagonal).

some zeolitic water is held in the structure. Weak absorption near 1400 cm^{-1} shows the presence in late samples of some carbonate and/or borate ion. To gain estimates of the rate of decay of the O-H stretch band, and thus of the proportion of $\text{Mg}(\text{OH})_2$ left at a given time, the following procedure was adopted:-

The ratio of the absorbances at 3700 cm^{-1} and 470 cm^{-1} was computed for each sample and plotted against time. The curve thus obtained was extrapolated to zero time and the values expressed as percentages of the zero-time value. The 470 cm^{-1} band is made up of MgO stretching and Si-O stretching, and should be a measure of total amount of $\text{Mg}(\text{OH})_2$ + silica in the sample. Thus the absorbance ratio should represent the proportion of unreacted magnesium hydroxide in the sample. There are, however, serious sources of error in this treatment. Firstly, the 470 cm^{-1} band is unlikely to be affected by the presence of alumina or of K^+ , both of which are present in increasing amounts as the reaction proceeds. Thus there will be a systematic error, tending to give high values for the absorbance ratio, which will become increasingly serious in later samples. Secondly, there is no guarantee that the Si-O stretch at 470 cm^{-1} will remain unchanged as the silica is incorporated into the structure: this leads to a further systematic error of unknown direction and magnitude. Finally, sampling inhomogeneity leads to random errors, especially in earlier samples.

Inspection of figure 7.03 shows that the proportion of unreacted $\text{Mg}(\text{OH})_2$ appears to fall rapidly

during the first 36 hours of the run, and more slowly thereafter. This behaviour is similar to that observed with hectorite and is believed to reflect initial rapid surface coverage with silica gel. It is interesting to note that the rate of increase in the proportion of silica in the samples is lower than the rate of removal of magnesium hydroxide in the early stages. Similar behaviour during the formation of hectorite was observed by Baird, Cairns-Smith and MacKenzie (15) and was explained by postulating the existence of a low-silica adsorbate which they termed "pseudo-smectite". In this case the low-silica adsorbate recrystallizes to form not hectorite but the much better crystallized phase observed.

The amount of silica in the samples changes little between 15.07 and 15.08. EM observations suggest, however, that 15.08 contains much more amorphous material, hectorite and magnesium hydroxide than 15.07. This suggests that the new phase is, in its turn, attacked by the reaction medium and broken down. It may thus be metastable with respect to hectorite under the reaction conditions used.

Sample 15.08 contains, from fig. 7.03, about 9% $\text{Mg}(\text{OH})_2$. Estimates from electron micrographs and X-ray traces put this figure at about 6%, the infrared estimate being high, as expected. Allowing for this, the X-ray fluorescence analysis figures give the approximate composition $\text{Al}_2\text{O}_3 \cdot 2\text{H}_2\text{O} \cdot 2\text{MgO} \cdot 3\text{K}_2\text{O} \cdot 10\text{SiO}_2$, neglecting components below 1%. This is extremely high in SiO_2 , a significant amount of which is probably present in the amorphous material rather than the new phase.

7.04 Conclusions.

At the higher temperature and pH of the experiment, the major product was a new crystalline magnesium silicate, possibly metastable with respect to hecrite + magnesium hydroxide + amorphous material. The new phase has a hexagonal or pseudo-hexagonal unit cell with $a = 18.2$ and $b = 7.5 \text{ \AA}$. The composition is uncertain but high in SiO_2 . The early stages of the reaction again involve adsorption of silicate ion onto the magnesium hydroxide. At what time and in what way the aluminium and potassium found in the product are incorporated, is not known.



15.6 Å

PLATE 7.01

CHAPTER 8. GENERAL HYPOTHESIS AND SUGGESTIONS FOR
FURTHER WORK.

The reactions studied give support to the thesis that, under these conditions, the early stages of silicate formation involve adsorption of silicate ion from solution onto the hydroxide crystals, penetration of the crystal structure by silicate ion and mechanical disruption of the hydroxide crystal structure. This process is signalled in the reaction by the following changes:-

(a) the main Si-O stretch band in the infrared appears in the adsorbate between 1000 and 1040 cm^{-1} , and is distinguishable from, although overlapping, the corresponding band of amorphous silica gel at 1070 - 1080 cm^{-1} .

(b) the hydroxide crystals break up to give a material, usually observable in the samples as a sol showing the Tyndall effect, having a weak, diffuse electron diffraction pattern, the nature of which depends of the hydroxide.

The rate of formation of the adsorbate depends on the crystal structure of the hydroxide, the most easily penetrated structures giving adsorbates in the shortest time. It is possible to define the 'adsorbate half-time' for the reactions studied, as the time at reflux required for the intensity of the 'adsorbate' Si-O stretch band to equal the intensity of the 'silica' Si-O stretch band. This was estimated from the spectra

for each of the hydroxides studied. The values obtained are correlated with the longest O-H group separation between structural units of the hydroxides, in table 8.01 and figure 8.01, in which the sample times at which the spectra bracketed the equality condition are used as error limits. There is a definite correlation between the adsorbate half-time and the O-H group separation. It is thus possible to predict that, for example, $Mn(OH)_2$ should have an adsorbate half-time of about three hours, and similar predictions can be made for the other air-sensitive C_6 hydroxides listed in table 1.02. These predictions could be tested if equipment were designed to handle and sample the reactions in an oxygen-free atmosphere.

It is not possible to predict with any certainty what silicate will be formed on recrystallization of the adsorbate, if this occurs at all. It was suggested by Henin and Robichet (54) that "synthetic clay minerals are most easily formed if the octahedral layer cation gives a brucite structure hydroxide". This suggestion concerns principally the thermodynamic stability of the cation in octahedral holes in an approximately close-packed oxide structure. Esquevin (51) used the formation of hemimorphite from zinc solutions as support for this contention, on the grounds that one of the metastable polymorphs of zinc hydroxide was supposed to have a brucite structure. The suggestion can be criticised on two grounds. Firstly, the silicates formed by the C_6 -hydroxide cations are not, in general, structurally related to the clay minerals and need not necessarily be layer silicates.

TABLE 8.01

Adsorbate half-times for some divalent hydroxides.

Hydroxide	Adsorbate Half-time, mins.	OH-group Separation, Å
Ca(OH) ₂	40	3.33
Mg(OH) ₂	240	3.22
Cd(OH) ₂	1200	2.98
Cu(OH) ₂	1250	2.97
γ-Zn(OH) ₂	1500	2.84
ε-Zn(OH) ₂	4750	2.83
β-Be(OH) ₂	7000	2.67

TABLE 8.02

Crystal radii of some ions common in silicate minerals.

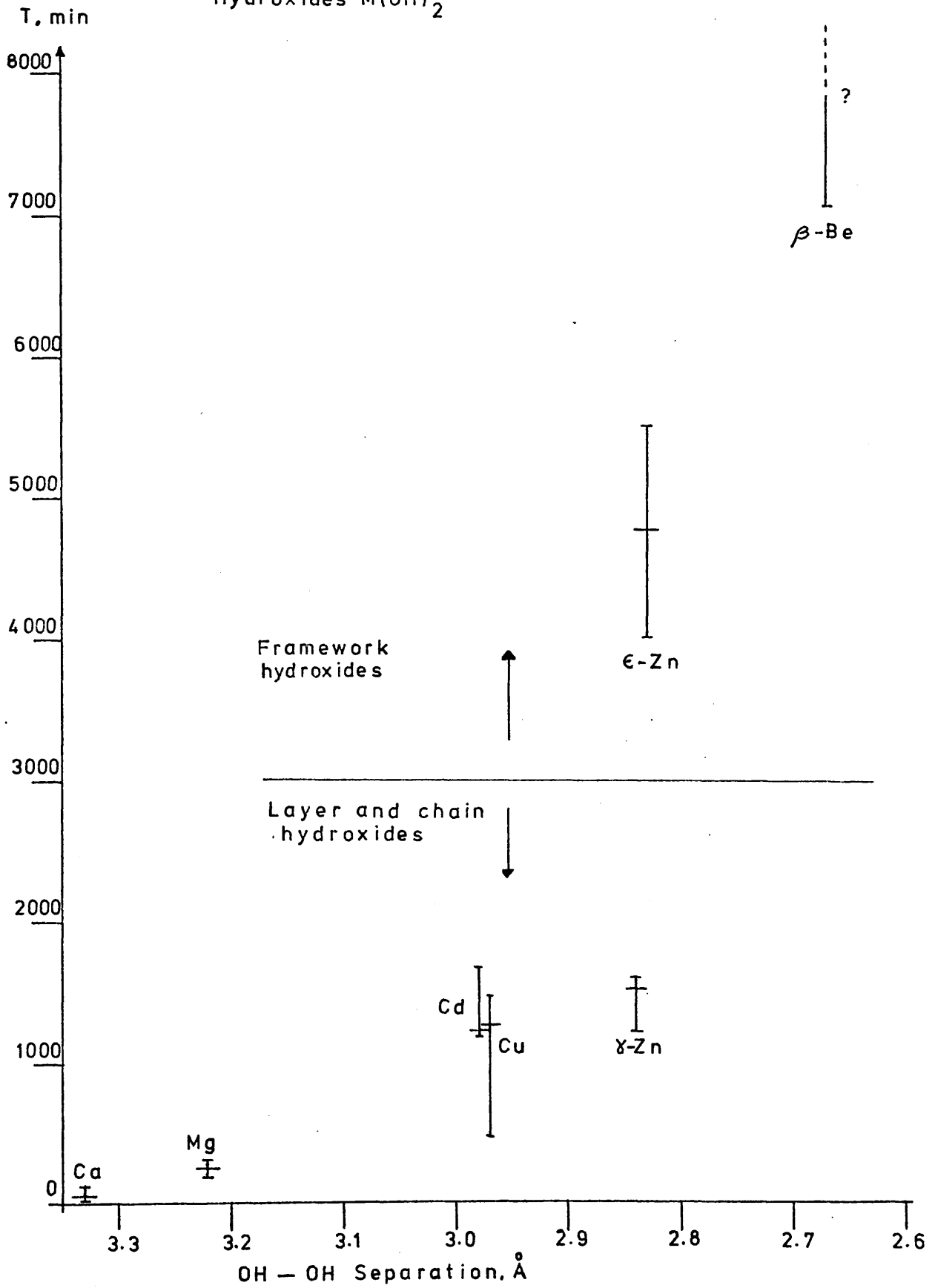
Ion	Crystal Ionic Radius, Å
Ca ²⁺	0.99
Cd ²⁺	0.98
Mn ²⁺	0.80
Zn ²⁺	0.74
Fe ²⁺	0.74
Cu ²⁺	0.72
Co ²⁺	0.72
Ni ²⁺	0.69
Li ⁺	0.68
Mg ²⁺	0.66
Fe ³⁺	0.64
Al ³⁺	0.51
Be ²⁺	0.35

(from the C.R.C. Handbook of Chemistry and Physics, 55th. Edn, CRC Press, Ohio, USA, 1974-1975, p. F-198)

Figure 8.01

'Adsorbate half-times' vs. OH-gp. separation.

Hydroxides $M(OH)_2$



Secondly, it is not certain that any of the zinc hydroxide polymorphs has a C_6 structure: hemimorphite, although it has a layer structure (figure 6.06) is not related to the clay minerals structurally. Nonetheless, the C_6 hydroxide cations do seem to form silicates readily, either from solution or by reactions of the type described in this work.

The radius of the octahedral hole in a close-packed oxide structure is approximately 0.61 \AA . If a clay-mineral-like structure is to be formed, it is necessary that the octahedral cation be of a suitable ionic radius so as not to distort the oxide packing too severely, and also to ensure that the silicate layer can arrange itself to provide a reasonable fit with the octahedral layer. Slight misfit is accommodated in layer silicates by a variety of subterfuges, notably the rolling up of the entire sheet in chrysotile. Cations larger than 0.7 \AA are unlikely to form octahedral sheets in silicates, the misfit between the octahedral and tetrahedral sheets leading to such severe distortion of the structure that it no longer has layer properties, as for example in the tobermorites and the chrysocollas. Table 8.02 lists the cation crystal radii of some ions common in silicate minerals. Considering only the radius, it is unlikely that any apart from Ni^{2+} , Li^+ , Mg^{2+} , Fe^{3+} and Al^{3+} would be found occupying octahedral holes in a clay mineral-like structure. Cations smaller than 0.5 \AA are likely to prefer tetrahedral holes in close-packed structures and hence not to appear in the octahedral layer.

This analysis is largely borne out by the results obtained in this work. The largest cations studied, calcium, cadmium and copper, did not form silicates with octahedral layers. Calcium hydroxide formed an adsorbate which recrystallized partially to a tobermorite-like structure; copper hydroxide similarly gave a chrysocolla-like product; and cadmium hydroxide produced an adsorbate which did not recrystallize, presumably because the activation energy for formation of any of the stable cadmium silicates was not available. Zinc hydroxide gave an adsorbate which recrystallized to hemimorphite, the zinc ion preferring tetrahedral coordination. The only phyllosilicate structure formed was the hectorite of chapter 2.

From figure 8.01 and table 8.02 it is possible to pick the hydroxide likeliest to give a talc-like layer silicate at reflux temperatures, and to state how long it would take to reach the adsorbate halfway stage. Nickel hydroxide has the C_6 structure with a hydroxyl group separation of 3.10 \AA , and should therefore reach the adsorbate halfway stage in around $8\frac{1}{2}$ hours. The cation radius is 0.69 \AA , so the adsorbate should recrystallize slowly to form a hectorite-like phyllosilicate with a variable c-axis spacing around 12 \AA . The reaction should be catalysed by the addition of LiF.

Figure 8.01 divides into two regions, as shown. Layer and chain structure hydroxides should give adsorbate half-times below 50 hours, while frame-

work hydroxides, if they form an adsorbate at all, should have half-times greater than this. Bear and Turnbull (55) described the metastable α - modification of beryllium hydroxide, the structure of which is unknown, although it is believed to have a tetragonal unit cell with $a = 10.84$ and $c = 8.74 \text{ \AA}$. The results of the present work suggest that, if the structure is a cross-linked tetrahedral framework like $\beta - \text{Be}(\text{OH})_2$, a reflux reaction with silica gel at pH 10 should have a very long adsorbate half-time of the order of 100 hours. If the half-time were under 50 hours, the structure is most probably layer- or chain-type, perhaps similar to $\gamma - \text{Zn}(\text{OH})_2$. If this is so, it should be possible to prepare bertrandite ($\text{Be}_4(\text{OH})_2\text{Si}_2\text{O}_7$) at reflux temperature.

The γ - series of trivalent metal oxide hydroxides have structures isomorphous with lepidocrocite (11,56). The hydrogen-bonded layer structure is analogous with that of $\text{Cu}(\text{OH})_2$ (figure 1.2, p. 8) with the intra-layer OH^- replaced by O^{2-} . The crystals show (010) cleavage between the layers and have hydroxyl group separations of $2.7 - 2.8 \text{ \AA}$: the crystal data are summarised in table 8.03. If extrapolation of the half-time hypothesis to the oxide hydroxides is valid, then bohmite, lepidocrocite, $\gamma - \text{ScOOH}$ and manganite should all have adsorbate half-times between 20 and 50 hours. Recrystallization of the adsorbate would not be expected at reflux, the formation of kaolinite from bohmite requiring a temperature of 200°C (12). The formation of an octahedral layer of the clay mineral type requires the splitting of the double octahedral layer in the lepidocrocite structure: this may explain the high recrystallization temperature needed.

By contrast, the α - series of metal oxide hydroxides (table 8.03) have cross-linked octahedral structures with all the oxygen atoms involved in hydrogen bonding (57). This places them in the "framework" area of figure 8.01: they should thus have adsorbate half-times greater than 50 hours.

A check on the sensitivity of the adsorbate half-time to structural differences in the hydroxides could be provided if the reaction were attempted with the metastable polymorphs of cadmium hydroxide, described by Glemser, Hauschild and Richert (58). The γ - polymorph is hydrogen bonded with an OH-group separation of 2.74 Å.

The effect of the hydroxide particle size on the adsorbate half-time is not known. Comparison of run 6 with run 22 (Ca(OH)_2 : chapter 3) suggests that the microcrystalline precipitate used in run 6 reacted faster than the large crystals of run 22, but the situation is complicated by the adsorption of CO_2 and the magnitude of the effect is uncertain. A series of comparative tests with samples of an hydroxide of different particle sizes should be attempted.

At first sight, there seems to be no limit set on the adsorbate half-time by the rate of dissolution of the silica gel, under the conditions used. No significant increase in rate was observed when the Mallinkrodt 100 mesh silica was replaced by wet silica gel freshly prepared by hydrolysis of SiCl_4 . The rate of adsorption observed in chapter 7, where the source of silicate was

Pyrex glass, was much less than in chapter 2, despite the higher temperature and pH, and was almost certainly controlled by the rate of dissolution of the Pyrex.

TABLE 8.03

Metal Oxy-Hydroxide Structure Data.

Name, Formula	System	Space Gp.	OHO _o dist., A	H-bond Energy, Kcal/mol.
γ -ScOOH	O	AmAm	2.72	
böhmite, γ -AlOOH		AmAm	2.70	
Lepidocrocite, γ -FeOOH (14)	O	AmAm	2.70	5.83
diaspore, α -AlOOH (57)	O	Pbnm	2.65	6.86
goethite, α -FeOOH (59)	O	Pbnm		6.28
groutite, α -MnOOH (60)	O	Pbnm	2.626	
manganite, γ -MnOOH (56)	M	B2 ₁ d	2.582	

O = Orthorhombic, M = Monoclinic.

H-bond energies from reference (5).

APPENDIX I

THE SYNTHESIS AND PROPERTIES OF TOBERMORITE, OF
C-S-H(I) AND OF C-S-H-GEL: A REVIEW. *

Introduction:

Interest in phylitic calcium silicate hydrates has increased since the realisation around 1950 of the part such species play in the setting and hardening of cement. In an effort to reduce the complexity of the study of cements, individual cement components have been studied in isolation by X-ray diffraction, IR Spectroscopy, Differential Thermal Analysis and the related thermal techniques, and Electron Microscopy. The individual components have been synthesised by hydrothermal treatment of lime/sand mixtures and by hydration of anhydrous calcium silicates and aluminates. The relationships between these species and the clay minerals have been explored and isomorphous substitution has been

* In press in J. Amer. Ceram. Soc., July/August, 1975.

reported. In 1952 it appeared that one of the components of hydrated cement possessed some resemblance to the natural mineral tobermorite, and interest in the natural tobermorites was stimulated, leading to a rigorous re-examination of these minerals.

In this review the literature on natural tobermorites, and on the synthetic methods used for tobermorite, C-S-H-Gel and C-S-H(I), is briefly surveyed before presenting a more detailed account of the application of the analytical techniques described above.

Natural Species.

Tobermorite was first described (1) in a "preliminary notice of substances which may prove to be new minerals". The mineral, the formula of which was calculated to be $3(\text{CaO}, \text{H}_2\text{O}), 5\text{SiO}_2 + 10\text{H}_2\text{O}$, intermediate between xonaltite (sic) and okenite", was found "totally filling small druses in the cliffs of the shore immediately to the north of the pier of Tobermory in the Island of Mull". Other locations were found at Loch Eynort (2) and at Ardtornish (3). The mineral was listed in the 1897 edition of "Handbuch der Mineralogie" (4), and in the sixth edition of Dana's "System of Mineralogy" (5), in which it was suggested that it might be identical with gyrolite. "Crestmoreite", a mineral from California described by Eakle in 1917 (6), was

later shown (7) to be an intimate intergrowth of tobermorite and wilkeite. By 1954, the "tobermorite group" of minerals was becoming defined, and it was observed that tobermorites of three distinct c-axis periodicities were possible, with $d_{002} = 9.6, 11.3,$ and 14.6 \AA . A dolerite-chalk contact at Ballycraigy, County Larne, yielded the 11.3 \AA variety (8), which could be converted into both the 14.6 \AA and the 9.6 \AA species simply by varying the degree of hydration. The most-investigated samples have been those of Ballycraigy and of Crestmore in California, but new locations continue to be reported (9 - 11).

Synthetic Work.

A material called calcium silicate hydrate I (CSH-I) was obtained by Taylor in 1950 (12) by "decomposition of tricalcium silicate" with water at unspecified solids ratio and temperature. A similar phase, also labelled CSH-I, was obtained by hydrothermal reaction of $\text{CaO}:\text{SiO}_2$ mixtures a) in the ratio $\text{Ca}:\text{Si}=1.0$ (13) or B) in the ratio $\text{Ca}:\text{Si}=1.5$ (14). Some of these were thought to be identical with tobermorite when the natural mineral was re-examined in 1952 by Claringbull and Hay (15), but later work has failed to substantiate the identity or even the close similarity of these phases (16). Further synthetic routes and conditions were explored in the remainder of Taylor's series of articles entitled "hydrated calcium silicates" (17,18), in which the

conditions of hydrothermal synthesis for best crystallinity of the product were determined. The hydrothermal synthesis has been exhaustively studied (19 - 25, 25a) and almost every author reporting on the properties of synthetic tobermorites has undertaken some such synthesis to provide himself with the necessary materials for study. Hydrothermal synthesis from materials other than silica gel has been reported. Calcium hydroxide reacts with quartz to yield tobermorite at temperatures between 120 and 200° (26 - 28) and with muscovite and feldspar under similar conditions (29). Hydrothermal reaction of calcium hydroxide with aggregate fines and slags can produce tobermorite-like crystals (30). Tobermorites are also formed on hydrothermal treatment of cement (25a, 59). Simultaneous formation of tobermorite and montmorillonite by autoclaving at 250° an $\text{SiO}_2/\text{MgO}/\text{Al}_2\text{O}_3/\text{CaO}$ glass has been reported (31).

The hydrothermal method has been used to bring about isomorphous substitution in the tobermorite structure. Aluminium-for-silicon substitution can occur (32 - 34) and a potassium-substituted tobermorite has been described (35). The aluminium-substituted minerals described by Kalousek (32) and Diamond, White and Dolch (33) were normal. An Al-substituted tobermorite synthesised from lime/zeolite slurries by Mituda (34a) was, on the other hand, anomalous (see the analytical section for a description

of the properties of the anomalous tobermorites).

Once formed, tobermorite can be induced to react with a variety of minerals under hydrothermal conditions. Thus, 11.3 Å⁰ tobermorite is transformed into xonotlite at 250 atm. and 380° (36) and reactions with aluminates, ferrites and sulphates have been described⁽³⁷⁾. The hydrothermal method was reviewed by Taylor in 1965 (38) and 1974 (16).

Atmospheric-pressure synthesis at or near reflux temperatures tend to produce samples of lower crystallinity, often lacking a basal reflection, which have been referred to as "tobermorite gels". An example of such a product is reported from refluxing of lime/sand slurries (39). Room temperature hydration of calcium silicates typically produces even more disordered phases with only a very few X-ray lines (typically 5 or less, often only 3). Such products have been reported from paste hydration of C_3S and β - C_2S (40 - 44); from precipitation of $Na_2H_2SiO_4$ solution with saturated $Ca(OH)_2$ solution (45); and as products of the hydration of Portland cement (reviewed by Venuat, 1961: (46)). The structural relationships among the atmospheric-pressure synthetic products and the tobermorites are, however, uncertain. It was suggested by Taylor in 1968 (47) that the disordered phases more closely resembled jennite (first reported in 1966: see reference (48) than tobermorite. This view, despite a fairly close similarity in composition, is now no longer held. Nor is the supposed relationship of these products to tobermorite considered to be necessarily correct (16). The c-axis aperiodic gels giving most of the $hk0$ reflections of tobermorite, are now referred to as C-S-H(I), the hyphens being used to avoid any compositional inference. The low-temperature, badly crystallized gels are now referred to as C-S-H-Gel.

In earlier work, however, the assumed structural identity of tobermorite, C-S-H(I) and C-S-H-Gel was given wide acceptance. Crystals and foils of "tobermorite" were identified from electron micrographs of hydrated cement pastes, and in one case Gaze and Robertson (49) claimed to have obtained unbroken tobermorite crystals from hydrated cement.

Comparisons between the tobermorite group minerals, both synthetic and natural, and the clay minerals, have been made (50,51).

Analytical techniques - Introduction.

Characterisation of the calcium silicate hydrates is usually achieved by applying in combination any or all of the analytical methods mentioned in the introduction. Few authors have relied on a single technique for the identification of their products, and where this has occurred, that technique has almost invariably been X-ray powder diffraction. In the subsequent sections of this work it has been attempted to avoid description of routine applications of these techniques, and to concentrate instead on areas of the subject where the application of a given physical method has increased our understanding of some aspects of the chemistry of the tobermorites. It may, however, be of use to be able to locate in the literature examples of the routine application of these techniques, and to this end a partial summary in approximately inverse order of publication of the application of X-ray diffractometry, electron microscopy, infrared spectroscopy and thermal methods is given

in table 1. Occasionally, the application of other physical methods, such as measurement of thermodynamic (52) and electrophoretic (53) parameters, calorimetry (54), or mechanical stability(38, 58 - 57) has been reported.

The standard techniques have also been used to study the carbonation of C-S-H(I), C-S-H-Gel and hydrothermally-produced tobermorites (55,57, 58 - 60).

X-ray Diffraction Analysis.

X-ray powder diffraction has been the principal technique for characterisation of the tobermorites. Patterns are recorded in the ASTM Powder Diffraction File for samples of natural materials from Crestmore (14 Å, ref. no. 6-0005; 10 Å, ref. no. 6-0020*) and Ballycraigy (11.3 Å, ref. nos. 10-0373 and 10-0374). Three patterns are recorded for synthetic products, nos. 6-0010 (poorly crystalline "tobermorite gel"); 19-1364, a hydrothermally-prepared 11.3 Å tobermorite; and 19-0052, an aluminium-substituted hydrothermal silicate with $d(002) = 11.8 \text{ \AA}$.

The first crystal structure analysis was performed in 1956 by Megaw and Kelsey (61) on the 11.3 Å hydrate from Ballycraigy. An orthorhombic pseudocell was proposed with $a_0=11.3$, $b_0= 7.33$ and $c_0= 22.6 \text{ \AA}$, and it was noted that the true unit cell was smaller and monoclinic. The silicate anion structure

* This card gives $a_0 = 7.3$, $b_0 = 11.2 \text{ \AA}$ which, to be consistent with the indices quoted, should be transposed.

consists of puckered chains of SiO_4 tetrahedra parallel to the \underline{b} -axis, in the "dreierketten" arrangement. Topotactic transformations in these dreierketten with consequent retention of the oxide packing structure can explain some of the interconversions among the calcium silicate hydrates. (62).

The silicate anion structure of the 9.6 \AA variety has been a matter of some debate. It has been claimed (63) that condensation of the chains to form a phyllosilicate sheet occurs, but this was challenged (64) by Wieker on the basis of molybdate analysis of a Crestmore sample, which showed that even in the 9.6 \AA variety the polysilicate anions were present as chains, and that a phyllosilicate structure did not appear until the sample had been heated to 600° . A discussion of the proposed structural models for the tobermorites appeared in Russian in 1972 (65).

The lattice contraction to 9.5 or 9.6 \AA displayed by normal tobermorites, occurs on heating the mineral to 300° . Further heating, to 800° , leads to the formation of $\beta\text{-CaSiO}_3$, twinned along the common \underline{b} -axis of product and starting material (66). Some tobermorites are regarded as anomalous in that they do not show the lattice contraction to 9.6 \AA , the 11.3 \AA basal spacing being stable up to the decomposition temperature of the mineral. A comprehensive account of the anomalous tobermorites, natural and synthetic, together with a possible structural

explanation of the absence of the lattice contraction, is given in Taylor's paper "Crystal Chemistry of Portland Cement Hydration Products" (16).

The unit cell of an hydrothermally-synthesised tobermorite has been reported (67) to be pseudo-orthorhombic with $a_0 = 11.27$, $b_0 = 7.35$, $c_0 = 22.74 \text{ \AA}$, in close agreement with with the results reported for the Ballcraig mineral.

Attempts by Dyczek and Taylor to determine tobermorite in autoclaved materials by quantitative diffractometry, were complicated by variable crystallinity of the tobermorite and by interference from C-S-H phases (16).

Electron Microscopy.

The combination of transmission electron microscopy and selected area electron diffraction has been of great value in identifying individual phases in calcium silicate hydrate mixtures. From the beginning of such investigations, micrographs were presented showing large foils, identified in many cases with tobermorite from the electron diffraction pattern: in some cases, needle-like or fibrous habits, apparently with the same diffraction pattern, were observed. (68,69). With careful sample preparation, it could be shown that the product of hydrothermal synthesis consisted of plate-like crystals of tobermorite similar to vermiculite, while at lower temperatures (ca. 100°) aggregates of extremely small crumpled foils of C-S-H(I) resulted (70). Such aggregates are typical of the poorly-crystallised gel (71) and yield an electron diffraction pattern having very fine-grained rings which correspond well with the (220), (400), (040), (620), (440), (800) and (260) spacings of the ASTM tobermorites (72). The (00 $\bar{1}$) spacings are absent, however, and the nearest spacing to the (201), reported at 5.5 Å, occurs at 5.3 Å. The fit is close enough to lead to an identification of these phases with tobermorite if a search of the

ASTM file is used as the principal method of identification, as it very often is.

The individual C-S-H(I) foils may be prevented from aggregation by dispersion in a non-aqueous medium before drying down onto the grid (73), but as yet no high resolution work on the crystallites has been reported. The 11 \AA lattice in hydrothermal samples has been resolved (73a).

Morphologies resulting from calcium silicate hydration have been reported (49,74,75), and hydrothermal hardening of a cement paste gave an 11.3 \AA tobermorite (59). Stereoscopic microscopy, and more recently scanning electron microscopy, have been undertaken both on cement products (59,75) and hydrothermal products (28). Plate- and leaf- shaped surfaces are observed which, presumably, correspond with the foils observed in transmission microscopy.

Shadowing has been used only rarely. A shadowed micrograph showing both sheet- and rod-shaped crystals of an hydrothermal product (53) was presented as additional characterisation of the material being studied. Many other authors have used electron microscopy routinely to characterise the products of various systems (45, 76 - 79).

The typical appearance of the crumpled foil aggregates resulting from aqueous dispersion of

C-S-H(I) samples might be supposed to reflect not only the structural stability of the material but also morphological uniformity of the individual crystallites. In the absence of high resolution

work on non-aggregated samples, no direct evidence for this view is available, but it is of interest to note the marked pseudomorphosis occurring on carbonation of tobermorites. Such pseudomorphosis has been noted in an 11 Å tobermorite from an autoclaved cement paste (59), and in a c-axis aperiodic gel prepared at reflux temperature (72). In view of the known occurrence of topotactic transformations among the calcium silicate hydrates (62, 62a), it may be that the carbonation reaction proceeds with little disturbance of the oxide packing structure of the crystallites, with resulting retention of their morphology.

Electron-optical examination of the anomalous tobermorite from Loch Eynort (80) revealed that the principal cleavage plane in this sample was (100), and the (001) cleavage was secondary. Not all the anomalous tobermorites share this property, however. (16, 34a).

Infrared Spectroscopy

Two regions of the infrared range of frequencies are of paramount importance in the study of silicate materials. The O-H stretching (3800 - 3000 cm^{-1}) and bending ($\sim 1600 \text{ cm}^{-1}$) regions of the spectrum yield information on a) the presence or absence of O-H groups in the material, and their bonding state, and b) the amount and in some cases the arrangement of bound water molecules. The Si-O stretch region (1200 - 800 cm^{-1}) may in favourable

cases provide an identification of the mineral from the number and position of the absorption maxima, and in all cases will provide general evidence on the state of the silicate anion structure, in particular any order-disorder relationships in the tetrahedral layer.

There are, however, complications which may arise from the preparation techniques necessary to record solid-state spectra. Mull and deposition techniques, for instance, tend to lead to orientation of phyllitic materials, thus enhancing the intensities of some bands and depressing or removing others; the widely-used alkali halide pressed-disc technique, although presumably providing a random geometrical arrangement of the particles, may interfere with bands in the O-H regions (because of the hygroscopicity of the matrix); and in all techniques excessive sample grinding can broaden bands and deform the structure of the material. These effects in the spectra of layer silicates have been carefully discussed by Farmer and his co-workers (81,82).

It follows that in infrared examination of the tobermorites, as with any solid-state materials, the preparative techniques used must be clearly defined if anomalies in the interpretation of the spectra are not to arise. The spectrum of a 14 Å tobermorite from Crestmore, recorded as a pressed disc, is almost identical with that of the 11.3 Å hydrate derived from it by heating to 90°. The mull spectrum of the unheated mineral is, however,

different, and the conclusion is that dehydration to the 11.3 \AA form occurs on preparing the disc (83).

It has been noted by Henning and Gerstner (84) that, in calcium silicate hydrates, "the spectra of similar substances, but by different authors, often differ strongly one from another". It was these authors' intention to provide a reference paper of standard spectra for the identification of natural and synthetic calcium silicate hydrates, but nowhere in this work do they mention any details of the conditions under which their spectra were obtained. The spectrum of a Crestmore sample which they present differs from that of Farmer (83) in several respects: there appears to be much more carbonate present (absorbing at 1450 cm^{-1}); the principal Si-O absorption maximum appears at 1050 cm^{-1} , much higher than the 962 cm^{-1} value quoted by Farmer; and there is no clear maximum of absorption in the O-H stretch region, while a strong H-bonded O-H band appears at 3350 cm^{-1} in Farmer's spectrum. How far these differences are caused by the sample, and how far they are caused by instrumental or sample-preparation effects, it is impossible to say in the absence of technical data.

These difficulties and inconsistencies would seem to detract seriously from the usefulness of infrared analysis in this context. However, many authors have recorded infrared spectra of tobermorites, and other calcium silicate hydrate phases, some limiting themselves to discussion of hydroxyl groups and interlayer water (32,85), some examining

the entire wavenumber region (e.g. 72,73,74,84, 86,87) and some others referring exclusively to the hydration of cements (88-90), and from consideration of this work certain generalisations concerning the spectra of C-S-H gels emerge:

a) In the absence of carbonate ion (absorbing around 1450 cm^{-1}) the principal Si-O absorption maximum appears around 950 cm^{-1} . This band can vary widely in width, a very broad band indicating a poorly crystalline sample.

b) Poorly crystalline gels with a high carbonate content show strong Si-O bands at 1050 cm^{-1} or higher, indicating partial decomposition to amorphous silica gel. In extreme cases the typical pattern of an acidic silica gel, with bands at 1200, 1070, 950 and 800 cm^{-1} becomes apparent.

c) No free O-H stretch at 3700 cm^{-1} appears. Hydrogen-bonded O-H bands between 3300 and 3600 cm^{-1} may be present, and may be masked by broad H_2O bands centred on 3400 cm^{-1} , especially in alkali halide disc spectra.

d) The Si-O-Si bending mode appears as two bands at 450 and 480 cm^{-1} in well-crystallised samples.

The quantitative infrared determination of hydrothermally hardened lime-sand masses has been claimed (91). Some literature on quantitative solid-state infrared exists (92,93), but the experimental difficulties described above greatly complicate any discussion of shape and intensity of infrared bands in solid state spectra (94), and most authors are

reluctant to make more than semiquantitative interpretations.

The spectra of thin films of 11.3 Å synthetic tobermorites of varying aluminium content have been recorded in the region 1700 - 600 cm⁻¹ (33)*.

Aluminium substitution up to 10% has little effect on the spectrum. Mitsuda presented KBr disc spectra of his synthetic 11 Å anomalous tobermorites (34a).

Thermal Techniques.

Weight-loss curves for the normal 14 Å tobermorite of Crestmore were reported by Farmer et al (83). A sharp loss of weight at 55° marked the contraction to the 11.3 Å hydrate, which dehydrated slowly, formation of the 9.35 Å tobermorite being complete by 450°. Between 450 and 660° the chains condensed and a 9.7 Å phyllosilicate was formed. Decomposition to wollastonite occurred at 850 - 900°.

Weight-loss (95) and DTA (95,70,73) curves for C-S-H(I) show the transformation to wollastonite as an exothermic effect at 800 - 850°. None of the dehydration steps of the natural tobermorites are observed, the sole other change being loss of adsorbed water at around 150°.

C-S-H-Gel samples show also a large endotherm around 560°, caused by dehydroxylation of Ca(OH)₂ (73,95). The absence of this endotherm in better-crystallised samples has been taken as an identification of C-S-H(I).

Normal, hydrothermal 11.3 Å tobermorites show the wollastonite transition, and dehydrate to

* In this work figs. 2,3&4 should read 4,2 & 3 respectively.

the 9.6 Å form at 275°. Al - substitution raises the peak temperature of the dehydration endotherm, and also raises the exotherm temperature. (33).

The anomalous tobermorites do not show the lattice contraction to 9.6 Å, and are in addition often Al - substituted. There appears to be a connection between Al - content and the stability of the anomalous structure, but it is not well understood (16).

The anomalous tobermorites described by Mitsuda (34a) showed no dehydration endotherm between 250 and 300°. The wollastonite transition temperature was, in common with other (normal) aluminium-substituted tobermorites, higher, and the exotherm sharper and more intense, than found with unsubstituted tobermorites.

References

- 1 M. F. Heddle, "Preliminary notice of substances which may prove to be new minerals", Mineral. Mag. 4 119 (1880)
- 2 M. F. Heddle, "Tobermorite from Loch Eynort", Trans. Geol. Soc. Glasgow, 9 254 (1893)
- 3 J. Currie, Tobermorite from Ardtornish, Mineral. Mag. 14 93 (1905)
- 4 C. Hintze, "Handbook of Mineralogy", Veit Verlag, 1897. Volume II, p. 1746, "Tobermorite".
- 5 E. S. Dana, "System of Mineralogy", 6th. Edn., 1892. page 570.
- 6 A. S. Eakle, report of crestmoreite, Bull. Dept. Geol. Univ. California, 10(19) 327 (1917).
- 7 H. F. W. Taylor, "Crestmoreite and Riversideite", Mineral. Mag. 30 155 - 165 (1953).
- 8 J. D. C. McConnell, "The hydrated calcium silicates riversideite, tobermorite and plombierite", Mineral. Mag. 30 293 - 305 (1954)
- 9 G. Gottardi and E. Passaglia, "Nonexpandable tobermorite and gyrolite from the Mount Biaena region of Trento, Italy", Period. Mineral. (Rome), 36(3) 1079 (1967).

- 10 E. Passaglia, "Zeolites and other minerals in the basalt from Monte Baldo (Trentino)",
Period. Mineral. (Rome) 35(1) 187 (1966).
- 11 A. B. St. J. Webb, "Tobermorite from Castle Hill near Kilbirnie, Ayrshire",
Mineral. Mag. 38(294) 253 (1971)
- 12 H. F. W. Taylor, "Hydrated Calcium Silicates I. Compound formation at ordinary temperatures",
J. Chem. Soc. (1950) 3682 - 3690.
- 13 L. Heller and H. F. W. Taylor, "Hydrated Calcium Silicates II. Hydrothermal reactions. Lime : Silica ratio 1:1",
J. Chem. Soc. (1951) 2937 - 2401.
- 14 L. Heller and H. F. W. Taylor, "Hydrated Calcium Silicates III. Hydrothermal reactions of lime:silica ratio 3:2",
J. Chem. Soc. (1952) 1018 - 1020.
- 15 G. F. Claringbull and M. H. Hey, "A re-examination of tobermorite",
Mineral. Mag. 29 960 - 962 (1952).
- 16 H. F. W. Taylor, "Crystal Chemistry of Portland Cement Hydration Products", Principal Paper, VIth. International Congress on the Chemistry of Cement, Moscow 1974.

- 17 L. Heller and H. F. W. Taylor, "Hydrated Calcium Silicates. IV. $\text{CaO}:\text{SiO}_2$ ratios 2:1 and 3:1 : Hydrothermal reactions",
J. Chem. Soc. (1952) 2535 - 2541.
- 18 H. F. W. Taylor, "Hydrated Calcium Silicates. V. Water content of calcium silicate hydrate I",
J. Chem. Soc. (1953) 163 - 171.
- 19 G. L. Kalousek, "Tobermorite and related phases in the system $\text{CaO} - \text{SiO}_2 - \text{H}_2\text{O}$ ",
J. Amer. Concrete Inst. 26 989 - 1011 (1955).
- 20 Yu. M. Butt and L. N. Rashkovich, "The synthesis of the individual hydrosilicates of calcium and their basic parameters",
Sbornik. Trudov. Resp. Nauch.-Issledovatel. Mestnykh Stroitel. Materialov. (1959) no. 15 13 -23.
Chem. Abs. 55 21531a.
- 21 T. M. Berkovich, D. M. Kheiker, O. I. Gracheva and N. I. Kupreeva, "Phase composition of the products of hydration of $3\text{CaO}.\text{SiO}_2$ and $\beta - 2\text{CaO}.\text{SiO}_2$ ",
Doklady Akad. Nauk SSSR 120 372 - 375 (1958).
- 22 A. Balandis, A. Razvadauskas and K. Sasnauskas, "Interaction of α - dicalcium silicate hydrate with monocalcium silicate hydrate and tobermorite under hydrothermal conditions",
Liet. TSR Aukst. Mokyklu Mokslo Darb., Chem. Chem. Technol. (1972) no. 14 277 - 284.
Chem. Abs. 80 51771m.

- 23 G. O. Assarsson, "Hydrothermal reactions between calcium hydroxide and amorphous silica: the reactions between 120 and 160°",
J. Phys. Chem. 62 223 - 228 (1958).
- 24 G. O. Assarsson, "Hydrothermal reactions between calcium hydroxide and siliceous materials at 120 - 220°",
Zement - Kalk - Gips 12 537 - 544 (1961).
- 25 Giichi Sudo, "Reaction in the system CaO - SiO₂(gel) - H₂O and their products",
Yogyo Kyokai Shi 69 401 - 409 (1961).
- 25a H. F. W. Taylor, "Hydrothermal reactions in the system CaO - SiO₂ + H₂O and the steam curing of cement and cement-silica products",
Proc. 4th. Int. Symp. Chem. Cement, Washington, 1960:
Vol. II 167 - 203 (pub. 1962).
- 26 G. O. Assarsson, "Hydrothermal reactions of calcium hydroxide - quartz at 120 - 220°",
J. Phys. Chem. 64 328 - 331 (1960).
- 27 A. Aitken and H. F. W. Taylor, "Hydrothermal reactions in lime - quartz pastes",
J. Appl. Chem. (London) 10 7 - 15 (1960).
- 28 O. Henning and B. Gerstner, "Interaction between quartz and calcium hydroxide under hydrothermal conditions",
Wiss. Z. Hochsch. Architekt. Bauw., Weimar, 19(1)
53 - 58 (1972).

- 29 G. O. Assarsson, "Hydrothermal reactions between calcium hydroxide and muscovite and feldspar at 120 - 200°",
J. Phys. Chem. 64 626 - 632 (1960)
- 30 H. G. Midgley and S. K. Chopkra, "Hydrothermal reactions between lime and aggregate fines",
Mag. Concrete Res. 12 73 - 82 (1960).
- 31 A. A. Govorov, N. A. Ovrachenko and F. D. Ovrachenko,
"Simultaneous formation of montmorillonite and tobermorite under hydrothermal conditions",
Ukr. Khim. Zh. 35(12) 1319 - 1320 (1969).
Chem. Abs. 72 71851a.
- 32 G. L. Kalousek, "Crystal chemistry of hydrous calcium silicates. I. Substitution of aluminium in lattice of tobermorites",
J. Amer. Ceram. Soc. 40 74 - 80 (1957).
- 33 S. Diamond, J. L. White and W. L. Dolch, "Effects of isomorphous substitution in hydrothermally synthesised tobermorite",
Amer. Mineral. 51(3-4) 388 - 401 (1966).
- 34 J. Petrovic, V. Rusnak and L. Stevula, "Isomorphous substitution of aluminium for silicon in tobermoritic structure. I. Mixtures of different forms of silicon dioxide and of different compounds of aluminium",
Chem. Zvesti. 23 129 - 133 (1969).

- 34a T. Mitsuda, "Synthesis of tobermorite from zeolite",
Mineral. J. 6 143 - 158 (1970).
- 35 Giichi Sudo and Hitoaki Mari, "Influence of potassium
hydroxide solution on the formation of tobermorite
phase at room temperature",
Yogyo Kyokai Shi 69 367 - 372 (1961).
- 36 H. F. W. Taylor, "Transformation of tobermorite
into xonotlite",
Mineral. Mag. 32 110 - 116 (1959).
- 37 L. E. Copeland, E. Bodor, T. N. Chang and C. H. Weise,
"Reactions of tobermorite gel with aluminates, ferrites
and sulphates",
J. PCA Res. Develop. Lab. 9 61 - 74 (1967).
(PCA = Portland Cement Association)
- 38 H. F. W. Taylor, "A review of autoclaved calcium
silicates",
Autoclaved Calcium Silicate Bldg. Prod., Pap. Symp.,
London 1965, 195 - 203 (pub. 1967).
Chem. Abs. 68 62387u.
- 39 S. A. Greenberg, "The chemical reactions of calcium
hydroxide, silica and water mixtures at 82°",
J. Phys. Chem. 61 373 - 374 (1957).
- 40 S. Brunauer, D. L. Kantro and L. E. Copeland, "The
stoichiometry of the hydration of β -C₂S and C₃S at
room temperature",
J. Amer. Chem. Soc. 80 761 - 767 (1958).

- 41 M. Colleparidi, L. Massida and G. Usai, "Kinetics and mechanism of aging of tobermoritic gel", *Cemento* 68(1) 3 - 8 (1971).
- 42 H. Funk, "Chemical investigation of silicates. XXII. On the products of the action of water on different forms of dicalcium silicate between 120 and 350^o, and their conditions of formation", *Z. Anorg. Allge. Chem.* 297 103 - 120 (1958).
- 43 S. Brunauer, L. E. Copeland and R. H. Bragg, "The stoichiometry of the hydration of C₃S at room temperature. I. Hydration in a ball mill", *J. Phys. Chem.* 60 112 - 115 (1956).
- 44 S. Brunauer, L. E. Copeland and R. H. Bragg, "The stoichiometry of the hydration of C₃S at room temperature. II. Hydration in paste form", *J. Phys. Chem.* 60 116 (1956).
- 45 H. Funk, "Lime-rich tobermorite phases", *Silikat Tech.* 11 375 - 377 (1960).
- 46 M. Venuat, "Composition and structure of the products of hydration of the calcium silicates in cements", *Rev. Materiaux Construct. et Trav. Publ. C*, No. 555, pp. 481 - 490, (1961).
Chem. Abs. 56 9718a.
- 47 H. F. W. Taylor, "The Calcium Silicate Hydrates", Principal paper, *Proc. 5th. Int. Symp. Chem. Cement*, Tokyo, 1968, Vol. 2, pp. 1 - 26.

- 48 A. B. Carpenter, R. A. Chalmers, J. A. Gard,
K. Speakman and H. F. W. Taylor, "Jennite, a
new mineral",
Amer. Mineral. 51(1-2) 56 - 74 (1966).
- 49 R. Gaze and R. H. S. Robertson, "Unbroken tobermorite
crystals from hydrated cement",
Mag. Concrete Res. 9(25) 25 - 26 (1957).
- 50 H. F. W. Taylor and J. W. Howieson, "Relationships
between calcium silicates and clay minerals",
Clay Minerals Bull. 3 98 - 111 (1956).
- 51 S. Diamond, "Tobermorite and tobermorite-like
calcium silicate hydrates: their properties and
relations to clay minerals",
Univ. Microfilms order no. 64-5722, 282 pp.
Diss. Abs. 24(12) 4979 (1964).
- 52 J. E. Taylor, "Heat of formation of xonotlite, tober-
morite, hillebrandite and afwillite",
Proc. Conf. Silicate Ind. 9 179 - 184 (1967).
- 53 H. N. Stein, "The zero-point charge of tobermorite",
J. Colloid Sci. 15 578 - 584 (1960).
- 54 V. M. Kazanskii and V. E. Leirikh, "Energy of the
binding of water by calcium hydrosilicate of tober-
morite structure",
Izv. Vyssh. Ucheb. Zaved., Khim. Khim. Technol.,
13(3) 394 - 396 (1970).
Chem. Abs. 73 48601f.

- 55 I. S. Shornikova, Yu. M. Butt, and S. A. Krzheminskii, "Properties of some single hydrated calcium silicates and of hydrogarnets",
Sb. Tr., Gos. Vses. Nauch-Issled. Inst. Stroit. Mater. Konstr. (1966) no. 8, 3 - 19.
Chem. Abs. 69 22830x.
- 56 K. G. Krásil'nikov and N. N. Skoblinskaya, "Deformation of the polycrystalline structure of tobermorite by the sorption and desorption of water vapour",
Dokl. Akad. Nauk SSSR 184 151 - 153 (1969)
- 57 L. N. Rashkovich, "The carbonation of the individual hydrosilicates of calcium",
Stroit. Materialy 8(6) 31 - 33 (1962).
- 58 S. Asano, Y. Kamatani and Y. Inoue, "Carbonation of calcium silicate compounds",
Yogyo Kyokai Shi 79 303 - 311 (1971).
- 59 Z. Sauman, "Effect of carbon dioxide on porous concrete"?
Cement Concr. Res. 2 541 - 549 (1972).
- 60 W. F. Cole and B. Kroone, "Carbonate minerals in hydrated portland cement",
Nature 184(4688) 57 (1959).
- 61 H. D. Megaw and C. H. Kelsey, "Crystal structure of tobermorite",
Nature 177 390 - 391 (1956).

- 62 H. F. W. Taylor, "Aspects of the crystal structures of calcium silicates and aluminates",
J. Appl. Chem. (London) 10 317 - 323 (1960).
- * 62a See footnote * .
- 63 Kh. S. Mamedov and N. V. Belov, "Crystal structure of tobermorites",
Doklady Akad. Nauk SSSR 123 163 - 165 (1958).
- 64 W. Wieker, "Chemical studies of silicates XXIV. Silicate anion structure of 14 Å tobermorite of Crestmore and its dehydration products",
Z. Anorg. Allge. Chem. 360 307 - 316 (1968).
- 65 Kh. S. Mamedov and M. I. Chiragov, "Structure of tobermorite",
Azerb. Khim. Zh. 1 120 - 124 (1972).
- 66 H. F. W. Taylor, "The dehydration of tobermorite",
Clays Clay Minerals, Proc. 6th. Natl. Conf.,
Berkeley (1957), pp. 101 - 109 (publ. 1959).
- 67 A. Takahashi, "X-ray diffraction data of synthetic tobermorite",
Osaka Kogyo Gijutsu Shikensho Kiho 22(2) 170-172 (1971)
Chem. Abs. 76 64753z.
- 68 Å. Grudemo, "An electronographic study of the morphology and crystallization properties of calcium silicate hydrates",
Svenska Forskningsinst. Cement Betong vid Kgl., Tek. Högskol. Stockholm, Handl. no. 26, (1955). 103 pp.
Chem. Abs. 50 5265b.
- * 62a L. S. D. Glasser, F. P. Glasser and H. F. W. Taylor, "Topotactic reactions in inorganic oxy-compounds",
Quart. Rev. 16 343 - 360 (1962).

- 69 D. S. Snell, "Studies on the Synthesis of Layer Silicates", Ph.D. Thesis, University of Glasgow, in press: Chapter 3, "Calcium Hydroxide".
- 70 R. Gaze and R. H. Robertson, "Calcium silicate hydrate I. Tobermorite",
Mag. Concrete Res. 8(22) 7 - 12 (1956).
- 71 J. A. Gard, J. W. Howieson and H. F. W. Taylor,
"Synthetic compounds related to tobermorite. A study by EM, X-ray and dehydration",
Mag. Concrete Res. 11 151 (1959).
- 72 T. Baird, A. G. Cairns-Smith and D. S. Snell, "Morphology, crystallinity and CO₂-uptake in tobermorite gel",
J. Colloid Interface Sci., ~~in press~~ 50[2] 387-391 (1975).
- 73 S. Diamond, W. L. Dolch and J. L. White, "Tobermorite-like calcium silicate hydrates",
Highway Res. Record, 62 62 - 79 (1965).
- 73a H. Grothe, G. Schimmel and H. zur Strassen, in a written discussion of the material of ref. 25a, appended to that paper.
- 74 G. L. Kalousek and A. F. Prebus, "Crystal chemistry of hydrous calcium silicates. III. Morphology and other properties of tobermorite and related phases",
J. Amer. Ceram. Soc. 80 761 - 767 (1958).

- 75 W. Czernin, "The electron microscopy of cement pastes in the process of setting",
Zement - Kalk - Gips 11 381 - 383 (1958).
- 76 H. Funk, "Hydration process of β -C₂S with formation of acicular tobermorite-like calcium silicate hydrate",
Silikat Tech. 11 373 - 375 (1960).
- 77 S. Diamond, J. L. White and W. L. Dolch, "Transformation of clay minerals by calcium hydroxide attack",
Clays Clay Minerals, Proc. 12th. Natl. Conf. (1963),
pp. 359 - 379, (publ. 1964).
- 78 V. R. Garashin and G. V. Sizov, "Structure of silicate concrete studied with an electron microscope",
Soversh. Metod. Issled. Tsem. Kamnya Betona (1968),
pp. 120 - 127.
Chem. Abs. 72 35385t.
- 79 H. E. Schwiete and G. Rehfeld, "Investigation of the structure of steam-hardened materials with the aid of the screen electron microscope",
Zement - Kalk - Gips 22(3) 109 - 111 (1969).
- 80 J. A. Gard and H. F. W. Taylor, "A further investigation of tobermorite from Loch Eynort, Scotland",
Miner. Mag. 31 361 - 370 (1957).
- 81 V. C. Farmer and J. D. Russell, "The infrared spectra of layer silicates",
Spectrochimica Acta 20 1149 (1964).

- 82 V. C. Farmer, "Infrared spectroscopy in clay mineral studies. A review",
Clay Minerals 7(4) 373 (1968).
- 83 V. C. Farmer, J. Jeevaratnam, K. Speakman and H. F. W. Taylor, "Thermal decomposition of 14 Å tobermorite from Crestmore",
Natl. Acad. Sci. - Natl. Res. Council Publ. no. 1389, pp. 291 - 299, (1966).
- 84 O. Henning and B. Gerstner, "Infrared- and X-ray-analytical characterisation of natural and synthetic calcium silicate hydrates",
Wiss. Z. Hochsch. Architekt. Bauw. Weimar 19(3) 287 - 293 (1972).
- 85 Ya. I. Ryskin, G. P. Stavitskaya et al., "Spectroscopic study of the chemical structure of synthetic tobermorite",
Izv. Akad. Nauk SSSR, Neorg. Mater. 5 954 - 961 (1969).
Inorganic Materials 5 810 - 816 (1969).
- 86 C. M. Hunt, "Infrared absorption spectra of some compounds in the CaO - SiO₂ - H₂O system",
Natl. Bureau Std. (US) Monograph 43(1) 297 - 305 (1960).
- 87 Ya. I. Ryskin, G. P. Stavitskaya and N. A. Toropov, "Infrared spectra of hydrated silicates",
Zh. Neorg. Khim. 5 2727 - 2734 (1960).
Russian J. Inorg. Chem. 5 1315 (1960).

- 88 A. Baron and R. Sierra, "Application of infrared spectroscopy to the study of the hydration of cement", *Method. Phys. Anal.* 4(4) 412 - 418 (1968).
- 89 T. Vazquez Moreno, "Application of infrared to the solution of some problems in the chemistry of cements", *Mater. Constr. (Madrid)* 140 51 (1970).
- 90 O. Henning and B. Kaessner, "Phase analysis of portland cement clinkers", *Epitoyanag* 25(11) 414 - 416 (1971).
Chem. Abs. 76 117119f.
- 91 O. Henning and B. Gerstner, "Quantitative infrared-spectroscopic investigations of hydrothermally - hardened lime-sand masses", *Wiss. Z. Hochsch. Architekt. Bauw. Weimar* 18 599-604 (1972).
- 92 W. C. Steele and M. K. Wilson, "Some comments concerning quantitative infrared spectroscopy", *ASTM Special Tech. Publ.* 269 185 - 189 (1960).
- 93 R. I. Arav, A. I. Boldyrev and L. G. Maragina, "Method for the quantitative determination of magnesium and calcium carbonates and hydroxides", *Ukr. Khim. Zh.* 36(12) 1295 - 1296 (1970).
- 94 K. S. Seshadri and R. N. Jones, "The shapes and intensities of infrared absorption bands - A review", *Spectrochim. Acta.* 19 1013 - 1085 (1963).

95 S. A. Greenberg, "Calcium silicate hydrate I",
J. Phys. Chem. 58 362 (1954).

Acknowledgement

The author thanks Professor H. F. W. Taylor
and Dr. V. C. Farmer for some helpful conversations.

TABLE 1.

ANALYTICAL TECHNIQUES INDEX

REF.	CODE	REF.	CODE	REF.	CODE	REF.	CODE
16	I	88	I	86	I	49	E
34a	XEIT	64	X	87	X I	39	XEIT
28	XEI	52	T	53	XE T	44	X
84	X IT	33	IT	62	X	43	X
91	I	83	X IT	20	X	70	XE T
65	X	55	M	60	X	61	X
59	XE M	73	XEIT	71	XE	68	E
58	XEI	38	XE M	36	X	95	X T
90	I	77	XE T	23	X	8	X T
67	X	57	X	40	X	15	X
89	I	27	X	74	XEIT		
85	X IT	26	X	63	X		
79	E	29	X	80	X		

KEY

X = X-ray Diffraction

E = Electron Microscopy

I = Infrared Spectroscopy

T = Thermal Techniques

M = Mechanical Properties.

References arranged in approximately inverse order of publication in columns.

APPENDIX II.

The Hypothesis of the Crystal Gene.

The reader is referred to the book "The Life Puzzle", by A. G. Cairns-Smith, Oliver and Boyd, (1971), for a summary of the literature on the following subject.

Defect patterns in crystals are known to be replicated throughout large regions of the crystal structure by the growth processes of the crystal. In this way, for example, growth spirals may develop around screw dislocations. It has been suggested that, given a defect pattern of suitable stability, subsequent cleavage processes may occur with retention of the pattern and hence any morphological and mechanical properties associated with it. There may be, in other words, parent-daughter relationships among crystals, the defect pattern providing the genotype, the macroscopic properties of the crystal the phenotype, and the normal processes of crystal growth and cleavage providing a replication mechanism. This reasoning leads to the concept of a "crystal gene" and to the possibility of such processes providing a basis for the evolution of crystal "communities" showing the "behaviour" normally associated with living systems.

The hypothesis depends for its feasibility on two conditions, namely (a) that there exist imperfections capable of surviving crystal cleavage processes as well as growth processes: and (b), that

these imperfections, in a given array, are capable of affecting the chemical or physical behaviour of the crystal in a given environment. These conditions may be met in a number of areas of crystal chemistry, but the most obvious field of enquiry would seem to be the phyllosilicate minerals, for the following reasons:

a) Isomorphous substitution in individual layers of the phyllosilicate structure can produce a stable charge pattern - the necessary "defect structure" or "genotype".

b) It is conceivable that this charge pattern may be copied among the layers during crystal growth - the "replication mechanism". Some evidence for this is available in the structures of natural muscovites.

c) The principal cleavage of phyllosilicate minerals is (001). This cleavage ought to have no disruptive effect on the "genotype".

d) specially in the clay minerals, a wide range of morphologies and mechanical properties, including for example thixotropy, is found for samples of the same or closely similar compositions. It seems that a choice among several "phenotypes" is available to the crystal.

The search for a crystal gene among the silicate minerals is complicated by the difficulty of recognising its presence. For instance, the observation of a particular morphology, occurring in a given sample of a silicate species, but not in

other samples of the same species, is not per se evidence of the inheritance of a structurally-determined genotype, since the conditions of growth of the crystal may influence its morphology independently of the existence of any such genotype. Evidence could be found, however, if it were observed that a sample of a given species, having a given morphology (or any other experimentally observable macroscopic property), when placed in an environment conducive to growth, produced more of the species having the same, or closely similar, morphology (or other property): in other words, if the crystal gene were observed to breed to type. Even this evidence is not necessarily conclusive: it would also be necessary to show that the breeding continued independently of the rate of growth, or perhaps that the rate of growth was influenced by the presence of the genotype - a seeding effect.

This, however, does not in itself provide a model of the life process, a fundamental aspect of which is the ability of the genotype to evolve-to respond to environmental conditions by the selection of phenotypes resulting from genetic mutation. The inherited charge pattern must not be too stable. Mistakes in transcription must occasionally occur, leading to a new genotype, the phenotype of which has the possibility of selection. Experimental justification of the crystal gene hypothesis thus requires not only the recognition of a genetic process but also the demonstration of evolutionary

adaptation of the species under investigation.

Mineral formation in nature is inconveniently slow for any such experimental approach. In our search for the right sort of crystal it seemed convenient to choose minerals which could be readily prepared under fairly mild conditions. Again, certain of the clay minerals seemed suitable. Here, the mechanism of formation of the crystal becomes an important consideration: unless it can be shown that the growth of one phyllosilicate layer depends on the structure of the layer on which it grows, further search for genetic properties in the product is pointless. An useful corollary is that if it can be shown that the individual layers of the crystal grow independently of each other, then the species under consideration may immediately be rejected, at least as prepared by the synthetic conditions used. From the beginning it seemed likely that this would be the case with the swelling clays, despite the enticing range of "phenotypes" which they might be expected to show.

The micas, on the other hand, may well have a transcription stage involved in their growth mechanism. It is unfortunate that, until recently, syntheses of micas had only been performed under high pressures. The report of a synthesis of a Phlogopite-like mica at atmospheric pressure led us to consider investigations of this new field, with

the results described in Chapter 7. It is of great interest to note that very recently Professor Weiss has shown that mica-type silicates are capable of propagating Al-for-Si substitutional features during the growth of new crystals on pre-existing seeds. (Naturwiss., in press).

APPENDIX III

Selected literature on the Copper Silicates.

1970 M. C. van Oosterwyck-Gastuche

The structure of Chrysocolla.

Comptes Rend. Acad. Sci. Paris D, 271, 1837, (1970).

U. Würtzburger

Copper silicates in the Timna' ore deposits.

Israeli J. Chem. 8, 443 - 457, (1970).

M. C. van Oosterwyck-Gastuche and Ch. Gregoire

Electron microscopy and diffraction identification
of some copper silicates.

Int. Mineral. Ass., Pap. Proc. Gen. Meet., 7th,
(1970) no. 1, 196 - 205, (pub. 1971).

1969 Rodriguez P., Carlos

The infrared spectra of some oxidic copper ores.

Bull. Soc. Quim. Peru 35, 38 - 55, (1969).

1968 M. C. van Oosterwyck-Gastuche

Nomenclature of some Katangan copper silicates.

Plancheite - shattuckite - bisbeeite - katangite
minerals.

Ann. Soc. geol. Belg. 91, 401 - 422, (1968).

M. C. van Oosterwyck-Gastuche

The plancheites viewed as a family of cupric amphiboles.

Comptes Rend. Acad. Sci. Paris D 266, 1546 - 1548, (1968).

- 1967 M. C. van Oosterwyck-Gastuche
Katanga plancheites and shattuckites.
Ibid 265, 836 - 839, (1967).
- L. Dell'anna and C. L. Garavelli
Plancheite of Capo Calamita, Elba Island.
Period. Mineral. (Rome) 36, 125 - 146, (1967).
- 1966 H. T. Evans, Jr. and M. E. Mrose
Shattuckite and placheite: a crystal chemical study.
Science 154, 506 - 507, (1966).
- 1965 J. J. Fripiat, A. Jelli and J. Uytterhoven
Congr. Int. du Verre, Brussels, 1965, comm. 14, p.1.
- M. E. Hilmy and L. A. Mohsen
Secondary copper minerals from west central Sinai.
J. Geol. UAR 9, 1 - 12, (1965) (pub. 1967).
- 1963 E. Martinez
Chrysocolla studied by DTA, TGA and IR.
Trans. AIME 226, 424 - 427, (1963).
- R. Baistrocchi and L. Nicolini
Spectrophotometry of Egyptian Blue Pigment.
Inst. Chim. Fiz. Univ. Firenze (1963), 7 pp. (separate)

- 1962 A. Graca da Cruz
Plancheite from Mavoio, Angola.
Angola, Serv. Geol. Minas., Bol. no. 5, 35 - 42, (1962)
- S. A. Williams
Stability relations and paragenesis of copper oxides
and chlorides at the Algomah mine, Ontonagon County,
Michigan.
Econ. Geol. 57, 111 -113, (1962).
- P. Tarte
IR spectra of copper silicates and the identification
of a "shattuckite" from La Rioja.
Bol. Acad. Nacl. Cienc. Cordoba (Rep. Argentina)
43, 55 - 68, (1962).
- 1961 C. Guellemin and R. Pierrot
Plancheite from Tantara, Katanga.
Bull. Soc. Franc. Miner. et Cryst., 84, 276, (1961).
- 1960 V. V. Klimov et al.
The IR spectroscopy of inorganic substances. IV.
Absorption spectra of some silicate minerals.
Tr. Kazakhsk. Nauchn.-Issled. Inst. Mineral'n
Syr'ya (1960) no. 3, 312.
- 1957 J. Toussaint
DTA study of the natural hydrated copper silicates.
Ann. Soc. Geol. Belg. 80, 287 - 295, (1957).
- C. Guellemin and R. Pierrot
Connellite and Spangolite from Trebas.
Bull. soc. franc. Mineral. et cryst. 80 235 - 6 (1957).

H. Neumann et al.

X-ray powder patterns for mineral identification.

Vol. III, Silicates.

Avhandl. Norskevidenskaps-Akad. Oslo, I, Mat.-Naturv.

Kl. (1957) no. 6, 18 pp.

1951 N. G. Sumin and N. K. Lasheva

New modifications of chrysocolla of the plancheite type from Mednorudyansk in the Ural.

Trud. Mineralog. Muzeya, Akad. Nauk SSSR. no. 3, 106 - 121, (1951).

1915 First report of Shattuckite.

W. E. Ford

Dana's System of Mineralogy (Wiley, N.Y., 1915),

Appendix III p. 72.

1907 First report of Plancheite.

A. Lacroix.

A new mineral species from the French Congo.

Comptes Rend. Acad. Sci. Paris, 146, 722 - 725, (1907).

REFERENCES

- 1 W. T. Granquist and S. S. Pollack
A study of the synthesis of hectorite.
Clays Clay Miner. 8 150 (1959).
- 2 S. Caillere and S. Henin
Synthèse des argiles cobaltifères.
Bull. Soc. franc. Miner. et Cryst. 78 227 (1955).
- 3 A. F. Wells
Structural Inorganic Chemistry, 3rd. Edn., p. 549.
Clarendon Press, 1962.
- 4 W. Lotmar and W. Feitknecht.
Über Änderungen der Ionenabstände in Hydroxid-
Schichtengittern.
Z. Krist. 93 368 - 378 (1936).
- 5 O. Glemser and E. Hartet
Untersuchungen über die Wasserstoff-Brücken-Bindung
in kristallisierten Hydroxiden.
Z. anorg. Chem. 283 111 - 122 (1956).
- 6 D. R. Dasgupta
Topotactic transformations in iron oxides and
oxyhydroxides.
Indian J. Phys. 35 401 - 419 (1961).
- 7 H. E. Petch
The hydrogen positions in portlandite, $\text{Ca}(\text{OH})_2$.
Acta Cryst. 14 950 - 957 (1961).
- 8 R. Giovanoli, H. R. Oswald and W. Feitknecht
Über die thermische Zersetzung der kristallinen
Zinkhydroxide.
Helv. Chim. Acta 49(7) 1971 - 1983 (1966).
- 9 H. Jaggi and H. R. Oswald
Die Kristallstruktur des Kupferhydroxids, $\text{Cu}(\text{OH})_2$.
Acta Cryst. 14 1041 (1961).
- 10 B. C. Lippens and J. H. de Boer
Study of phase transformations during calcination
of aluminium hydroxides.
Acta Cryst. 17 1312 - 1321 (1964).
- 11 W. O. Milligan and J. L. MacAtee
The crystal structure of γ - AlOOH and γ - ScOOH .
J. Phys. Chem. 60 273 - 277 (1956).
- 12 A. Oberlin and R. Couty
Conditions de formation de la kaolinite à basse
température.
Bull. Groupe. franç. des Argiles 22 111 - 113 (1970).

- 13 A. Seitz, U. Rösler and K. Schubert
Crystal structure of β -Be(OH)₂.
Z. anorg. Chem. 261 94 (1950).
- 14 F.J. Ewing
The crystal structure of lepidocrocite.
J. Chem. Phys. 3 420 - 424 (1935).
- 15 T. Baird, A.G. Cairns-Smith and D.W. MacKenzie
An EM study of magnesium smectite synthesis.
Clay Minerals 10 17 (1973).
- 16 S. Caillere and S. Henin
Vues d'ensemble sur le probleme de la synthèse des
mineraux argileux à basse temperature.
Clay Mins. Bull. 5 265 - 272 (1963).
- 17 J.F. Schipko and D.L. Douglas
Stability of ferrous hydroxide precipitates.
J. Phys. Chem. 60 1519 - 1523 (1956).
- 18 H. Besson, S. Caillere and S. Henin
Experimental formation of a micaceous mineral
similar to phlogopite.
CR Acad. Sci. D 272(1) 1 - 3 (1971).
- 19 T. Baird, A.G. Cairns-Smith, D.W. MacKenzie and
D.S. Snell
EM studies of synthetic hectorite.
Clay Minerals 8 250 (1971).
- 20 V.C. Farmer
The IR spectra of talc, saponite and hectorite.
Miner. Mag. 31 829 - 845 (1958).
- 21 M. Hino and T. Sato
IR absorption spectra of silica gel - H₂¹⁶O, D₂¹⁶O and
H₂¹⁸O systems.
Bull. Chem. Soc. Japan 44 33 - 37 (1971).
- 22 J.M. Serratosa
IR analysis of the orientation of pyridine
molecules in clay complexes.
Clays Clay Mins., Proc. 14th. Natl. Conf., 1967, p. 385.
- 23 T. Baird, A.G. Cairns-Smith and D.S. Snell
Morphology and CO₂-uptake in tobermorite gel.
J. Coll. Interfac. Sci. 50(2) 387 - 391 (1975).
- 24 G. Brauer, Ed.
Handbook of preparative inorganic chemistry.
2nd. Edn., Vol. I, p. 935.
Academic Press, 1963.
- 25 J.A. Gard, J.W. Howieson and H.F.W. Taylor
Synthetic compounds related to tobermorite.
Mag. Concrete Res. 11(33) 151 (1959).

- 26 H. F. W. Taylor
Private communication to ASTM JCPDS.
- 27 J. D. C. McConnell
The hydrated calcium silicates riversideite,
plombierite and tobermorite.
Miner. Mag. 30(224) 293 - 305 (1954).
- 28 O. Henning and B. Gerstner
Zür Infrarot- und Röntgenanalytischen Charakteris-
ierung natürlicher und synthetischer Kalziumsilikat-
hydrate.
Wiss. Z. Hochsch. Architek. Bauw. (Weimar) 19 287 -
293 (1972).
- 29 V. C. Farmer, J. Jeevaratnam, K. Speakman and
H. F. W. Taylor
Thermal decomposition of 14Å tobermorite from
Crestmore.
Natl. Res. Council Publ. 1389, pp. 291-9, (1966).
- 30 W. F. Cole and B. Kroone
Carbonate minerals in hydrated portland cement.
Nature 184(4688) 57 (1959).
- 31 L. N. Rashkovich
The carbonation of the individual hydrosilicates of
calcium.
Stroit. Mater. 8(6) 31 (1962).
- 32 S. Asano, Y. Kamatani and Y. Inoue
The carbonation of calcium silicate compounds.
Yogyo Kyokai Shi 79 303 (1971).
- 33 Z. Sauman
The effect of carbon dioxide on porous concrete.
Cem. Concr. Res. 2 541 (1972).
- 34 K. Nakamoto
The IR spectra of inorganic and coordination compounds.
J. Wiley & Sons, Inc., 1963. P. 93.
- 35 H. F. W. Taylor
Aspects of the crystal structure of calcium silicates
and aluminates.
J. Appl. Chem. (London) 10 317 - 323 (1960).
- 36 L. S. D. Glasser, F. P. Glasser and H. F. W. Taylor
Topotactic reactions in inorganic oxy-compounds.
Quart. Rev. 16 343 - 360 (1961).
- 37 Gmelins Handbuch Anorganische Chemie
Auflage 8, System-nummer 60 (Copper) B1
Gmelin-Institut, Frankfurt-am-Main
Verlag Chemie, GMBH, (1958).
- 38 P. Tarte
Spectres infrarouge des sels basiques de cuivre.
Spectrochim. Acta 13 107 - 119 (1958).

- 39 C. Carbannes-Ott
Ann. Chim. (Paris) vol. 5, p. 925, (1960).
- 40 H. T. Evans, Jr. and M. E. Mrose
Shattuckite and Plancheteite, a crystal chemical study.
Science 154 506 - 507 (1966).
- 41 C. Guellemin and R. Pierrot
Plancheteite from Tantara, Katanga.
Bull. soc. franc. Minéral. et Crist. 84 276 - 281
(1961).
- 42 P. Tarte
IR spectra of copper silicates.
Bol. Acad. Nacl. Cienc. Cordoba 43 55 - 68 (1962).
- 43 M. C. van Oosterwyck-Gastuche
The structure of crysocolite.
CR Acad. Sci. D 271 1837 (1970).
- 44 I. J. Bear, G. M. Lukaszewski and A. G. Turnbull
IR spectra of the solid phases in the system
BeO - H₂O.
Aust. J. Chem. 18 1317 - 1330 (1965).
- 45 O. K. Srivastava and E. O. Secco
Thermal analysis of zinc derivatives.
Can. J. Chem. 45 579 - 583 (1967).
- 46 R. B. Corey and R. W. G. Wyckoff
The crystal structure of zinc hydroxide.
Z. Krist. A 86 8 - 18 (1933).
- 47 H. G. Schnering
Zur Konstitution des ϵ -Zn(OH)₂.
Z. anorg. Chem. 330 170 (1964).
- 48 A. Nørlund Christensen
The crystal structure of γ -Zn(OH)₂.
Acta Chem. Scand. 23 2016 - 2020 (1969).
- 49 H. G. Dietrich and J. Johnston
J. Amer. Chem. Soc. 49 1419 - 1431 (1927).
- 50 A. G. Merkulov and B. S. Khristoforov
Low-temperature synthesis of zinc silicates.
Izv. Sib. Otd. Akad. Nauk SSSR, Ser. Khim. Nauk,
4 70 - 74 (1969).
Chem. Abs. 72 27871h
- 51 M. J. Esquévin
Synthèse de la calamine et de la willémitte à
basse température.
CR Acad. Sci. D 243 1334 - 1336 (1956).

- 52 W. D. Keller, J. H. Spotts and D. L. Biggs
IR spectra of some rock-forming minerals.
Amer. J. Sci. 250 453 - 471 (1952).
- 53 W. S. McDonald and D. W. Cruickshank
Refinement of the structure of hemimorphite.
Z. Krist. 124(3) 180 - 191 (1967).
- 54 S. Hénin and O. Robichet
CR Acad. Sci. 236 517 (1953)
- 55 I. J. Bear and A. G. Turnbull
The heats of formation of beryllium compounds.
J. Phys. Chem. 69(9) 2828 - 2833 (1965).
- 56 H. Dachs
Neutron and x-ray investigation of manganite.
Z. Krist. 118 303 - 326 (1963).
- 57 reference 3, p. 556.
- 58 O. Glemser, U. Hauschild and H. Richert
Eine neue polymorphe Modifikation des Cadmiumhydroxyds.
Z. anorg. Chem. 290 58 - 67 (1957).
- 59 C. F. Sampson
The lattice parameters of goethite.
Acta Cryst. B25 1683 - 5 (1969).
- 60 L. S. Dent Glasser and L. Ingram
Refinement of the crystal structure of groutite.
Acta Cryst. B24 1233 - 6 (1968).

